



5-2019

The Development of a Dual-ligand PEGylated Liposome Nanotechnology for Cell-selective Targeted Vascular Gene Therapy

Richard Kern Fisher III
University of Tennessee, rkf3wolf@earthlink.net

Follow this and additional works at: https://trace.tennessee.edu/utk_graddiss

Recommended Citation

Fisher, Richard Kern III, "The Development of a Dual-ligand PEGylated Liposome Nanotechnology for Cell-selective Targeted Vascular Gene Therapy. " PhD diss., University of Tennessee, 2019.
https://trace.tennessee.edu/utk_graddiss/5432

This Dissertation is brought to you for free and open access by the Graduate School at TRACE: Tennessee Research and Creative Exchange. It has been accepted for inclusion in Doctoral Dissertations by an authorized administrator of TRACE: Tennessee Research and Creative Exchange. For more information, please contact trace@utk.edu.

To the Graduate Council:

I am submitting herewith a dissertation written by Richard Kern Fisher III entitled "The Development of a Dual-ligand PEGylated Liposome Nanotechnology for Cell-selective Targeted Vascular Gene Therapy." I have examined the final electronic copy of this dissertation for form and content and recommend that it be accepted in partial fulfillment of the requirements for the degree of Doctor of Philosophy, with a major in Comparative and Experimental Medicine.

Deidra Mountain, Major Professor

We have read this dissertation and recommend its acceptance:

Oscar Grandas, Michael Best, Stephen Kania

Accepted for the Council:

Dixie L. Thompson

Vice Provost and Dean of the Graduate School

(Original signatures are on file with official student records.)

The Development of a Dual-ligand PEGylated Liposome Nanotechnology for Cell-selective Targeted Vascular Gene Therapy

A Dissertation Presented for the
Doctor of Philosophy
Degree
The University of Tennessee, Knoxville

Richard Kern Fisher III

May 2019

Copyright © by Richard Kern Fisher III
All rights reserved.

DEDICATION

To my wife

Lauren Fisher

my daughter

Harper Fisher

my sister

Ashley Fisher

my father

Rick Fisher

and my mother

Tammy Fisher

ACKNOWLEDGEMENTS

I would like to express sincere gratitude to Dr. Deidra Mountain for her support and guidance during my time as a student in graduate school and as a research associate in the Vascular Research Lab over the past 7 years. She has created a learning environment that has allowed me to flourish as a graduate student and a scientist. She has taught me the values of work ethic, accountability, and attention to detail. I will always be indebted to her for the opportunity to pursue my doctoral studies and the wisdom she has provided me during that pursuit. I would like to thank Dr. Oscar Grandas for his support and oversight throughout my research training and for assisting with my education in comparative and experimental medicine. I would also like to thank Dr. Mei-Zhen Cui and Dr. Michael Best for serving on my committee and their career advice that has proven invaluable. I want to thank Stacy Kirkpatrick for her aid and assistance in my work tenure at the Vascular Research Lab. I will always treasure the friendship that we have shared. Finally, I would like to offer thanks to Connor West for his contributions to the bench work herein and all the long hours spent working through this scientific process.

I would like to express my sincere appreciation for the support and counsel Dr. Michael Freeman and Dr. Mitchell Goldman, as well as the entire staff and faculty associated with the Department of Surgery. I want to thank Dr. Stephen Kania and Kim Rutherford for all of the administrative guidance throughout my PhD candidacy. Finally, I would like to express gratitude to the University of Tennessee, UT Graduate School of Medicine, UT Health Science Center, and the Comparative and Experimental Medicine program, and the Biochemistry and Molecular Biology Department for providing support and funding for my research and graduate education.

ABSTRACT

Percutaneous transluminal angioplasty (PTA) is a common endovascular procedure that restores blood flow in peripheral vascular disease. Unfortunately, endovascular procedures inherently cause injury to intimal layer. This exposing the medial layer and vascular smooth muscle cells (VSMCs) to hemodynamic flow. The injury response induces dysfunctional VSMC phenotypes, leading to thickening of the vessel wall known as intimal hyperplasia (IH). Eventually, IH leads to restenosis, a common complication of PTA.

Most therapeutic strategies for IH are aimed at reducing VSMC migration and proliferation. However, recent studies have shown healing of the VEC layer is crucial mitigating factor in IH. We postulate that an optimal intervention could be achieved by employing both therapeutic strategies simultaneously in a cell-type specific manner at the site of PTA-induced injury. Gene therapy techniques provide an opportunity to accomplish this goal. Many IH-associated genetic targets have been successfully modulated to improve reendothelialization of VECs and inhibit the proliferation of VSMCs. However, clinical success of vascular gene therapy is limited due to the lack of a translational delivery vehicle.

Liposomes have been shown to be effective gene vectors with translational efficacy. The addition of polyethylene glycol (PEG) to liposomes (PLP) can improve *in vivo* pharmacokinetics, but reduces cellular uptake of liposomal cargo. Ligand-modified liposomes provide an opportunity to enhance transfection of neutral PLPs and target specific cell types for gene delivery. Cell-penetrating peptides (CPPs) containing arginine-rich motifs have the ability to enhance membrane translocation of their conjugated cargo. Cell-targeting peptides (CTP) can also be used to decorate the liposome surface, providing cell-type specificity. In this *in vitro* proof-

of-concept study, we aim to develop a modified PLP comprised of neutral lipids and capable of enhanced transfection and cell-type specific delivery to VSMCs and VECs, respectively.

Using a Ca^{2+} -mediated ethanol injection technique, a novel method for the self-assembly of CPP-modified PLPs with enhanced transfection, optimized siRNA loading efficiency, minimal cytotoxicity, and cell-targeting capabilities was developed. These nanocarriers convey chemical stability to siRNA in the presence of nuclease activity. This liposomal delivery system could provide the foundation necessary to increase the bench-to-bedside success of systemically administered vascular gene therapy.

TABLE OF CONTENTS

CHAPTER 1: Introduction	1
1.1 Overview	2
1.2 Introduction to Peripheral Arterial Disease	3
1.2.1 Anatomy of the Vessel Wall.....	4
1.2.2 Pathogenesis of Atherosclerosis	7
1.2.3 Treatment of Atherosclerotic Lesions	10
1.3 Restenosis – Vessel Response to Injury.....	12
1.3.1 Intimal Hyperplasia in a Balloon Injury Model.....	12
1.3.2 Timeline of IH-associated Restenosis after Balloon Injury	14
1.3.3 Novel Therapeutic Strategies to Prevent PTA-induced Restenosis.....	16
1.4 Gene Therapy.....	18
1.4.1 Mechanism of RNA Interference	19
1.4.2 siRNA Targets in the Treatment of Intimal Hyperplasia.....	20
1.5 Gene Delivery	22
1.5.1 Introduction to Liposomes.....	24
1.6 Research Summary.....	30
1.6.1 Specific Aims	32
CHAPTER 2: The Scalable Assembly of Noncationic PEGylated Liposomes with Octaarginine-potentiated siRNA Encapsulation	33
2.1 Introduction	34
2.2 Materials and Methods	36
2.2.1 PLP Assembly via Ethanol Injection Technique.....	36
2.2.2 CPP Modification via R8 Amphiphile Incorporation.....	37
2.2.3 Liposome Characterization Studies.....	39
2.2.4 Vascular Smooth Muscle Cell Culture.....	42
2.2.5 Cell Association Studies.....	42
2.2.6 Statistical Analysis	42
2.3 Results	43
2.3.1 Incorporation of R8-PEG via Pre-insertion, Post-insertion, and Post- conjugation Resulted in Significant siRNA Leakage and Reduced Total siRNA Retention.	43
2.3.2 Incorporation of STR-R8 via Pre-insertion Resulted in Significantly Enhanced siRNA Encapsulation and Retention.....	43

2.3.3	Ca ²⁺ -mediated EtOH injection of R8-PLPs Resulted in Homogenous Liposome Samples Between 50-60nm with Increased siRNA Retention and EE%.....	46
2.3.4	Increasing Lipid:siRNA Enhanced R8-PLP EE% to ~100%.....	46
2.3.5	Partial Heparin Displacement Indicated siRNA Complexation to R8-PLP Surface in Addition to Internalized R8-PLP Entrapment.....	49
2.3.6	R8-PLP Nanoparticles Sufficiently Protected Encapsulated and Complexed siRNA Against RNase A Degradation.	51
2.3.7	Slower Injection Rates During R8-PLP Assembly Resulted in Increased Sample Homogeneity but Showed No Correlation to EE%.	52
2.3.8	R8-PLP Nanoparticles Demonstrated Enhanced Cell Association <i>in vitro</i>	52
2.4	Discussion.....	56
CHAPTER 3: Improving the Efficacy of Liposomal-mediated Vascular Gene Therapy via Lipid Surface Modifications		63
3.1	Introduction	64
3.2	Materials and Methods	66
3.2.1	Neutral and Cationic Liposome Assembly via EtOH Injection.....	66
3.2.2	Liposome Characterization Studies.....	68
3.2.3	Vascular Smooth Muscle Cell Culture.....	69
3.2.4	Cytotoxicity Assays.....	70
3.2.5	Cell Association Experiments	70
3.2.6	Liposome Transfection and Gene Expression Analysis	71
3.2.7	Statistical Analysis	71
3.3	Results	72
3.3.1	EtOH Injection Assembly of PLPs, R8-PLPs, and CLPs Results in Nanoparticles with Similar Physical Characteristics.....	72
3.3.2	R8 Modification of PLPs Increases Encapsulation Efficiency of siRNA in a Concentration Dependent Manner.	72
3.3.3	Non-cationic Liposomes Exhibited Significantly Less Cytotoxic Effects Compared to Cationic Liposomes.....	75
3.3.4	R8 Lipid Surface Modification Significantly Increases the Cell Association of PLPs.....	75
3.3.5	Transfection with R8-PLPs, Modified at 10mol% STR-R8, Resulted in Significant GAPDH silencing, in a Manner Dependent on Lipid-to-siRNA Load Capacity.....	75
3.4	Discussion.....	81
CHAPTER 4: The Assembly of Ligand-modified PEGylated Liposomes for Cell-type Selectivity in Vascular Cell Types.....		87
4.1	Introduction	88

4.2	Materials and Methods	90
4.2.1	PLP Assembly via Ethanol Injection Technique.....	90
4.2.2	CTP-PLP assembly via VAPG and REDV Amphiphile Incorporation	91
4.2.3	Liposome Characterization Studies.....	92
4.2.4	Vascular Cell Culture.....	93
4.2.5	Cell Association Experiments	93
4.2.6	Statistical Analysis	94
4.3	Results	94
4.3.1	The Incorporation of CTP Does Not Significantly Affect Size or Homogeneity of CTP-PLPs Compared to PLP Controls.....	94
4.3.2	The Incorporation of VAPG-PEG into PLP Base Formulations Results in Desired Morphological Characteristics.....	94
4.3.3	The Incorporation of VAPG-PEG into SMC-PLPs Increases Cell Association Above PLP Controls in VSMC but Not VEC.	98
4.3.4	The Incorporation of VAPG-PEG into SMC-PLPs via Post-insertion Does Not Significantly Increase Cell Association in SMCs Compared to PLP Controls.	98
4.3.5	The Incorporation of REDV-PEG into EC-PLPs Increases Cell Association Above PLP Controls in VEC but Not VSMC at Early Exposure.	98
4.3.6	The Incorporation of REDV-PEG into EC-PLPs Does Not Significantly Increase Cell Association Above PLP Controls at Later Time Points.	102
4.4	Discussion.....	102
CHAPTER 5: Conclusions and Future Directions.....		107
5.1	Study Conclusions and Future Directions	108
BIBLIOGRAPHY		113
VITA		122

LIST OF TABLES

TABLE 2.1: QUALITY BY DESIGN APPROACH WHICH PROVIDES ESTABLISHED CRITERIA, OR CQAs, REQUIRED FOR EFFECTIVE SYSTEMIC ADMINISTRATION OF LIPOSOMAL DRUG DELIVERY SYSTEMS.	36
TABLE 2.2: BULK LIPID CONSTITUENTS THAT COMPRISE THE LIPOSOME FORMULATIONS USED IN THIS STUDY.	37
TABLE 2.3: R8-PLP MODIFICATION CONDITIONS. THE siRNA RETENTION AND FINAL EE% ARE LISTED AS A RESULT OF R8-MODIFICATION.	44
TABLE 2.4: R8-PLP MODIFICATION CONDITIONS. SIZE, PDI, AND ZETA POTENTIAL ARE MEASURED BEFORE AND AFTER R8-MODIFICATION.	45
TABLE 3.1: LIPOSOME CONSTITUENTS.....	67
TABLE 3.2: LIPOSOME CHARACTERIZATION.	73
TABLE 4.1: LIPOSOME FORMULATION CONSTITUENTS AND ASSOCIATED ACRONYMS.....	91

LIST OF FIGURES

FIGURE 1.1: PROGRESSION OF ATHEROSCLEROTIC DEVELOPMENT.	5
FIGURE 1.2: ANATOMY OF THE ARTERIAL VESSEL WALL.	6
FIGURE 1.3: ILLUSTRATION OF MAJOR CELLULAR EVENTS AND POSSIBLE CRITICAL OUTCOMES OF ATHEROGENESIS.....	9
FIGURE 1.4: SURGICAL BYPASS AND PERCUTANEOUS TRANSLUMINAL ANGIOPLASTY REVASCULARIZATION PROCEDURES ARE COMPARED.....	11
FIGURE 1.5: DIAGRAM OF MAJOR EVENTS IN THE DEVELOPMENT OF IH-INDUCED RESTENOSIS IN RESPONSE TO VASCULAR INJURY COMMONLY SEEN IN PTA PROCEDURES.	13
FIGURE 1.6: STAGED DEVELOPMENT OF INTIMAL HYPERPLASIA DEVELOPMENT AFTER PTA-INDUCED INJURY. ²⁷	15
FIGURE 1.7: MECHANISM OF RNAI.....	21
FIGURE 1.8: COMPARISON OF COMMONLY USED VIRAL AND NONVIRAL VECTORS.....	22
FIGURE 1.9: ADVANTAGES OF LIPOSOMES AS PHARMACEUTICAL NANOCARRIERS IN MEDICINE.....	26
FIGURE 1.10: GRAPHICAL ILLUSTRATION SHOWING EXPONENTIAL GROWTH OF LIPOSOME-RELATED PUBLICATIONS IN MEDICINE AS WELL AS THE USE OF COMPUTATIONAL MODELING IN DEVELOPING LIPOSOMAL DRUGS.	26
FIGURE 1.11: SCHEMATIC REPRESENTATION OF DIFFERENT CLASSIFICATIONS OF LDS CAPABLE OF ENCAPSULATING HYDROPHILIC AND HYDROPHOBIC DRUGS.	29
FIGURE 1.12: LISTING OF LIPID CLASSES USED IN DISSERTATION WITH ASSOCIATED NOMENCLATURE AND STRUCTURE.....	31
FIGURE 2.1: MALDI-TOF SPECTROSCOPY CONFIRMATION OF SUCCESSFUL “CLICK” REACTION USED TO CONJUGATE AZIDE-MODIFIED R8 WITH DSPE-PEGDBCO USING AZIDE-ALKYNE CYCLOADDITION.	38
FIGURE 2.2: EE% OF siRNA FOLLOWING ALL R8-MODIFICATION TECHNIQUES AS COMPARED TO PLP CONTROL USING CA ²⁺ -MEDIATED ETOH INJECTION METHOD.....	44
FIGURE 2.3A: COMPARISON OF siRNA EE% IN PLP AND R8-PLP ASSEMBLIES WITH VARIED AMOUNTS OF CALCIUM DURING INJECTION.	47
FIGURE 2.3B: COMPARISON OF PDI UPON PLP AND R8-PLP ASSEMBLY USING 0-50 mM [CA ²⁺].....	47
FIGURE 2.3C: COMPARISON OF AVERAGE SIZE (D.NM) UPON PLP AND R8-PLP ASSEMBLY USING 0-50 mM [CA ²⁺].....	48
FIGURE 2.4A: COMPARISON OF siRNA EE% IN R8-PLP ASSEMBLIES WITH VARIED LIPID:siRNA (WT-TO-WT).	48
FIGURE 2.4B: PHYSICAL CONFIRMATION OF EE% USING siRNA GEL EXCLUSION ASSAYS.	49
FIGURE 2.5A: HEPARIN DISPLACEMENT ASSAY THAT INDICATES THE MINIMUM AMOUNT OF [HEPARIN] TO REMOVE ALL OUTER-ASSOCIATED siRNA (WHITE BOX; 100UG/ML).....	50
FIGURE 2.5B: GEL EXCLUSION/HEPARIN DISPLACEMENT ASSAYS USED TO CHARACTERIZE COMPLEXATION OF siRNA WITH R8-PLP ASSEMBLIES.....	50
FIGURE 2.6A: RNASE STABILITY ASSAY INDICATING THE MINIMUM AMOUNT OF RNASE A REQUIRED TO DIGEST ALL FREE siRNA USED FOR ASSAY (WHITE BOX; 0.5 UG/ML).....	51
FIGURE 2.6B: RNASE STABILITY ASSAY SHOWING NEARLY COMPLETE PROTECTION OF siRNA-LOADED R8- PLPs.....	52
FIGURE 2.7A: COMPARISON OF siRNA EE% WITH VARIED INJECTION RATES DURING ETOH INJECTION ASSEMBLY OF R8-PLPs WITH 10:1 LIPID:siRNA.....	53
FIGURE 2.7B: COMPARISON OF PDI UPON R8-PLP ASSEMBLY USING VARIED INJECTION RATES (P=NS VS ALL GROUPS; N=3)	54

FIGURE 2.7C: COMPARISON OF AVERAGE SIZE (D.NM) UPON R8-PLP ASSEMBLY USING VARIED INJECTION RATES.....	54
FIGURE 2.8: QUALITATIVE FLUORESCENT IMAGES OF HASMCs TREATED WITH R8-PLP ASSEMBLIES WITH 10MOL% STR-R8 AND PLP CONTROLS AT 30 MINS AND 24 HOURS.....	55
FIGURE 2.9: SCHEMATIC ILLUSTRATION OF EMPIRICALLY DERIVED CA ²⁺ -MEDIATED ETOH INJECTION TECHNIQUE USED TO ASSEMBLE NONCATIONIC R8-MODIFIED PLPs WITH NEARLY COMPLETE siRNA EE% AND ENHANCED CELL ASSOCIATION.....	62
FIGURE 3.1: ILLUSTRATION OF LIPID CONSTITUENTS AND THEIR ASSEMBLY WITHIN IN LIPOSOME CLASSIFICATION USED FOR EXPERIMENTAL ANALYSIS.....	67
FIGURE 3.2: SCANNING TRANSMISSION ELECTRON MICROSCOPY (STEM) IMAGES CONFIRMING LIPOSOME MORPHOLOGY AND LAMELLARITY.....	73
FIGURE 3.3: GRAPH SHOWING INCREASED siRNA ENCAPSULATION WITH INCREASING MOL% OF STR-R8.....	74
FIGURE 3.4: CYTOTOXICITY OF R8-PLPs WITH INCREASING MOL% R8 AS COMPARED TO PLP AND CLP CONTROLS.....	76
FIGURE 3.5: GRAPH OF CELL ASSOCIATION OF R8-PLPs AS COMPARED TO CLPs AND NORMALIZED TO PLPs.....	77
FIGURE 3.6: GRAPH OF SILENCING EFFICIENCY OF R8-PLP siRNA COMPARED CLP-LOADED siRNA.....	79
FIGURE 3.7: GRAPH OF SILENCING EFFICIENCY OF R8-PLP-LOADED siRNA COMPARED TO NC siRNA.....	80
FIGURE 4.1: COMPARISON OF AVERAGE SIZE (D.NM) AS A RESULT OF VAPG INCORPORATION INTO PLPs USING PRE-INSERTION AND POST-INSERTION TECHNIQUES.....	95
FIGURE 4.2: COMPARISON OF POLYDISPERSITY INDEX (PDI) AS A RESULT OF VAPG INCORPORATION INTO PLPs USING PRE-INSERTION AND POST-INSERTION TECHNIQUES.....	96
FIGURE 4.3: COMPARISON OF AVERAGE SIZE (D.NM) AS A RESULT OF REDV INCORPORATION INTO PLPs USING PRE-INSERTION TECHNIQUE.....	96
FIGURE 4.4: COMPARISON OF AVERAGE SIZE (D.NM) AS A RESULT OF REDV INCORPORATION INTO PLPs USING PRE-INSERTION TECHNIQUE.....	97
FIGURE 4.5: STEM IMAGES OF SMC-PLPs MODIFIED WITH 5 MOL % VAPG.....	97
FIGURE 4.6: THE RELATIVE CELL ASSOCIATION OF VAPG MODIFIED CTP-PLPs COMPARED IN HASMCs AND HAECs.....	99
FIGURE 4.7: THE RELATIVE CELL ASSOCIATION OF VAPG MODIFIED CTP-PLPs USING POST-INSERTION TECHNIQUE COMPARED IN VSMCs AND VECs.....	100
FIGURE 4.8: THE RELATIVE CELL ASSOCIATION OF REDV MODIFIED CTP-PLPs USING PRE-INSERTION COMPARED IN VSMCs AND VECs AFTER 1 HOUR TREATMENT.....	101
FIGURE 4.9: THE RELATIVE CELL ASSOCIATION OF REDV MODIFIED CTP-PLPs SING PRE-INSERTION COMPARED IN VSMCs AND VECs AFTER 4 HOUR TREATMENT.....	103

CHAPTER I: Introduction

1.1 Overview

As our society ages, peripheral vascular disease (PVD) is increasingly problematic, and remains a major risk factor contributing to stroke and cardiovascular disease.¹ In severe or complex forms of PVD, surgeons have typically relied on surgical bypass procedures for vessel revascularization. Fortunately, advanced technology has given rise to endovascular procedures with comparable success rates and fewer patient risks compared to surgical revascularization.² Unfortunately, a gold standard intervention is still elusive due to common occurrence of neointima formation and late vessel restenosis induced by endovascular angioplasty, atherectomy, and stenting procedures.

Gene therapy has emerged as a promising therapeutic modality in the treatment of a variety of disease pathologies. A dual gene delivery strategy aimed at reducing neointima formation and regenerating injured endothelium provides an encouraging pharmacological approach when implemented in conjunction with surgical and endovascular interventions.³ This combinatorial gene therapy approach could improve long-term outcomes of patients undergoing revascularization procedures for PVD, while also limiting further medical interventions, and significantly reducing PVD-associated costs.

Many gene targets have been elucidated for modulation in the prevention of late vessel restenosis in a surgical setting, which includes matrix metalloproteinases (MMPs), transforming growth factor-beta (TGF- β 1), and nitric oxide synthase (NOS).⁴ However, the primary hurdle of effective gene therapy is the accessibility of a safe and efficacious delivery system. The preponderance of evidence shows liposomes to be promising nonviral gene vectors due to biocompatibility and reduced toxicity profile compared to viral and polymeric vectors.⁵ Liposomal

nanoparticles also exhibit multifunctional potential for targeted gene therapy applications through lipid surface modifications.⁶ Due to these advantageous characteristics and validated pharmacokinetic superiority compared to other common gene vectors, the volume of drug delivery research in gene therapy continues to shift towards liposomal delivery systems (LDS).

The research herein is a proof-of-concept approach that lays the foundation for the development of a liposomal gene therapy platform aimed at the efficient and cell-type specific delivery of siRNA to vascular smooth muscle cells (VSMCs) and vascular endothelial cells (VECs), respectively. This platform could provide a translational avenue towards the ultimate goal of delivering gene therapeutics to vascular injury sites in order to inhibit neointima formation and improve long-term outcomes of surgical interventions performed in vascular disease. This project is interdisciplinary in nature, which requires the discussion of a variety of academic research areas. This includes peripheral arterial disease (PAD), mechanisms of atherosclerosis development, surgical and pharmacological interventions for PAD, and the pathophysiology of restenosis. Current developments in modern gene therapy and liposomal delivery systems will also be discussed. The specific aims of this study conclude the introductory chapter.

1.2 Introduction to Peripheral Arterial Disease

PAD affects over 200 million people worldwide, and is the leading cause of disability in people over the age of 60.⁷ PAD is the most common form of PVD, and is defined as the atherogenic progression of disease in arterial vasculature whereby oxygenated blood flow is occluded to the extremities. PAD is most often caused by atherosclerosis, but can include aneurysms, thromboembolisms, congenital defects, chronic inflammation, and traumatic injury.⁸ For the purposes of this dissertation, the term PAD will strictly refer to atherosclerotic

pathological processes that affect normal function of the aorta, its visceral branch arteries, and the arteries of the lower extremity. Progression of occlusive arterial flow in PAD shown in Figure 1.1 is associated with deficits in quality of life, reduction of functional capacity, limb amputation, and often signals systemic atherosclerosis development.⁹ In fact, myocardial infarction and stroke are more common in PAD patients than major adverse limb events (i.e. limb amputation).¹⁰ For this reason, early diagnosis of PAD is crucial, and it should be assumed that PAD patients require aggressive medical interventions to prevent secondary cardiovascular and cerebrovascular events.

1.2.1 Anatomy of the Vessel Wall

Restenosis is defined as the “loss of greater or equal to 50% of the gain produced at angioplasty or a >50% stenosis at follow-up angiography.”¹² The pathogenesis of restenosis involves the entire multi-laminar structure of the blood vessel wall. This includes the *tunica adventitia*, *tunica media*, and *tunica intima* as shown in Figure 1.2. The *intimal layer* comprises a thin, continuous layer of VECs anchored to a subendothelial collagenous matrix. VECs help maintain homeostasis within the vasculature by modulating vascular tone, local cell proliferation and migration, and regulating extracellular matrix (ECM) deposition.¹³ Injury to the endothelium exposes the subendothelial matrix to blood components, which initiates pathogenesis of atherosclerotic disease. For this reason, reendothelialization is an important pharmacological strategy for mitigating the progression of vascular disease.

The *tunica intima* is delineated from the *tunica media* by the internal elastic lamina (IEL). The IEL is made up of ECM components such as collagen Type IV, laminin, and proteoglycans. The underlying *tunica media* makes up the bulk of the arterial tissue, and is primarily made up of densely packed VSMCs within an interstitial matrix. It is this muscle layer that provides

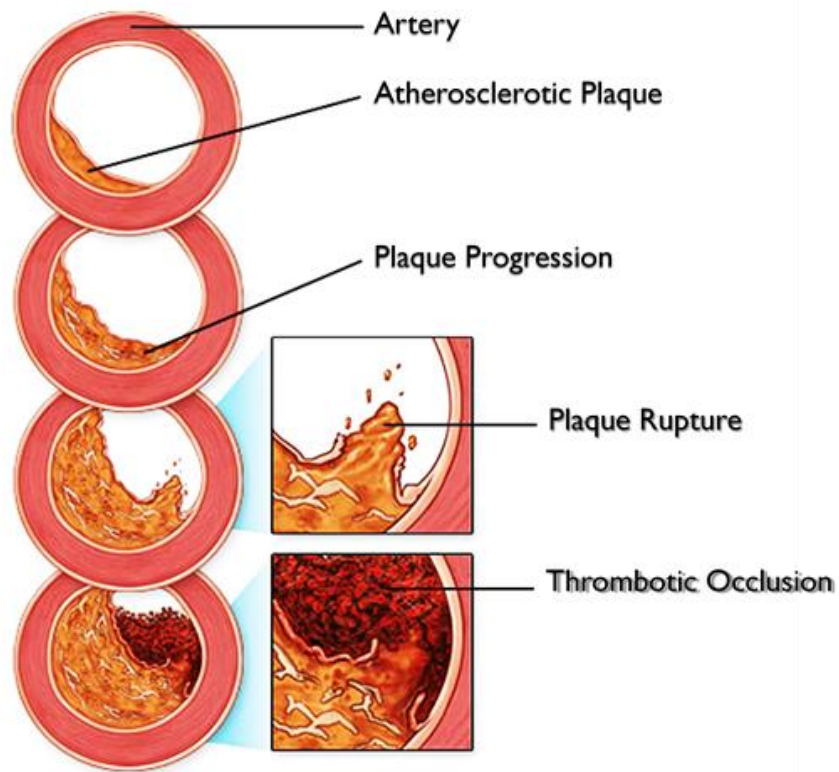


Figure 1.1: Progression of atherosclerotic development. As the atherosclerotic plaque forms, the artery experiences increased occlusion. Plaque growth continues leading to eventual plaque rupture and thrombosis. Adapted from atherosclerosis figure in Mayo Clinic, by Mayo clinic staff, Retrieved January 15, 2019 from <https://www.mayoclinic.org/>.¹¹ Copyright 2019 by Mayo Foundation for Medical Education and Research (MFMER).

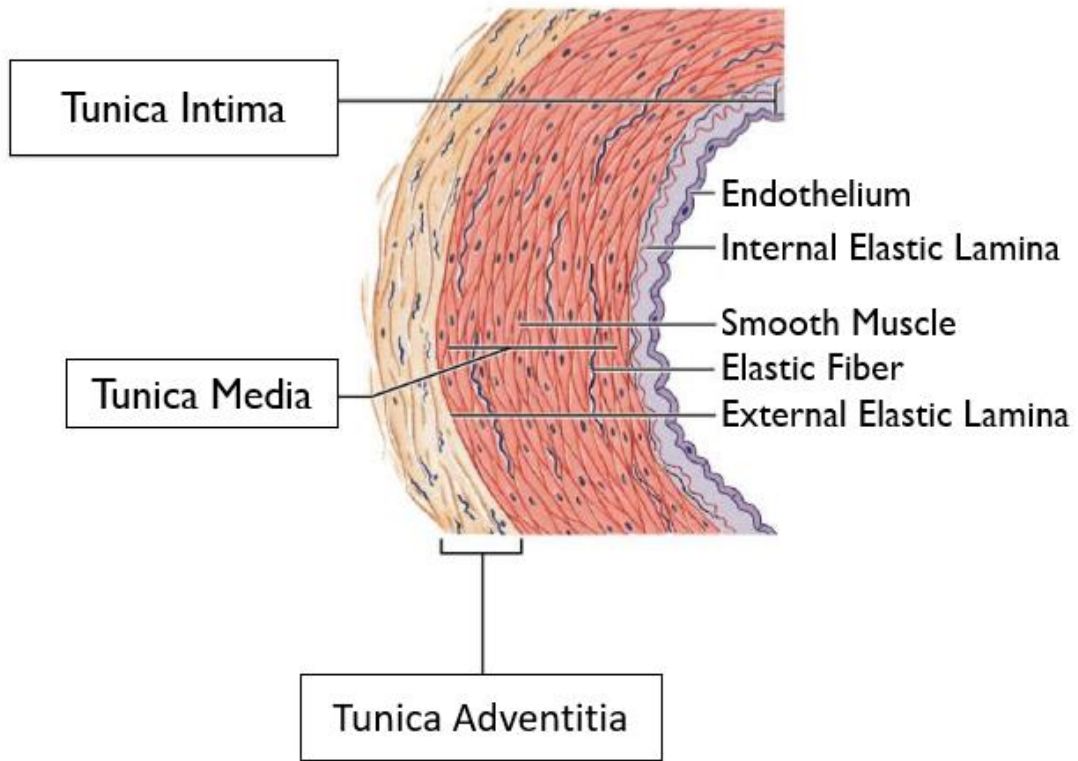


Figure 1.2: Anatomy of the arterial vessel wall. The tunica intima and tunica media is separated by the IEL. The tunica media and the tunica adventitia are separated by the EEL. Adapted from Human Anatomy and Physiology, 11th Edition (pg. 709), by E. N. Marieb, 2019, New York, NY: Pearson Inc. Copyright 2018.

contraction and relaxation functionality to blood vessels to maintain adequate blood flow and pressure. In normal, healthy vessels, VSMCs exhibit a quiescent, non-proliferative phenotype.¹⁴ When exposed to inflammatory factors and vascular injury, VSMCs can switch from a contractile phenotype to a synthetic phenotype.¹⁵ VSMCs of a synthetic phenotype exhibit substantial increase in migratory and proliferative potential, and have been shown to contribute to neointima formation and vascular disease progression. Due to the acute response of VSMCs to a synthetic phenotype after surgically-induced injury, VSMC proliferation is the most common therapeutic target to preserve post-operative lumen diameter and prevent restenosis.

Finally, the outer layer, or *tunica adventitia*, is comprised mainly of fibroblasts and perivascular nerves within a collagen-rich matrix. The adventitia is delineated from the medial layer by the external elastic lamina (EEL).¹⁶ This layer has been shown to aid in communication between VSMCs and VECs, and is also the site of resident immune cells such as macrophages, T-cells, B-cells, mast cells, and dendritic cells. Although the *adventitia* is often ignored as a pharmacological target in vascular disease, this layer is primed for the immune response that is critical to the pathophysiology of atherosclerotic PAD and restenosis in response to vascular injury.

1.2.2 Pathogenesis of Atherosclerosis

Atherosclerosis, the primary cause of PAD, is the buildup of subendothelial plaques within the arterial wall, which leads to thickening and hardening of blood vessels. The pathological buildup of an atheroma, or fatty plaque, is a slow process that begins in the *tunica intima*. As plaque progression proceeds, the *intima* becomes distorted, resulting in negative remodeling and lumen diameter loss.¹⁷ The major atherosclerotic events are delineated in Figure 1.3, which

illustrates the chronic progression of atherogenesis and potential critical outcomes. Ultimately, patients with these complicated lesions can experience potentially lethal ischemia and thrombotic occlusion of arteries supplying blood to the heart, brain, legs, and other major organs. The presence of atherosclerotic plaques in PAD typically signals systemic disease burden, therefore, it is important to identify and treat PAD patients early in disease progression in order to prevent more serious cardiovascular and cerebrovascular issues.

First, the *intimal layer* of the vessel is damaged, resulting in endothelial dysfunction. This initial process can begin in childhood and is precipitated by a host of risk factors including hypertension, dyslipidemia, diabetes, smoking, hemodynamic factors, and inflammation. As dysfunction of the endothelium ensues, the inflammatory process in atherosclerosis is initiated. This process typically originates as platelet adherence and monocyte infiltration within the compromised endothelium. Next, circulating cholesterol bound to low density lipoprotein (LDL) begins to cross the endothelial barrier into the *intima* where it accumulates and becomes oxidized. Upregulation of monocyte adhesion molecules (MAM), such as P-selectin and vascular cell adhesion molecule (VCAM-1), leads to enhanced entry of inflammatory cells within the vessel wall. Monocyte infiltration and cytokine production is continuous throughout disease progression, which maintains chronic activity of proinflammatory cascade. Invading and activated resident immune cells upregulate growth factor expression, which promotes VSMC migration and proliferation within the *intimal layer*. Eventually, monocytes differentiate into macrophages within the vessel wall, which slowly absorb oxidized LDL components leading to foam cell formation. Finally, as these macrophages undergo apoptosis and dump their cellular debris, a lipid-rich, fibrous cap begins to form through unregulated MMP expression and excessive ECM

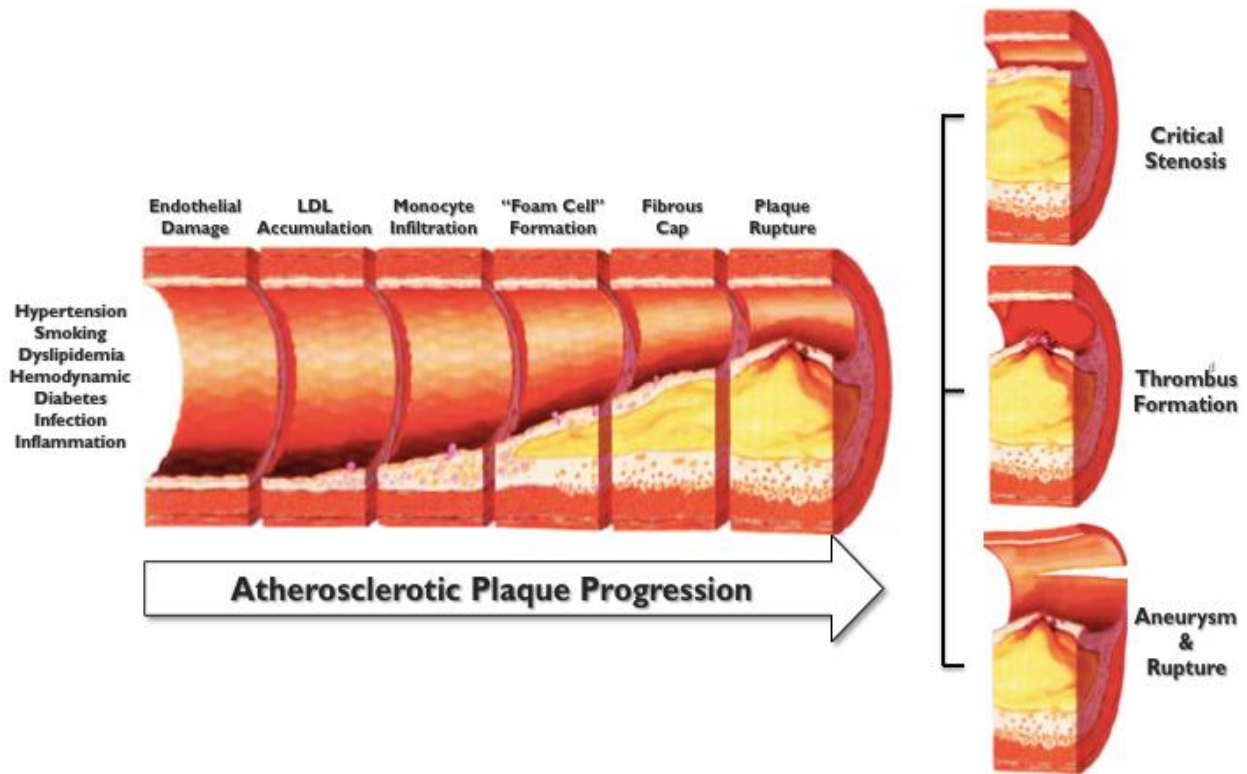


Figure 1.3: Illustration of major cellular events and possible critical outcomes of atherogenesis. Chronic exposure to major risk factors for atherosclerosis leads to endothelial damage. LDL begins to attach to dysfunctional endothelium and accumulate within intimal layer. Monocytes are also attracted to lesion site by monocyte adhesion molecules and cytokine production. Once monocytes infiltrate the lesion, they differentiate into macrophages and engulf lipid-rich particles within plaque forming "foam cells". As foam cell growth continues, a fibrous cap is formed. Continuous ECM remodeling leads to vulnerability and eventual plaque rupture. This can lead to critical stenosis, thrombus occlusion, or aneurysmal rupture. Adapted from "Biomarkers of Atherosclerotic Plaque Instability and Rupture," by W. Koenig and N. Khuseynova, 2006, *Arteriosclerosis, Thrombosis, and Vascular Biology*, 27;1, p. 15-26, Copyright 2006 by American Heart Association.

remodeling within the plaque. Chronic atherogenesis can eventually lead to plaque vulnerability where thrombosis, plaque rupture, or aneurysmal rupture may ensue.¹⁸

1.2.3 Treatment of Atherosclerotic Lesions

The treatment of atherosclerotic peripheral artery occlusion typically begins with non-invasive interventions like exercise prescription and pharmacological approaches. The goal of these interventions is to relieve pain, improve exercise tolerance, mitigate progressive artery occlusion, and prevent dangerous secondary cerebrovascular and cardiovascular events. Examples of medications to treat PAD include anticlotting agents, statins to lower cholesterol, and medications for hypertension (i.e. beta-blockers, angiotensin converting enzyme inhibitors, calcium channel blockers, etc.). Adverse lifestyle habits may also be addressed such as diet, exercise, smoking, and sleep schedule.¹⁹ Once conservative strategies fail, the patient is typically referred for surgical revascularization through surgical bypass or endovascular interventions. The pros and cons of these two surgical options are compared in Figure 1.4.

Surgical intervention for PAD involves the use of an autologous vein graft or a synthetic graft (i.e. Polytetrafluoroethylene) as a conduit, which is anastomosed into the diseased vasculature, bypassing the arterial occlusion and revascularizing distal areas to the lesion site. Long-term patency rates are comparable to endovascular procedures, especially when using autologous grafts. However, a recent retrospective meta-analysis has shown that there is no significant difference in amputation-free survival or all-cause mortality when comparing surgical bypass to endovascular interventions.²⁰ For this reason, along with minimal risks to patient, percutaneous endovascular procedures appear to be the most cost-effective and safest surgical option for PAD intervention.

Surgical Bypass	Angioplasty
<p>Advantages</p> <ul style="list-style-type: none"> • Considered “gold standard” • Better for complex lesions with multiple stenoses • Better long-term patency <p>Disadvantages</p> <ul style="list-style-type: none"> • Higher rate of morbidity • Potential systemic complications • Requires general anesthesia • Requires autologous veins, which may be needed for future coronary artery bypass 	<p>Advantages</p> <ul style="list-style-type: none"> • Faster recovery • Shorter hospital stay • No anesthesia • Maintain future revascularization options • Preserves autologous grafts (i.e. saphenous vein) • Repeatable • Can be combined with surgery <p>Disadvantages</p> <ul style="list-style-type: none"> • Lower patency rates • Reintervention due to restenosis is common • Limited in complex lesions

Figure 1.4: Surgical bypass and percutaneous transluminal angioplasty revascularization procedures are compared.

Undeniably, endovascular approaches have become increasingly popular over the past 20 years due to simplicity and continued advancements in surgical technology. Percutaneous transluminal angioplasty (PTA) is a minimally invasive endovascular procedure commonly administered in the treatment of PAD. PTA involves the utilization of a catheter-guided balloon that is inflated at the atherosclerotic lesion site, pressing the plaque into the artery wall in order to expand the arterial lumen for revascularization.²¹ Sometimes, stenting, or the implant of a metallic mesh tube, is used after PTA to hold the artery open after lesion repair. In other cases, an atherectomy is performed in conjunction with PTA to remove or de-bulk plaque components at the lesion site with the aid of a mechanical blade or laser. PTA with or without stenting is associated with shorter recovery times and lower costs for the patient, and preserves downstream surgical revascularization options that may be needed for coronary interventions.²²

I.3 Restenosis – Vessel Response to Injury

Restenosis is the arterial response to injury that is incurred during surgical and endovascular procedures. In a clinical setting, restenosis is typically defined as a loss of greater or equal to 50% of the luminal diameter gain produced by surgical intervention observed in follow-up angiography.¹² Despite advances in biotechnology and pharmacological treatments, late-vessel restenosis remains a consistent complication in all interventions designed to treat atherosclerotic lesions. Restenosis also occurs at sites of anastomosis in surgical bypass grafts, and is a leading cause of graft failure. However, restenosis is more prevalent after percutaneous interventions due to the mechanical injury inherent in PTA procedures.²³ Elimination of restenotic development would alleviate most complications associated with percutaneous interventions, thus, reducing the demand for open surgery. For this reason, the focus of this dissertation is directed towards restenosis as a result of PTA-induced vascular injury.

I.3.1 Intimal Hyperplasia in a Balloon Injury Model

In every form of percutaneous intervention, vascular injury is unavoidable due to the inherent stress and mechanical stretch placed on the vessel wall during balloon inflation. This surgically-induced damage is characterized by denudation of the *intimal layer* comprised of VECs, exposing the underlying subendothelial matrix and VSMCs to hemodynamic flow. An inflammatory cascade ensues, marked initially by platelet adhesion and leukocyte infiltration into the injured vessel wall. This ultimately triggers VSMC migration and proliferation into the *intima*, leading to a gradual thickening of the vessel wall known as intimal hyperplasia (IH; Fig 1.5).²⁴

‘Intimal hyperplasia’ literally is defined as an increase in the number of cells in the *intima*. As a clinical term, IH also refers to the simultaneous increase in ECM components and VSMCs

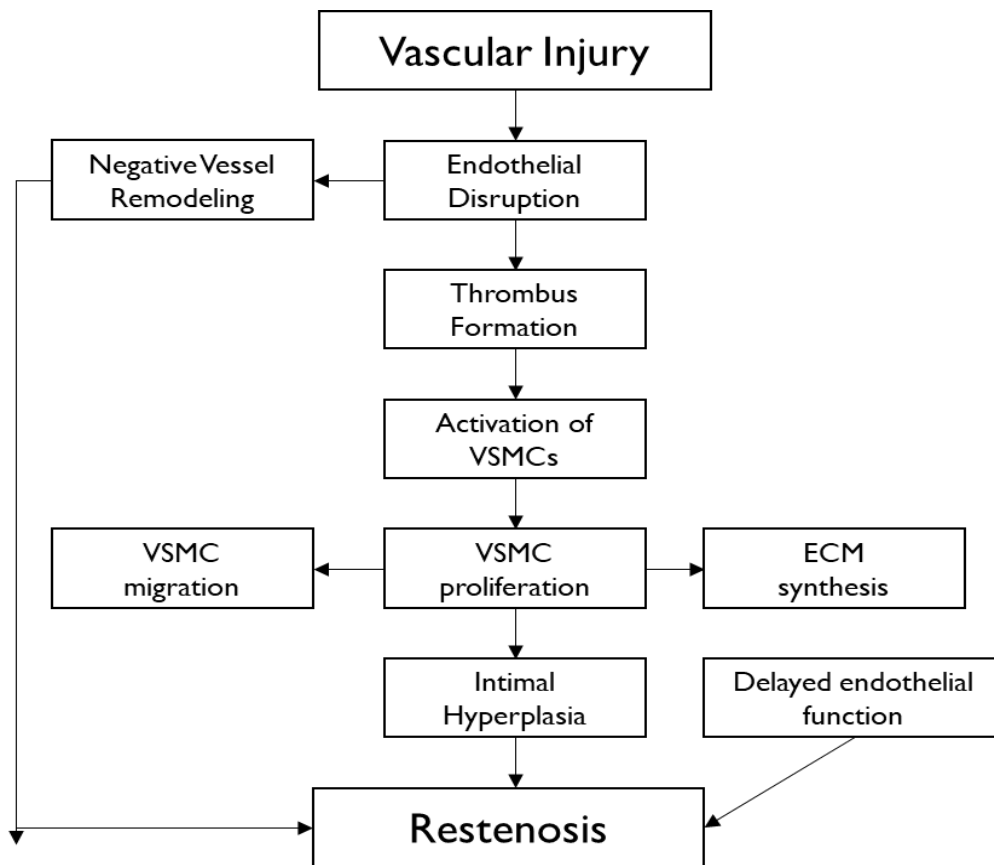


Figure 1.5: Diagram of major events in the development of IH-induced restenosis in response to vascular injury commonly seen in PTA procedures.

that leads to intimal distortion and reduced vessel lumen diameter. In the case of balloon injury in PTA, the atherosclerotic plaque is crushed, ruptured, and dislocated, as the entire vessel wall is mechanically stretched. Platelets contribute to release of basic fibroblast growth factor (bFGF) and platelet-derived growth factor (PDGF) within the vessel wall. These growth factors, along with transforming growth factor beta (TGF- β 1) and angiotensin, promote VSMC migratory and proliferative expansion into the *intimal layer*. PDGF and bFGF also enhance the expression of MMPs, or proteolytic enzymes capable of degrading the ECM near the cell surface, which further potentiates the migratory capacity of VSMCs.²⁵ Recent literature has also confirmed that VEC preservation and regeneration in response to balloon injury is crucial to mitigating VSMC dysfunction. This is possibly due to nitric oxide (NO) production by resident VECs. Long-term success without development of restenosis is unattainable when accompanied by delayed endothelial recovery.²⁶

1.3.2 Timeline of IH-associated Restenosis after Balloon Injury

Stage I – During a PTA procedure with or without stenting, the endothelium is denuded, exposing the subendothelial matrix and VSMC medial layer. Activated platelets immediately begin to adhere to injury site, which promotes fibrinogen deposition. This leads to a preliminary fibrin-rich thrombus.

Stage II – Thrombosis (48-72 hours): In the days following surgery, thrombus formation begins to accelerate. Red blood cells aggregate at platelet-rich mass forming fibrin/erythrocyte complex. The inflammatory process is exponentiated with an upregulation in cytokines, such as MCP-1, IL-6, and IL-8. As a result, leukocytes, including neutrophils and macrophages, are recruited to the initial injury site.

Stage III – Recruitment Phase (1st week): Monocyte infiltration continues to intensify at subendothelial thrombus site. Monocytes differentiate into macrophages within the vessel wall. Immune cell infiltration and local vascular cells begin to release large number of growth factors such as bFGF, PDGF, TGF- β , and vascular endothelial growth factor (VEGF). This increase in growth factor expression is concomitant with increased MMP expression. Exposed VSMCs begin to change from a quiescent phenotype into a synthetic, proliferative phenotype.

Stage IV – Proliferative Phase (1-4 weeks): VSMC residency within the intima continues to increase. This leads to inward growth of the vessel wall, known as negative remodeling, which decreases lumen diameter. The intimal layer at the injury site begins to transition from a mural thrombus into a lesion comprised mostly of neointimal cells.

Stage V – Restenosis (5-12 weeks): ECM deposition accumulates in the intimal layer due to dysfunctional MMP expression. Proliferation and migration of VSMCs will continue until endothelial layer is healed, and inflammatory cascade is halted.

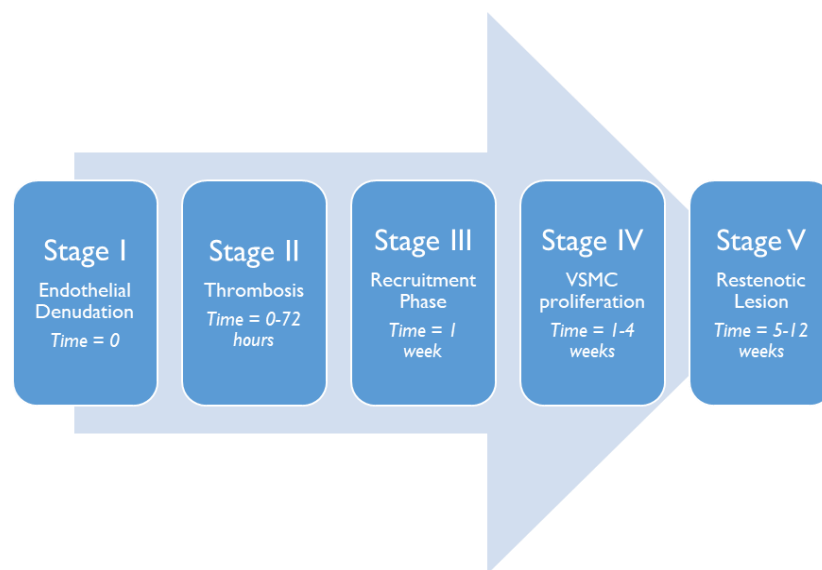


Figure 1.6: Staged development of Intimal Hyperplasia development after PTA-induced injury.²⁷

I.3.3 Novel Therapeutic Strategies to Prevent PTA-induced Restenosis

There have been several therapeutic strategies developed to mitigate the hyperplastic response and negative remodeling associated with PTA. Most therapeutic interventions are aimed at reducing the uncontrolled proliferation of VSMCs after vessel injury. Recently, the use of coated devices to deliver pharmacologics locally to injury site has increased. This typically comprises a combinatorial approach that fuses antiproliferative pharmacology with drug-eluting devices (balloons and stents).²⁸ Other novel approaches include polymeric coated stents and balloons, endoluminal cryotherapy, and intravascular brachytherapy (IVBT).

The use of intravascular stents began in the 1990's as small mesh-metal conduits used to support diseased arteries once cleared of atherosclerotic lesions. Stenting with PTA procedures is geared towards the prevention of arterial dissection and elastic recoil induced after balloon injury. Unfortunately, restenosis is still a significant problem, which is sometimes delineated as in-stent restenosis (ISR).²⁹ Drug-eluting stents (DES) or balloons (DEB) that release antiproliferative agents into the vessel wall have shown promise in preventing IH-induced restenosis after PTA. DES and DEB technology often use anti-mitotic agents like paclitaxel and sirolimus, which are aimed at reducing neointima formation through overall reduction in VSMC migration and proliferation. Though DES and DEB have decreased acute restenosis and improved initial success rates of endovascular interventions, they still have a propensity to cause late stent thrombosis and delayed restenosis months or even years after surgery.³⁰ For this reason, many vascular surgeons are apprehensive in using DES or DEB due to adverse interactions between pharmacological agent and human tissue.

Polymer coatings have been used in conjunction with DEB and DES with the specific aim of mimicking the endothelial lining of the vessel wall. By creating a pseudo endothelial layer with a polymer coating, late vessel thrombotic complications can be prevented. However, clinical findings show that polymer-coated technology can upregulate genes related to inflammation, proliferation, thrombosis, and vasoconstriction.³¹ These unwanted effects can actually increase rates of restenosis, and have limited the efficacy of polymeric coatings in endovascular procedures. Current research in this area has moved to the production of biodegradable polymers, which could improve long-term efficacy of drug-eluting devices in the vasculature.

Endoluminal cryotherapy was developed in 2004 to combat late vessel restenosis associated with PTA. This therapeutic application involves the use of cold thermal energy in conjunction with balloon dilatation force. This process essentially “freezes” the vessel wall, altering elastin fiber behavior and promoting VSMC apoptosis, which reduces the overall VSMC contribution to the hyperplastic response.³² This therapeutic modality is very appealing to surgeons due to the fact that permanent implants are unnecessary. Even though primary patency rates have been encouraging in cryotherapy applications, further randomized-controlled trials are necessary to confirm long-term success as compared to traditional treatments.

IVBT involves the introduction of radiation to suppress VSMC proliferation and migration at the target lesion site. This strategy was originally tested in oncological applications but has recently been explored in vascular surgery. The theory behind the use of IVBT is that proliferating VSMC cells are more susceptible to radiation damage than normal cells.³³ Also, the arterial lesion induced by PTA is less prone to platelet adhesion and thrombus formation when exposed to IVBT radiation therapy. When combined with PTA, IVBT has shown a significant reduction in

restenosis rate at 6-month follow-up when compared to PTA alone. However, this beneficial effect disappears after 24 months. Further comparative analysis and clinical testing is required to determine the overall efficacy of this therapeutic modality.³⁴

The main drawback of these novel therapeutic strategies is that they only focus on the dysfunctional proliferation of VSMC in IH. Considering the non-specific nature of these modalities, endothelial recovery is typically compromised. As mentioned earlier, reendothelialization is essential to halting long-term neointima formation and thrombosis. An optimal preventative therapeutic strategy for restenosis after PTA should comprise a cell-type specific inhibition of migration and proliferation in VSMCs, while promoting intimal healing through VEC growth and recovery. The use of gene therapy to modulate expression of factors implicated in IH-induced restenosis in these primary cell types (VSMC vs. VEC) could provide a path to accomplishing this goal.

1.4 Gene Therapy

Gene therapy is the delivery of genetic material to a cell to correct, replace, augment, silence, mark, or edit the expression of genes implicated in the pathological presentation of disease. There are essentially three phases of gene expression that can be targeted for therapeutic intervention: transcriptional, post-transcriptional, and post-translational. Post-translational modifications are rarely used, and involve epigenetic changes to DNA to alter gene expression.³⁵ The most well-established form of gene modulation is the delivery of a deficient gene via a plasmid DNA (pDNA) vector. The plasmid DNA hijacks host cell transcription machinery once delivered inside the nucleus. Plasmids can be modified in bacterial hosts using recombinant DNA technology allowing the insertion of virtually any gene sequence. To provide

functionality for plasmid expression of therapeutic genes, bacterial gene sequences (i.e. prokaryotic origin of replication, antibiotic resistance markers, etc.) are required, which limits how small the double-stranded DNA molecule can be. Also, since pDNA molecules require the use of foreign bacterial sequences, adverse immunogenic responses are common *in vivo*, which has limited its translational success.³⁶

RNA medicine comprises a variety of nucleic acid structures including messenger RNA (mRNA), microRNA (miRNA), transfer RNA (tRNA), short-interfering RNA (siRNA), ribosomal RNA (rRNA), and short-hairpin RNA (shRNA).³⁷ The use of RNA therapeutics, or short oligonucleotides, has increased considerably due to the discovery of double stranded RNA-mediated interference (RNAi) by Fire and Mello in 1996.³⁸ RNAi methods utilize double-stranded siRNA to hijack normal cellular machinery within the cell to provide highly specific, post-transcriptional degradation of target mRNA. The small size (<30 nucleotide base pairs) of siRNA makes it easier to package RNAi technology within common vectors, such as liposomes and polymers, which can be modified for multifunctional potential. Also, unlike pDNA, siRNA is not required to enter the nucleus, and can be functionally deployed within the cytosol.

1.4.1 Mechanism of RNA Interference

The RNAi pathway begins when a long double-stranded RNA molecule is cut by an enzyme called Dicer to create a small nucleotide fragment between 21 and 25 nucleotides long. These small fragments represent what is known as siRNA, and can be directly introduced to the cell for improved therapeutic efficacy. These RNA fragments are then loaded into the RNA-induced silencing complex (RISC), which includes the Argonaute-2 protein (Ago-2). In this protein complex, the “passenger” strand of the siRNA molecule is removed by Ago-2

leading to activation of the RISC complex which now contains the single-stranded “guide” RNA molecule. This complexed “guide” RNA can now interact in a gene specific manner through complementary base-pairing with its mRNA target. Once bound to its target, the mRNA molecule is cleaved and degraded by the mature RISC complex before protein translation can commence.³⁹ In this way, the gene is effectively silenced, which reduces overall expression at the post-transcriptional level. The mechanism of action of RNAi is illustrated in Figure 1.7.

1.4.2 siRNA Targets in the Treatment of Intimal Hyperplasia

The use of siRNA to silence genes that contribute to neointima formation have been investigated. Potential targets include growth factors like TGF- β 1, connective tissue growth factor (CTGF), and insulin-like growth factor (IGF-I) to reduce VSMC proliferative cascade within the injury site. Angiotensin II (AngII), a potent vasoconstrictor and contributor to vascular remodeling in IH, can be targeted to reduce VSMC growth response to injury. Mitotic promoters such as C-myc can be inhibited to similarly downregulate VSMC contribution to neointima formation. Immune mediators such as toll-like receptor 4 (TLR4) and Nuclear factor kappa β (NF- κ) are common siRNA targets in IH that have been shown to contribute to dysregulation of the inflammatory response in vascular injury. MMPs are of particular interest as gene therapy targets due to their contribution to ECM remodeling and VSMC migration within the *intimal layer*.⁴⁰ Our group has shown that, with the use of siRNA, the inhibition of membrane type 1 metalloproteinase (MT1-MMP) is effective in reducing overall MMP activity and corresponding VSMC migration and proliferation *in vitro*.⁴¹ There are many other potential targets implicated in IH development, but the primary hurdle to an adequate gene therapeutic with translational efficacy is the delivery mechanism. The development of a gene vector that can provide enhanced

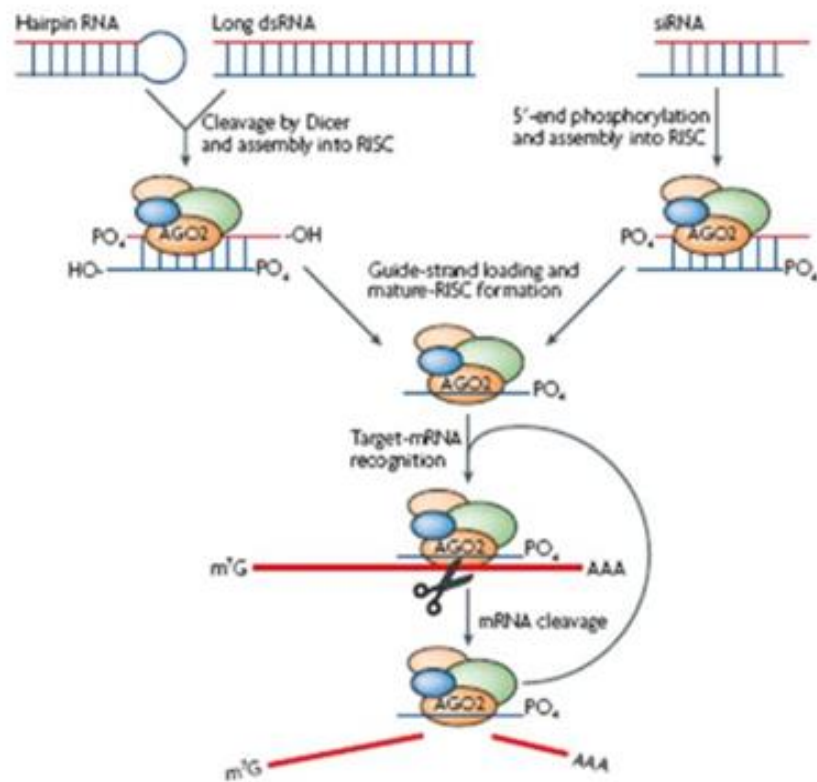


Figure 1.7: Mechanism of RNAi. DICER cleaves long dsRNA produce siRNA molecule, or synthetic siRNA is directly introduced into cell. siRNA is loaded into RISC complex, where Ago-2 removes “passenger” strand from siRNA molecule. Mature RISC complex uses remaining “guide” strand to target gene-specific mRNA. Target mRNA is cleaved and degraded by mature RISC complex before translation. Adapted from Patenting Interfering RNA (Slide 4), by J. D. Schultz.

pharmacokinetics and cellular uptake, biocompatibility, low toxicity, and targeted delivery within the vasculature is required.

1.5 Gene Delivery

The delivery of naked RNA or DNA across the cell membrane is generally inefficient due to hydrophilic character and molecular instability. To accomplish functional gene transfer, a carrier, or gene vector is required. Generally, a suitable vector system will include extracellular targeting and delivery minus unwanted off-site effects. Gene vectors can be given to a patient directly (*in vivo*) or to cells that have been extracted and maintained in culture conditions (*ex vivo*). Vectors are typically classified as viral or nonviral vectors and the most common vectors are shown in Figure 1.8.

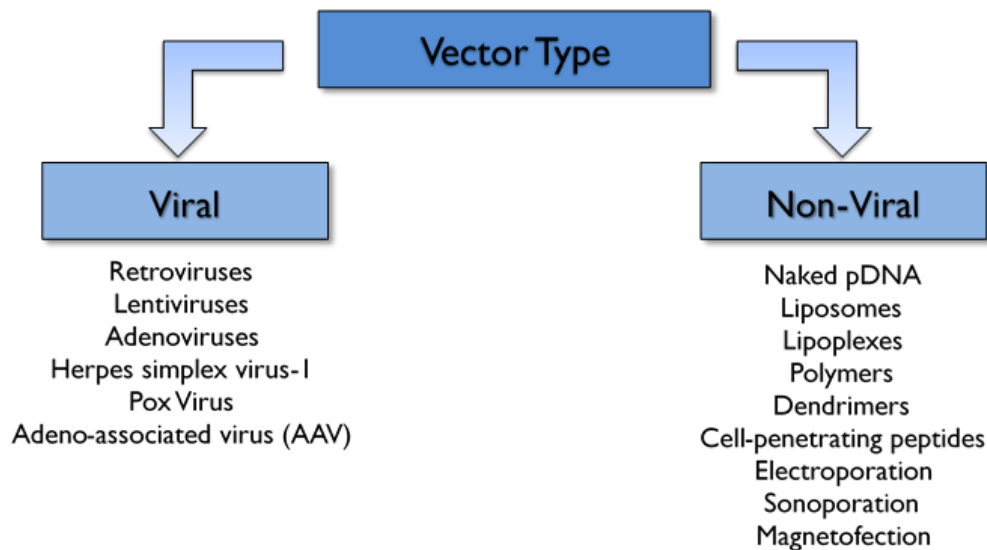


Figure 1.8: Comparison of commonly used viral and nonviral vectors.

The first approved gene therapy techniques utilized viral vectors to incorporate therapeutic genes into cells. Viruses are popular gene vectors due to their inherent ability to invade cells and deliver nucleic acid cargo into the cellular genome. The most common viral vectors are derived from lentiviruses, retroviruses, adenoviruses, and adeno-associated viruses (AAV). Herpes simplex virus-1 and Pox virus have shown some success *in vitro*, but are less commonly used.⁴² Regrettably, viral vectors exhibit toxicity in many cases, and can be highly immunogenic and unpredictable. The use of many classes of viral vectors is limited in repeat applications due to increased immune response, which limits overall therapeutic efficacy. Also, particularly with lentiviral and retroviral applications, insertional mutagenesis is a common problem, which can exacerbate other medical issues.⁴³ To reduce immunogenic and toxic effects associated with viral vectors, non-viral approaches have been investigated extensively.

Nonviral vectors are generally classified into three categories: (a) naked DNA delivery, (b) polymer-based delivery (c) and lipid-based delivery. The use of pDNA is an intriguing nonviral vector due to its simplicity and ease of production in bacteria. Therapeutic pDNA molecules can be manipulated using established recombinant DNA techniques to express specific genes of interest. Once injected to the target site, it rarely disseminates to distant sites of the body and does not typically induce antibodies against itself.

Physical methods can also be used to enhance the delivery of naked DNA locally. Electroporation is a method that uses short bursts of high voltage aimed at the target site to carry DNA across the cell membrane via temporary pore formation. Unfortunately, electroporation is associated with high rates of cell death, and its clinical potential is limited. Similarly, sonoporation uses ultrasonic frequencies to deliver nucleic acid into cells, but has shown

inconsistent results. DNA and RNA can also be complexed with magnetic nanoparticles. In a process known as magnetofection, a magnet is used to attract these complexes to the tissue site of interest. Even though advancements have been made in physical methods to aid naked nucleic acid transfection, unprotected forms of nucleic acid are generally unstable and have limited application without a delivery vehicle to mitigate nuclease and oxidative degradation.⁴⁴

Polymeric vectors are often comprised of nucleic acid complexed with polycationic molecules in what is otherwise known as polyplexes. Some examples of polycationic polymers used in gene therapy include poly(L-lysine), poly(L-ornithine), both linear and branched polyethyleneimine (PEI), poly(amidoamine) dendrimers, and poly(dimethylaminoethyl methacrylate). These molecular carriers typically contain positively charged amine groups, and therefore form electrostatic complexes with negatively charged nucleic acid molecules.⁴⁵ These “polyplexes” carry an overall positive charge that enhances its association with cell membranes, where it eventually becomes endocytosed within an endosome. Once inside the cell, the positively charged amino groups and reduced pH contribute to increased osmotic potential and subsequent endosomal release within the cytosol. Even though polymeric gene transfer has allowed us to understand feasibility and efficacy of gene therapy candidates, *in vivo* success is limited due to systemic toxicity and rapid clearance by the reticuloendothelial system (RES) and mononuclear phagocytic system (MPS) located primarily in the blood, liver, and spleen.

1.5.1 Introduction to Liposomes

Since their original observation by Alec Bangham over 40 years ago, liposomes have emerged as the most common nanocarriers for drug delivery applications.⁴⁶ Liposomes can be defined as a discrete internal aqueous compartments surrounded by a phospholipid bilayer. The

phospholipid bilayer mimics the cellular membrane and, therefore, exhibits high biocompatibility and low toxicity. Also, liposomes have the ability to encapsulate both hydrophobic and hydrophilic drugs unlike most other pharmacological nanocarriers. Liposomes are generally simple to make due to their innate ability to self-assemble, and exert a wide range of physiochemical and biophysical properties that can be altered to control and accentuate *in vitro* and *in vivo* delivery performance.⁶ The most intriguing feature of liposomal vectors is their flexibility of modification and multifunctional potential, which could allow for enhanced therapeutic index and reduced off-site effects. These liposomal characteristics provide numerous advantages compared to other gene vectors, which are listed in Figure 1.9.

Our improved understanding of pharmacokinetic properties and modification techniques with liposomal vectors has led to hundreds of successful *in vivo* studies. Unfortunately, the bench-to-bedside success has progressed much slower than the flux of successful preclinical research. Figure 1.10 illustrates the exponential increase of published papers related to liposomal drug delivery along with the sparse sum of FDA-approved liposomal drugs. This discrepancy is even more intense when only considering liposomal gene vector applications.

Liposomes can be classified into 4 types of liposomal delivery systems (LDS): 1) Conventional liposomes, 2) Sterically-stabilized liposomes, 3) Ligand-targeted liposome, and 4) Multifunctional liposomes. Conventional liposomes are typically comprised of phospholipids and cholesterol in a bilayer that wraps the aqueous core. Conventional liposomes successfully improved the pharmacokinetics of doxorubicin and amphotericin in the 1980's. Traditional liposome formulations are simplistic in nature, and could be directly correlated to a reduction in toxicity and improved pharmacokinetic profile when compared to free drug alone. Unfortunately,

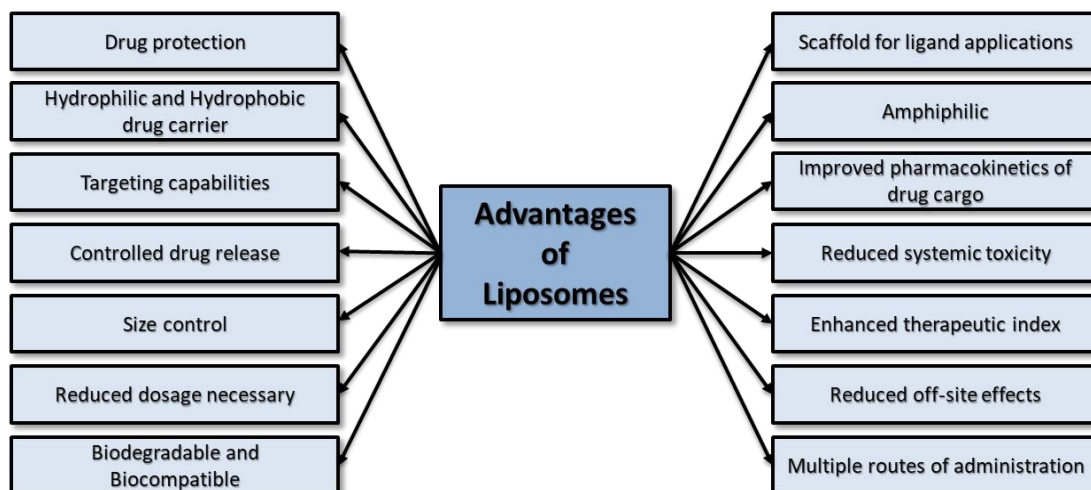


Figure 1.9: Advantages of liposomes as pharmaceutical nanocarriers in medicine.

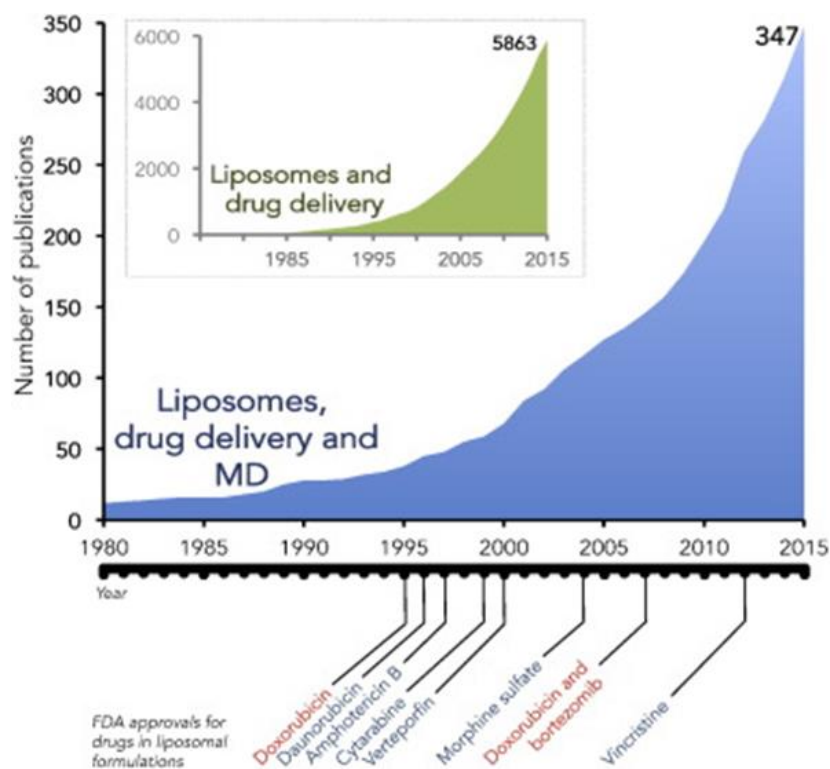


Figure 1.10: Graphical illustration showing exponential growth of liposome-related publications in medicine as well as the use of computational modeling in developing liposomal drugs. This contrasted with the small number of approved therapies. Adapted from “Rational design of liposomal drug delivery systems, a review: Combined experimental and computational studies of lipid membranes, liposomes and their PEGylation,” by A. Bunker, A. Magarkar, and T. Viitala, 2016, *Biochimica et Biophysica Acta*, 1858(10), p. 2337. Copyright 2016 by Elsevier.⁴⁷

conventional liposomes are subject to rapid clearance due to complement activation, opsonization, and macrophage uptake of the RES within the liver and spleen and are rarely used in translational models.⁴⁸

To improve pharmacokinetics of conventional liposomal cargo, sterically stabilized liposomes were created. Surface-linked polyethylene glycol (PEG) has proven to be the most optimal method for stabilizing conventional liposomes *in vivo*. These so-called PEGylated liposomes have a steric barrier that produces an aqueous cage around the lipid nanoparticle that inhibits complement activation, opsonization, and RES clearance. The steric effect of the PEG shell helps to prolong circulation half-life of liposomal constituents, whereby more drug can reach its target. Due to the observed ability of these PEGylated liposomes (PLPs) to evade clearance from circulation, sterically-stabilized liposomes are often referred to as “Stealth” liposomes, and have been shown to passively accumulate in leaky vasculature of tumor sites due to enhanced retention and permeation effect (EPR).⁴⁹ Regrettably, the introduction of PEG on the liposome surface also reduces cellular uptake of liposomal cargo in what is known as the “PEG dilemma”. To improve delivery of PLPs, the addition of cell-penetrating peptides (CPPs), such as arginine-rich peptides (i.e. octaarginine; R8), on the liposome surface is commonly employed.⁵⁰

The addition of PEG to LDS has also provided a polymeric scaffold to attach functional ligands on the liposome surface. This offers the potential to target LDS to specific disease sites in the body. These ligands include peptides, carbohydrates, and antibodies. Specifically, the conjugation of antibodies (i.e. immunoliposomes) with cell- or tissue-specific binding affinity has expanded the research area of targeted liposome delivery. However, immunoliposomes still exhibit high levels of immunogenicity and poor pharmacokinetics seen in conventional liposomes

and viral vectors. It may be appropriate to elucidate peptides or peptide fragments that exhibit similar binding affinity and specificity of antibody counterparts. The integration of these technologies has led to the development of multifunctional liposomes. For instance, the incorporation of PEG into immunoliposomes has improved pharmacokinetics of antibody-targeted LDS. There are a variety of technologies that can be incorporated into liposomes as shown in Figure 1.11, and the combinatorial possibilities are numerous.

1.5.1.1 Liposomal Gene Therapy

Liposomes are the most widely investigated nonviral gene vectors due to their biocompatibility and unique ability to encapsulate and protect nucleic acids within an aqueous environment. Liposomes have been successfully combined with a wide range of nucleic acid therapies including siRNA, pDNA, miRNA, and modern gene-editing systems. The first liposomal vectors were assembled using neutral phospholipids like 1,2-Oleoyl-sn-Glycero-3-phosphocholine (DOPC) and 1,2-Dioleoyl-sn-Glycero-3-phosphoethanolamine (DOPE). Neutral liposomes enhance the pharmacokinetic capacity and physical stability of nucleic acid delivery, and were eventually shown to produce significant siRNA-mediated silencing in cancer cells *in vivo*. However, the long-term translational success of this liposomal paradigm is limited due to low levels of transfection and limited encapsulation efficiency nucleic acid cargo.

Soon, synthetic cationic lipids like 1-oleoyl-2-[6-[(7-nitro-2-1,3-benzoxadiazol-4-yl)amino]hexanoyl]-3-trimethylammonium propane (DOTAP) were created to help improve nucleic acid load and cellular uptake of liposomal cargo. The encapsulation efficiency of cationic liposomes (CLP) is improved due to the electrostatic complexation of negatively charged nucleic acid with positively charged lipids like DOTAP. The overall positive charge of the fully assembled

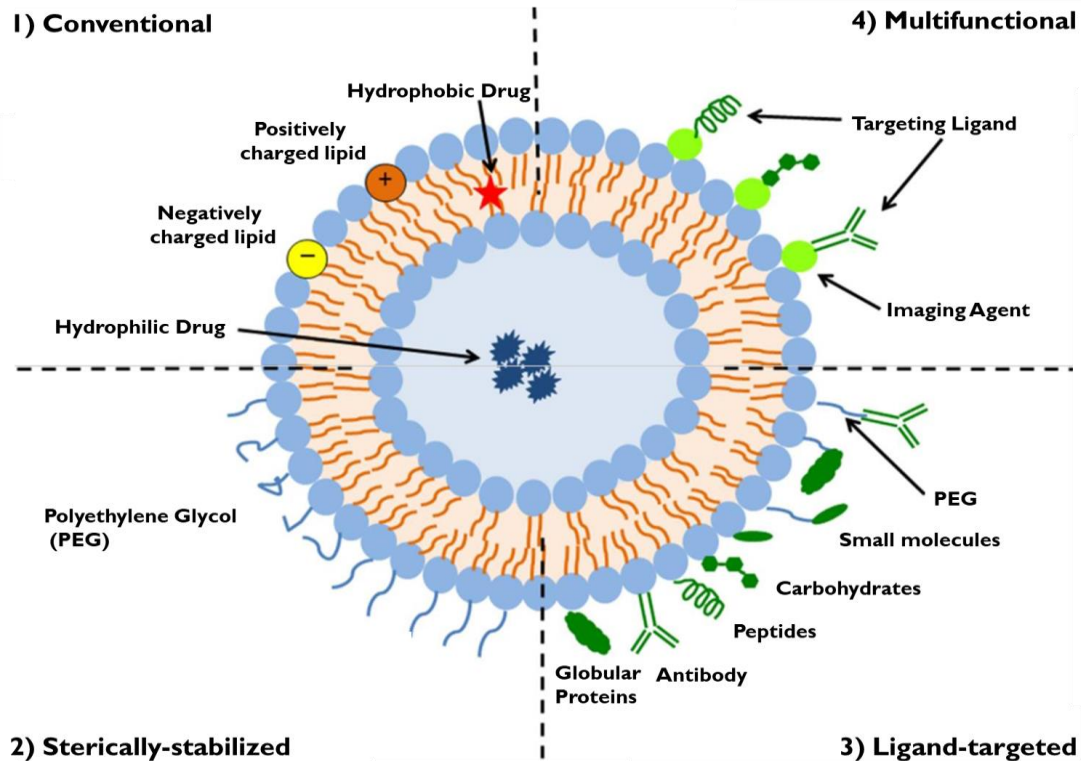


Figure 1.11: Schematic representation of different classifications of LDS capable of encapsulating hydrophilic and hydrophobic drugs. 1) Conventional liposomes have a phospholipid bilayer comprised of charged or neutral lipids and cholesterol. 2) Sterically-stabilized, or PEGylated, liposomes improve pharmacokinetic characteristics of LDS in vivo. 3) Ligand-targeted liposomes incorporate ligands onto liposome surface or PEG chains to confer targeting capacity. 4) Multifunctional liposomes can consist of a multitude of ligand applications which includes imaging agents, targeting ligands, and PEGylation. Adapted from “Ligand-targeted liposome design: challenges and fundamental considerations,” by G. T. Noble, et al., 2014, Trends in Biotechnology, 32(1), p. 34. Copyright 2014 Elsevier.51

CLP, or lipoplexes, provides enhanced cellular uptake of nucleic acid cargo due to cellular association with negatively charged cell membranes.⁵² However, the charged nature of CLPs results in unwanted interactions with serum proteins and rapid RES clearance *in vivo* compared to neutral liposomes and PLPs. Also, CLPs comprised of synthetic lipids induce cytotoxicity *in vitro* and *in vivo*, and can lead to adverse inflammatory effects. To improve the translational potential of liposomal gene vectors, further investigation of the assembly and application of noncationic liposomes is required.⁵³ Figure 1.12 illustrates the lipid classes we used within this dissertation project, along with nomenclature and chemical structure, to provide comparative analysis and assembly parameters for development of noncationic liposome platform.

1.6 Research Summary

PTA procedures inherently cause mechanical injury to the vessel marked by denudation of VECs within the *intimal layer*. This exposes the underlying *medial layer* of the vessel to hemodynamic flow. An acute inflammatory response is triggered through platelet adhesion to the sub-endothelial matrix, followed by monocyte attachment and infiltration of the vessel wall. This acute inflammatory response stimulates dysfunctional migration and proliferation of VSMCs into the *intimal layer* leading to a gradual thickening of the vessel wall known as IH. Chronic vessel diameter reduction ensues, clinically referred to as restenosis, eventually requiring surgical revascularization with increased morbidity rates. Most therapeutic interventions for IH-induced restenosis are aimed at attenuating VSMC proliferation at the site of the treated lesion. This approach has been successful in reducing acute intimal thickening. However, chronic restenosis still occurs in an estimated 60% of patients at 12-month follow-up due to the concomitant inhibition of VEC recovery inherent in anti-proliferative interventions.⁵⁴ We postulate that a

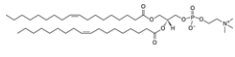
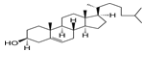
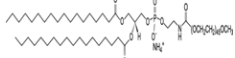
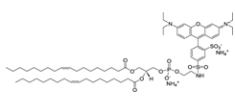
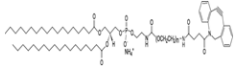
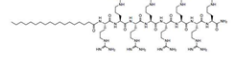
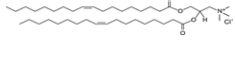
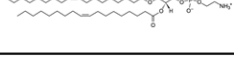
Lipid	Abbreviation	Structure	Molecular Weight (g/mol)	Lipid Type
1,2-dioleoyl-sn-glycero-3-phosphocholine	DOPC		786.113	Natural Phospholipid
cholesterol (ovine wool, >98%)	Chol		386.654	Natural Sterol
1,2-distearoyl-sn-glycero-3-phosphoethanolamine-N-[methoxy(polyethylene glycol)-2000] (ammonium salt)	DSPE-PEG		2805.497	Sterically-stabilized Phospholipid
1,2-dioleoyl-sn-glycero-3-phosphoethanolamine-N-(lissamine rhodamine B sulfonyl) (ammonium salt)	Rho-PE		1301.715	Fluorescent Phospholipid
1,2-distearoyl-sn-glycero-3-phosphoethanolamine-N-[dibenzocyclooctyl(polyethylene glycol)-2000] (ammonium salt)	DSPE-PEGdbco		3077.798	Sterically-stabilized Phospholipid (activated for click reaction)
Stearylated Octaarginine	STR-R8		1533.01	CPP-modified fatty acid
1,2-dioleoyl-3-trimethylammonium-propane (chloride salt)	DOTAP		698.542	Cationic Lipid
1,2-dioleoyl-sn-glycero-3-phosphoethanolamine	DOPE		744.034	Natural Phospholipid

Figure 1.12: Listing of lipid classes used in dissertation with associated nomenclature and structure.

targeted drug delivery scheme, designed to inhibit VSMC migration and proliferation while simultaneously enhancing VEC recovery, could prove to be an optimal therapeutic strategy in the treatment of chronic IH-induced restenosis in a surgical model.

1.6.1 Specific Aims

PLPs have proven to be promising drug delivery agents due to high biocompatibility, increased half-life *in vitro* and *in vivo*, and high degree of flexibility. Specifically, CPPs are short peptides that can provide enhanced cellular uptake of biomolecular cargo by temporarily perturbing the cell membrane, leading to direct translocation through the phospholipid bilayer. Similarly, cell-targeting peptides (CTP) have been conjugated to liposome surfaces to mediate cell-type specific delivery. Dual-ligand strategies have been developed for multiple disease pathologies that employ both CPP and CTP for synergistic cell selectivity and enhanced cytosolic delivery of gene therapeutics.⁵⁵ There are two specific aims of this dissertation:

- 1) We aim to develop a CPP-modified PLP (CPP-PLP) with efficient siRNA encapsulation and functionally enhanced transfection capacity in vascular cell types.

Hypothesis: An effective noncationic CPP-PLP will provide a liposomal vector with reduced cytotoxicity and greater translational potential for *in vivo* applications in the vasculature.

- 2) We aim to incorporate previously established CTP fragments, specific for VSMC and VECs, onto lipid surface via click chemistry techniques to impart cell-type specificity of noncationic PLP assemblies in primary vascular cell types.

Hypothesis: The development of a cell-type specific PLP (CTP-PLP), equipped with VSMC-specific and VEC-specific functional motifs, will provide a drug delivery vehicle capable of differentially targeting vascular cell types for siRNA delivery.

CHAPTER 2: The Scalable Assembly of Noncationic PEGylated Liposomes with Octaarginine-potentiated siRNA Encapsulation

The following chapter is currently under consideration for publication in a peer-reviewed manuscript format. We anticipate publication of this material at a future date.

2.1 Introduction

Ribonucleic acid interference (RNAi) is a biological process that inhibits the post-transcriptional expression of mRNA in the cytoplasm of eukaryotic cells. The gene-specific nature of small-interfering RNA (siRNA), an active biological molecule of RNAi, provides a therapeutic avenue for silencing abnormal or unwanted gene expression often exemplified in vascular disease, cancers, and other rare genetic disorders. However, siRNA is vulnerable to enzymatic degradation *in vivo*, and lacks the ability to traverse cell membranes due to large molecular weight and hydrophilic properties. Therefore, the issue of delivery remains a primary hurdle to clinical application of siRNA therapeutics.

Liposomes are the most widely studied nonviral gene vectors, with the ability to encapsulate nucleic acid cargo within an aqueous compartment, protecting it from the external environment.⁵⁶ Many multifunctional modification strategies aimed at improving the clinical efficacy of liposome-mediated gene therapy have been elucidated.⁵⁷ This includes the incorporation of polyethylene glycol (PEG) on the surface, resulting in PEGylated liposomes (PLPs) with increased stability and half-life of siRNA cargo *in vivo* (2nd generation liposomes),^{58,59} and the development of ligand-conjugated liposomes for enhanced cell uptake and targeted drug delivery (3rd generation liposomes).^{60,61} The use of cationic lipids in liposomal formulations (CLPs) has helped improve encapsulation of negatively-charged nucleic acid cargo through the electrostatic-mediated “lipoplexes”.⁶² However, many synthetic, “unnatural” cationic lipids are associated with cytotoxicity through toll-like receptor activation,⁵³ mitochondrial membrane

disruption⁶³, and induction of reactive oxygen species.⁶⁴ Due to the cytotoxic effects of cationic liposomes, along with rapid opsonization and macrophage clearance, translational success of CLP-mediated gene therapy has been limited despite approval of numerous Phase I clinical trials.⁴⁸ An alternative strategy would be constructing nucleic acid lipoplexes with “natural” noncationic lipids in the presence of divalent cations (i.e. calcium; Ca^{2+}), whereby electrostatic bridging between the phosphate backbone of nucleic acid and the zwitterionic phospholipid head group enhances nucleic acid loading during self-assembly.⁶⁵ However, inadequate cell uptake of standard PLP assemblies has limited basic science investigations using noncationic lipid formulations.⁶⁶ Cell-penetrating peptides (CPPs) have been incorporated into PLP bilayers to promote membrane translocation of liposomal cargo and subsequent cellular uptake.^{50,67} Unfortunately, due to their inherent membrane perturbation, the incorporation of CPP-amphiphiles into PLP formulations often results in cargo leakage and heterogeneous size dispersity as a result of aggregation.⁶⁸ Consequently, most of the techniques used to assemble CPP-modified PLPs with siRNA or other nucleic acid cargo are inefficient and costly.

Using octaarginine (R8), a well-established CPP,⁶⁹ we aimed to elucidate optimal process parameters required to assemble noncationic, CPP-modified PLPs with efficient siRNA loading and functionally enhanced transfection capacity. Modification strategies for incorporating R8 into non-cationic PLPs (R8-PLP) were surveyed to empirically derive an assembly method that maximizes siRNA retention and encapsulation efficiency (EE%), and produces liposomal nanoparticles with critical quality attributes necessary for *in vivo* translation (Table 2.1). This strategy could provide the ground-breaking advancement required to augment bench-to-bedside success of liposomal-based RNAi technology.

Table 2.1: Quality by design approach which provides established criteria, or CQAs, required for effective systemic administration of liposomal drug delivery systems.

Quality by Design Experimental Approach		
Critical Quality Attribute (CQA)	Units Measured	Desired Range
Encapsulation Efficiency (EE%)	mol% siRNA	>50%
Zeta Potential (ζ)	millivolts (mV)	<10 mV
Average Size	diameter (d.nm)	< 100 nm
Polydispersity Index (PDI)	N/A	<0.2

2.2 Materials and Methods

2.2.1 PLP Assembly via Ethanol Injection Technique

Liposome Constituents

All liposome formulation constituents are defined in Table 2.2. Lipids and cholesterol were purchased from Avanti Polar Lipids (Alabaster, AL, USA). Custom R8 peptide was purchased with an azido-modified lysine (RRRRRRRRK(N3)-NH₂) from P3 Biosystems (Louisville, KY, USA). STR-R8 was purchased from LifeTein LLC (Somerset, NJ, USA). GAPDH siRNA was purchased from ThermoFisher Scientific (Waltham, MA, USA).

Liposome Assembly

Base PLP nanoparticles were formed with bulk lipid DOPC:chol at 7:3mol plus 10mol% DSPE-PEG, and were assembled using a previously described EtOH injection technique.⁷⁰ Briefly, lipids were dissolved in CHCl₃, combined as indicated, and dried under N₂ gas and vacuum to remove remaining solvent. Dried lipids were then resuspended in molecular grade 100% EtOH. GAPDH siRNA at 20-50ug/300uL 10mM Tris-HCl, pH 8.0 with 0-50mM CaCl₂ was injected with 200-5,000ug total lipid/200uL 100% EtOH, under constant vortexing at room temperature (RT).

Table 2.2: Bulk lipid constituents that comprise the liposome formulations used in this study. The appropriate acronyms are listed for reference.

PLP Formulation Components	
Lipid Constituent	Acronym
1,2-dioleoyl-sn-glycero-3-phosphocholine	DOPC
cholesterol	chol
1,2-distearoyl-sn-glycero-3-phosphoethanolamine-N-[amino(polyethylene glycol)-2000]	DSPE-PEG
1,2-distearoyl-sn-glycero-3-phosphoethanolamine-N-[dibenzocyclooctyl(polyethylene glycol)-2000]	DSPE-PEGdbco
1,2-dioleoyl-sn-glycero-3-phosphoethanolamine-N-(lissamine rhodamine B sulfonyl) octaarginine (RRRRRRRK(N3)-NH2)	Rho-PE R8

Liposomes were purified from EtOH and un-encapsulated siRNA via 24hr dialysis against PBS, pH 7.4 at 4 °C. Liposomes were extruded using 100nm polycarbonate NanoSizer™ extruders from T&T Scientific prior to characterization (Knoxville, TN, USA).

2.2.2 CPP Modification via R8 Amphiphile Incorporation

R8-PEG Synthesis

DSPE-PEGdbco, a form of DSPE-PEG with a cyclooctyne modification commonly used in azide-alkyne cycloaddition reactions (i.e. click chemistry), was used to form R8-PEG amphiphiles for PLP incorporation via pre- and post-insertion. Briefly, equimolar azido-modified R8 peptides and DSPE-PEGdbco were combined at RT under constant agitation for 2hr, according to previously established reaction conditions.^{71,72} Mass spectrometry confirmed peptide conjugation and reaction efficiency (Fig. 2.1).

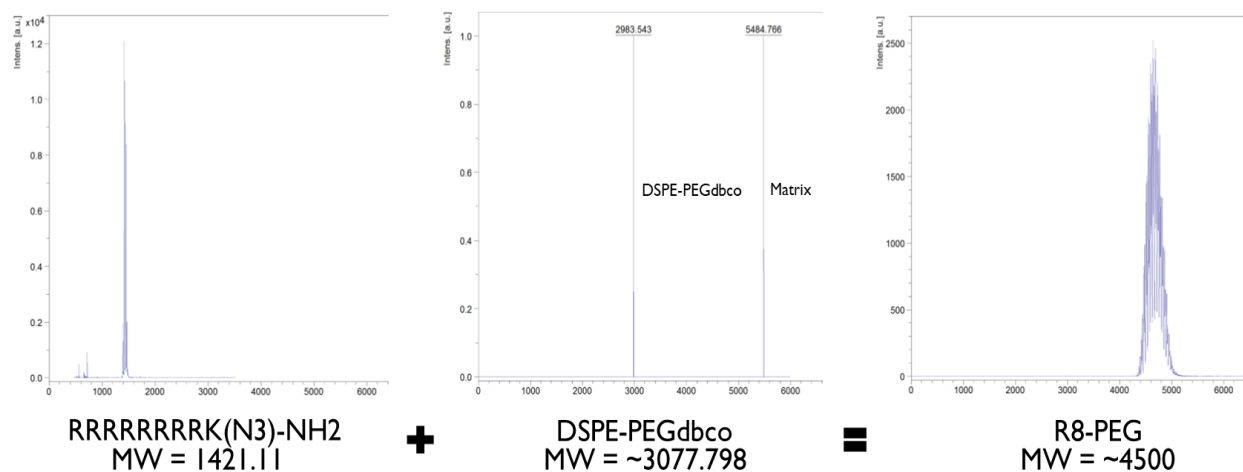


Figure 2.1: MALDI-TOF spectroscopy confirmation of successful “click” reaction used to conjugate azide-modified R8 with DSPE-PEGdbco using azide-alkyne cycloaddition.

Modification of R8-PEG or STR-R8

For all modification strategies, base PLPs were assembled via EtOH injection as described, and were modified by substituting DSPE-PEG or 7:3 DOPC/chol with R8-PEG or STR-R8 amphiphiles at equal mol%, respectively. In this way mol% PEG was kept constant across all conditions to control PEG-mediated membrane stability and assay encapsulate retention as a function of R8 modification alone.

Modification via Pre-insertion

R8-PEG or STR-R8 were combined at 1-10mol% with base PLP lipid constituents at the time of lipid drying under N₂ gas. Likewise, lipid hydration with EtOH was performed in one-step and all lipid constituents were incorporated at the time of initial liposome assembly. Liposomes were purified from un-encapsulated siRNA as described, prior to extrusion and characterization.

Modification via Post-insertion

Base PLPs were assembled as described without the incorporation of R8 amphiphiles. Following PLP purification by dialysis, R8-PEG or STR-R8 were combined with pre-formed base PLPs and incubated at 4°C overnight or 37°C for 4 hours, according to previously established conditions for lipid transfer. A second overnight dialysis was performed following R8-amphiphile insertion to remove any un-retained siRNA encapsulate, prior to extrusion and characterization.

Modification via Post-conjugation

Base PLPs were assembled as described, without the incorporation of R8, but with DSPE-PEGdbco added at the time of lipid drying. Following, purification by dialysis, azido-modified R8 peptides were added in an equimolar amount to DSPE-PEGdbco, and incubated at 4°C overnight or 37°C for 4 hours, according to previously established parameters of the azide-alkyne cycloaddition reaction. A second overnight dialysis was performed following R8 conjugation to remove any un-retained siRNA encapsulate, prior to extrusion and characterization.

2.2.3 Liposome Characterization Studies

Size, Homogeneity, and Charge Characterization

The mean size, associated polydispersity index (PDI), and zeta potential of all liposome preparations were measured by dynamic light scattering and relative electrophoretic mobility in water using the Zetasizer Nano ZS instrument (Malvern Instruments Ltd., Worcestershire, UK).

siRNA Encapsulation Efficiency (EE%)

The siRNA encapsulation and retention of all liposome preparations was determined using the Quant-iT RiboGreen RNA Assay Kit (Thermofisher Scientific). Following purification from un-

encapsulated and/or un-retained siRNA, liposomes were denatured and solubilized in 1% Triton X-100 at 37°C for 15min to release siRNA cargo. Released siRNA was mixed with RiboGreen reagent for fluorescent labeling, and emission was read at 525nm. Fluorescence units of solubilized liposomes was fit to a known standard curve of siRNA in 1% Triton X-100. EE% of each liposome formulation was calculated as (pmols siRNA encapsulate / original pmols siRNA used) x 100.

Gel Electrophoresis

The stability of siRNA-loaded liposomes was assessed using gel electrophoresis techniques. Stability assays were run using 4% agarose gels with 1ug/mL Ethidium Bromide (EtBr) and 1X Tris-Boric-EDTA (TBE) buffer for gel preparation and running. All siRNA bands were visualized by EtBr binding via transillumination through a GFP filter.

Gel Exclusion Assay

For a qualitative analysis of EE%, siRNA-loaded liposome sample aliquots were taken prior to purification by dialysis, and equal fractions were loaded onto agarose gels. Un-encapsulated, un-complexed siRNA, free in solution, was ran into gel at 50V for 30mins while liposomes with encapsulated/complexed siRNA were excluded from gel penetration and isolated to the wells. To examine total encapsulated siRNA and/or total lipoplexed siRNA, liposome samples were taken after purification by dialysis, exposed to 1% Triton X-100 and 100 ug/mL heparin to denature liposome nanoparticles and release all complexed siRNA, and equal fraction were loaded and ran as described.

Heparin Displacement Assay

siRNA-loaded liposomes from 100:1 lipid:siRNA wt-to-wt samples were exposed to varying concentrations of heparin (0-400 ug/mL) for 30 minutes at room temperature. Equal fractions were loaded onto agarose gels and displaced siRNA was ran into gel at 50V for 30 mins to determine minimum heparin concentration necessary for complete siRNA displacement from liposome surface. In follow-on experiments, to examine the proportion of lipoplexed siRNA that was outer associated and vulnerable to heparin displacement, liposome samples were taken after purification by dialysis, exposed to 100ug/mL heparin, and equal fractions were loaded and ran as described. To examine total encapsulated siRNA and/or total lipoplexed siRNA, liposome samples were taken after purification by dialysis, exposed to 1% Triton X-100 and 100 ug/mL heparin to denature liposome nanoparticles and release all complexed siRNA, and equal fractions were loaded and ran as described.

RNase Stability Assay

Free siRNA controls were exposed to varying concentrations of RNase A enzyme (0.001-100ug/ml) for 30mins at 37°C to determine minimum RNase necessary for complete siRNA degradation. In follow-on experiments, siRNA-loaded liposomes were prepared with and without the exposure to 0.5ug/mL RNase A, RNase digestion was stopped by flash freezing in liquid N₂, and liposome samples were exposed to 1% Triton X-100 and 100 ug/mL heparin to denature liposome nanoparticles and release all complexed siRNA. The protection of outer associated siRNA demonstrated via heparin displacement was validated by the protection from RNase enzyme degradation compared to the degradation of free siRNA controls.

2.2.4 Vascular Smooth Muscle Cell Culture

Human aortic smooth muscle cells (HASMCs) were obtained from LifeLine Cell Technology (Walkersville, MD) as cryopreserved primary cultures of 49yr old male single-donor cells. Cells were incubated at 37°C in an environment of 5% CO₂ and 95% humidity and grown in VasuLife growth medium (VasuLife Basal Medium + VasuLife smooth muscle cell supplement kit + gentamycin/amphotericin; LifeLine Cell Technology). Prior to experimental use, a quiescent state was induced using Dulbecco's Modified Eagle Medium (DMEM; ThermoFisher Scientific) + gentamycin/amphotericin overnight.

2.2.5 Cell Association Studies

To measure cell association, liposomes were assembled as described with the addition of Rho-PE at 0.5mol%. At ~80% confluency, HASMCs were treated with Rhodamine-labeled neutral PLPs and R8-PLP groups at 100uM total lipid in DMEM. After 30min and 24hr liposome exposure, cells were washed three times in PBS and qualitatively imaged by fluorescent microscopy. Images were acquired with a Texas Red fluorescent filter at 400X under 400msec exposure across all groups.

2.2.6 Statistical Analysis

All data are reported as mean \pm SEM. Statistical analyses were performed using Student's *t*-test or one-way ANOVA and a post-hoc Student-Newman-Keuls test using SPSS 25 software (Systat Software, Inc., San Jose, CA). Probability (*P*) values ≤ 0.05 were considered to be significant.

2.3 Results

2.3.1 Incorporation of R8-PEG via Pre-insertion, Post-insertion, and Post-conjugation Resulted in Significant siRNA Leakage and Reduced Total siRNA Retention.

Modification of neutral PLPs with 5mol% R8-PEG via post-insertion at 4°C and 37°C, and via post-conjugation at 4°C and 37°C resulted in 5.11±1.64%, 1.63±0.89, 6.66±2.80%, and 4.98±1.78% final siRNA EE%, respectively (Table 2.3, Fig. 2.2). Pre-insertion of 5mol% R8-PEG resulted in 16.61±7.06% total siRNA retention, significantly higher than all other R8-PEG groups (*P<0.05 vs. other R8-PEG groups; n=5-6; Table 2.3, Fig. 2.2), but still significantly lower than unmodified PLP controls. Additionally, incorporation of R8-PEG by both pre-insertion and postconjugation resulted in increased nanoparticle size and/or aggregation and increased PDI (Table 2.4).

2.3.2 Incorporation of STR-R8 via Pre-insertion Resulted in Significantly Enhanced siRNA Encapsulation and Retention.

Pre-insertion of 5mol% STR-R8 into base PLP resulted in 55.86±6.12% total siRNA encapsulation, significantly higher than all other STR-R8 modification techniques, all R8-PEG modification groups, and unmodified PLP controls (**P<0.05 vs. all other groups; n=3-5; Table 2.3, Fig 2.2). Additionally, pre-insertion of STR-R8 resulted in a more favorable nanoparticle characterization profile of size, PDI, and charge compared to other groups (Table 2.4).

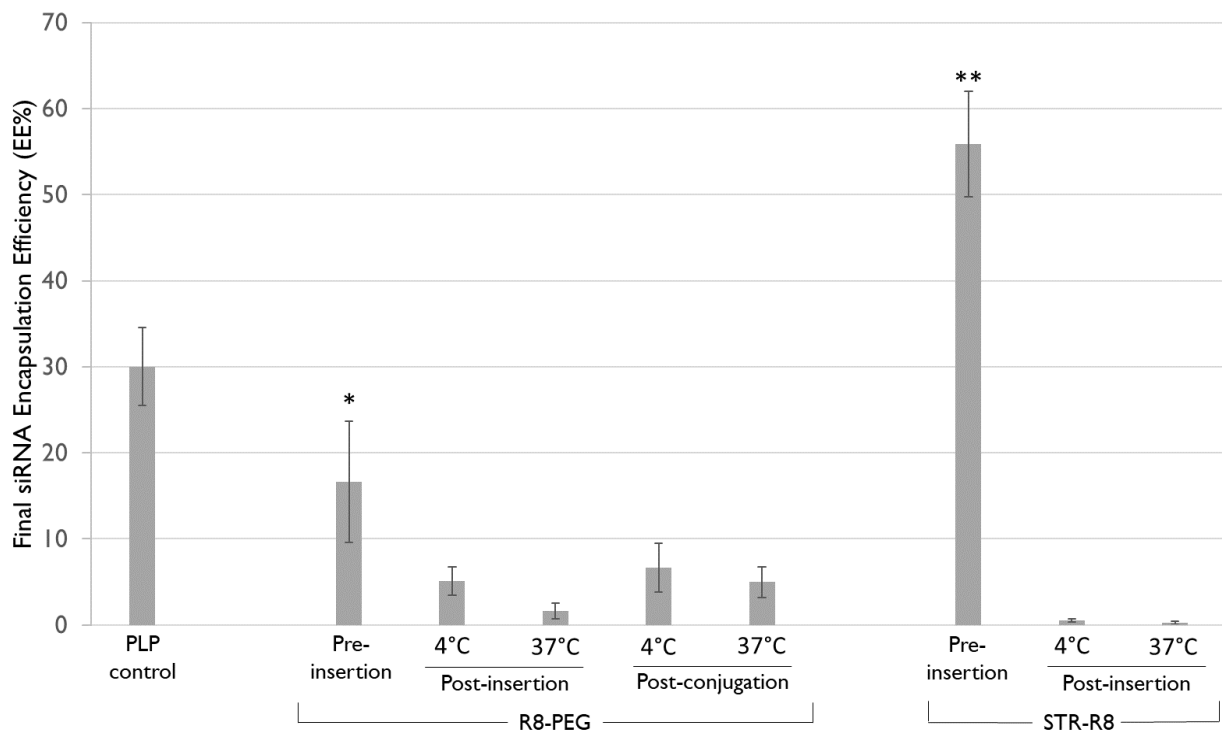


Figure 2.2: EE% of siRNA following all R8-modification techniques as compared to PLP control using Ca²⁺-mediated EtOH injection method. The pre-insertion of R8-PEG results in highest siRNA EE% among all R8-PEG modification groups. (*P<0.05 vs R8-PEG groups) The pre-insertion of STR-R8 enhanced siRNA EE% above all R8-PEG and STR-R8 modification groups and PLP control. (**P<0.05 vs. all other groups)

Table 2.3: R8-PLP modification conditions. The siRNA retention and final EE% are listed as a result of R8-modification.

R8-PLP Modification Conditions			R8-modification		
Liposome Type	R8-Lipid Conjugate	Modification Type	% Leakage	% siRNA Retention	Final EE%
PLP	N/A	N/A	N/A	N/A	30.011
R8-PLP	R8-PEG	Pre-insertion	N/A	N/A	16.614
	R8-PEG	Post-insertion (4°C)	71.468±4.758	28.532±4.758	5.108
	R8-PEG	Post-insertion (37°C)	93.394±3.091	6.606±3.091	1.631
	R8-PEG	Post-conjugation (4°C)	81.615±7.211	18.385±7.211	6.661
	R8-PEG	Post-conjugation (37°C)	79.386±10.866	20.614±10.866	4.984
	STR-R8	Pre-insertion	N/A	N/A	55.856
	STR-R8	Post-insertion (4°C)	95.296±2.000	0.522±.195	0.522
	STR-R8	Post-insertion (37°C)	97.448±1.472	0.256±.159	0.256

Table 2.4: R8-PLP modification conditions. Size, PDI, and zeta potential are measured before and after R8-modification.

R8-PLP Modification Conditions			Pre-modification			Post-modification		
Liposome Type	R8-Lipid Conjugate	Modification Type	Size (d.nm)	PDI	Zeta Potential (mV)	Size (d.nm)	PDI	Zeta Potential (mV)
PLP	N/A	N/A	55.836±5.003	.251±.035	9.736±1.024	55.836±5.003	.251±.035	9.736±1.024
R8-PLP	R8-PEG	Pre-insertion	N/A	N/A	N/A	820.842±375.680	.521±.126	9.934±1.436
	R8-PEG	Post-insertion (4°C)	58.318±1.745	.176±.012	10.208±1.164	68.012±5.881	0.217	10.720±2.153
	R8-PEG	Post-insertion (37°C)	61.749±3.174	.222±.021	10.698±1.484	72.546±5.449	0.180	11.916±1.445
	R8-PEG	Post-conjugation (4°C)	59.702±6.139	.211±.045	10.436±1.439	176.778±47.892	0.313	10.640±1.271
	R8-PEG	Post-conjugation (37°C)	55.982±5.470	.210±.043	10.574±1.493	172.398±52.063	0.354	9.106±.940
	STR-R8	Pre-insertion	N/A	N/A	N/A	49.650±1.77	.220±.006	7.40±1.90
	STR-R8	Post-insertion (4°C)	51.140±.973	.162±.012	1.54±6.870	53.740±2.368	.211±.022	13.700±2.633
	STR-R8	Post-insertion (37°C)	49.000±1.752	.206±.001	8.54±2.350	48.830±1.995	.206±.003	12.100±.551

2.3.3 Ca²⁺-mediated EtOH injection of R8-PLPs Resulted in Homogenous Liposome Samples Between 50-60nm with Increased siRNA Retention and EE%.

We have previously reported that STR-R8 increases EE% in a dose dependent manner, with 10mol% resulting in the highest of all tested modification levels.⁷³ Here 10mol% STR-R8 was pre-inserted into our R8-PLP assembly, both with and without the presence of Ca²⁺ at injection. STR-R8 incorporation without calcium results in EE% of 35.24±2.18%, while the addition of 10mM Ca²⁺ significantly increased EE% to 66.28±9.14% (*P<0.05 vs. 0mM Ca²⁺; n=4; Fig. 2.3A). The addition of 20-50mM Ca²⁺ also increased EE% above 0nM, but not to a degree greater than 10mM. Therefore, R8-PLP siRNA EE% is synergistically enhanced by STR-R8 incorporation and assembly in the presence of calcium. Additionally, the combinatorial addition of Ca²⁺ and STR-R8 had no effect on nanoparticle size, with all liposome groups at 50-60nm in diameter, while samples had a slightly elevated size distribution compared to PLP controls, but PDI values still <0.25 (Fig. 2.3B and 2.3C).

2.3.4 Increasing Lipid:siRNA Enhanced R8-PLP EE% to ~100%.

Using the empirically defined assembly parameters for the incorporation of 10mol% STR-R8 via pre-insertion in the presence of 10mM Ca²⁺ at injection, the effect of lipid:siRNA wt-to-wt ratio was tested from 5:1-100:1. Ratios of 5, 10, 20, 50, and 100:1 achieved EE% of 59.31±4.26%, 77.22±3.42%, 80.64±2.36%, 90.62±4.76%, and ***97.06±5.34%, respectively (***P<0.05 vs. all groups ≤20:1; n=6; Fig. 2.4A). Gel exclusion assays ran on unpurified liposome samples showed siRNA bands of decreasing intensity, representing decreasing amounts of un-encapsulated, un-complexed siRNA with increased lipid:siRNA (Fig. 2.4B). Notably, the siRNA band representing

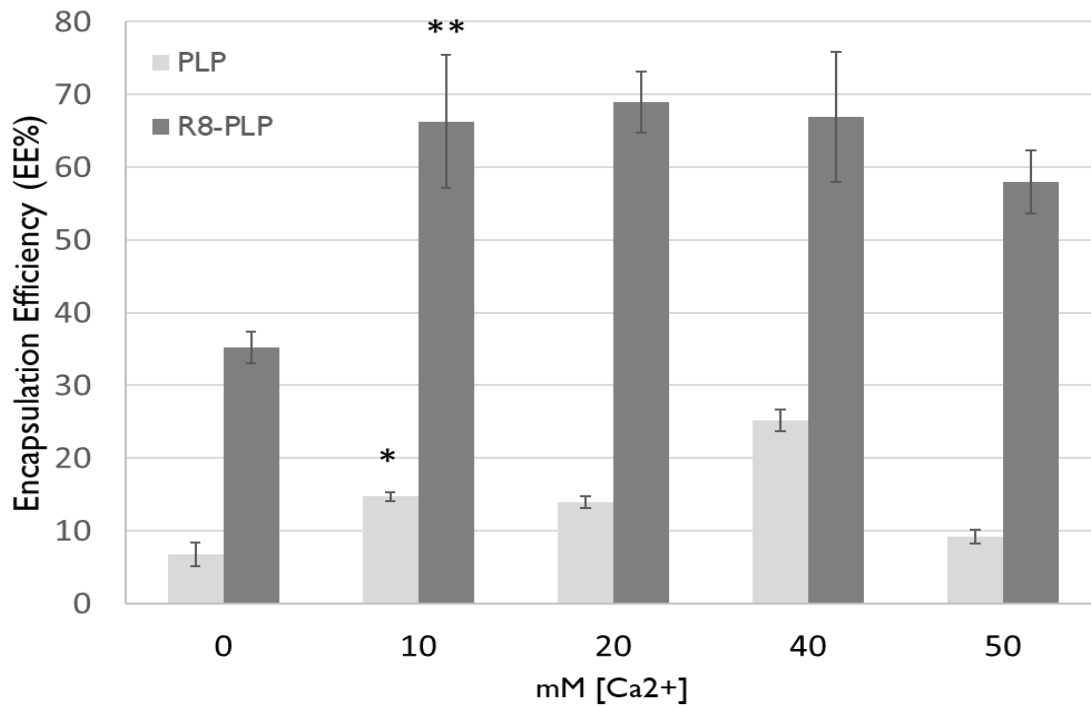


Figure 2.3A: Comparison of siRNA EE% in PLP and R8-PLP assemblies with varied amounts of calcium during injection. The addition of 10mM calcium enhanced siRNA EE% PLP and R8-PLP controls with no calcium. (*P<0.05 vs. 0mM calcium in PLP assembly; **P<0.05 vs. 0mM calcium in R8-PLP assembly)

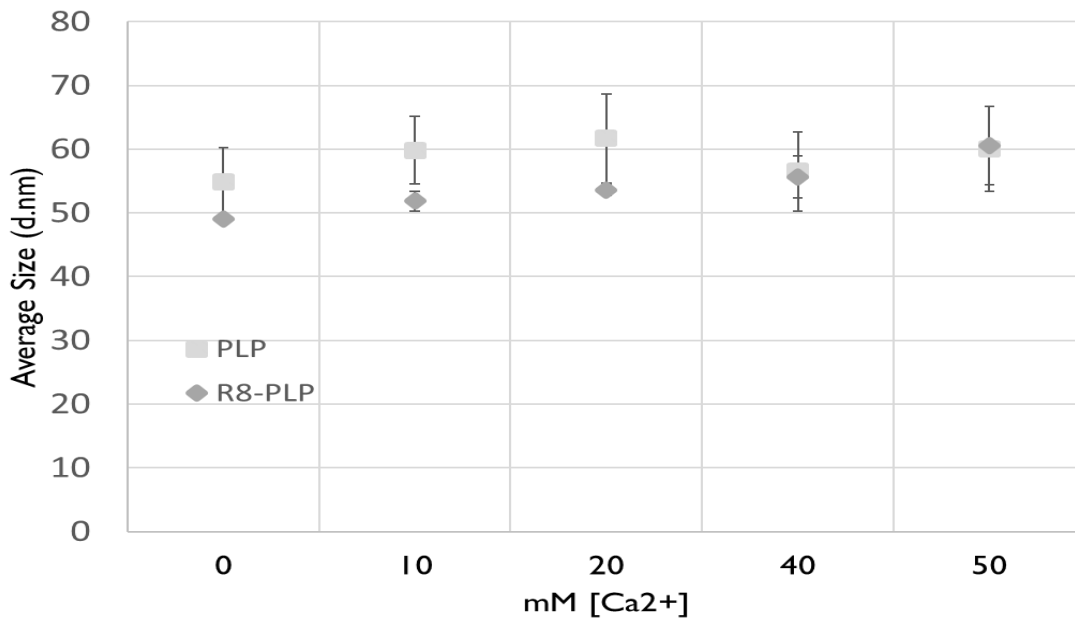


Figure 2.3B: Comparison of PDI upon PLP and R8-PLP assembly using 0-50 mM [Ca²⁺].

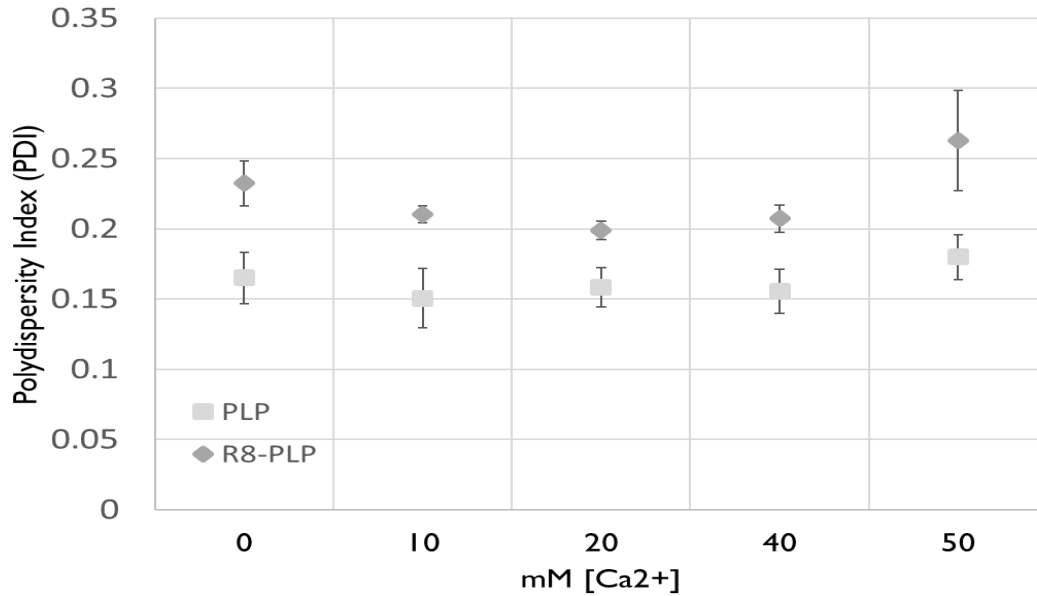


Figure 2.3C: Comparison of average size (d.nm) upon PLP and R8-PLP assembly using 0-50 mM [Ca²⁺].

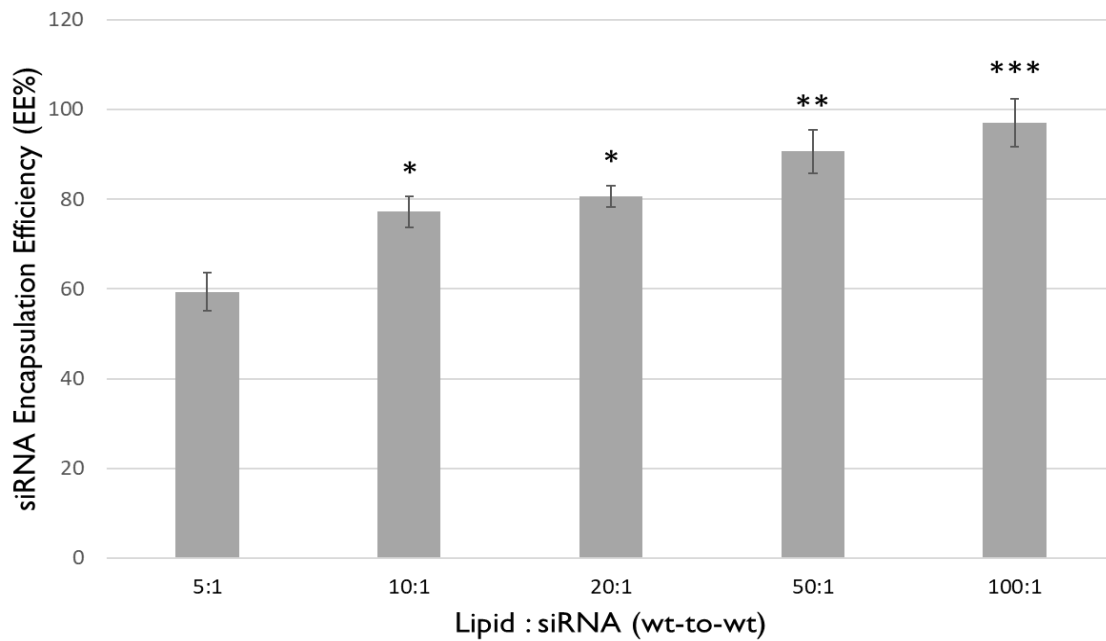


Figure 2.4A: Comparison of siRNA EE% in R8-PLP assemblies with varied lipid:siRNA (wt-to-wt). The 20:1 lipid:siRNA assembly group showed significantly higher EE% than the 5:1 lipid:siRNA group (* $P < 0.05$ vs. 5:1; $P = \text{NS}$ vs. 10:1). The 50:1 lipid:siRNA assembly group exhibited EE% significantly higher than the 5:1 lipid:siRNA group (** $P < 0.05$ vs. 10:1; $P = \text{NS}$ vs. 20:1). The 100:1 lipid:siRNA assembly group showed significantly higher EE% than the 20:1 lipid:siRNA group (** $P < 0.05$ vs. 20:1; $P = \text{NS}$ vs. 50:1).

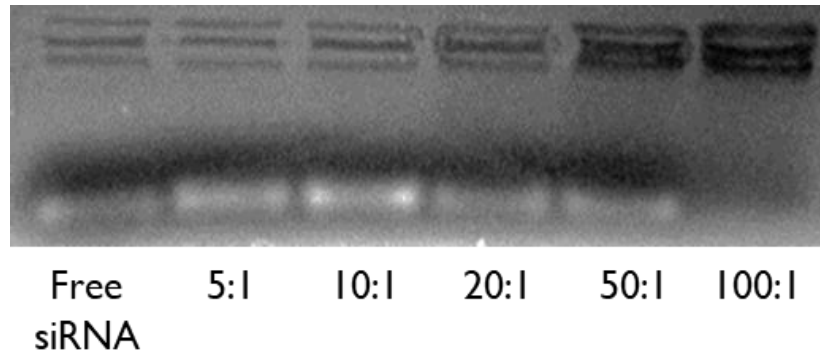


Figure 2.4B: Physical confirmation of EE% using siRNA gel exclusion assays. R8-PLPs of varying lipid:siRNA wt-to-wt ratio were run on 4% agarose gels stained for siRNA content using ethidium bromide. The siRNA band becomes more faint with increasing lipid:siRNA which indicates, via gel exclusion, increasing EE%.

the 100:1 sample was fully excluded from the gel, indicating ~100% complexation of siRNA with the R8-PLP nanoparticles (Fig. 2.4B).

2.3.5 Partial Heparin Displacement Indicated siRNA Complexation to R8-PLP Surface in Addition to Internalized R8-PLP Entrapment.

Heparin displacement assays using 100:1 R8-PLP samples, assembled as empirically defined, demonstrated that treatment with 100ug/ml heparin for 30min at RT resulted in maximal siRNA displacement from the liposome surface (Fig. 2.5A). When lipid:siRNA samples (5:1-100:1) were treated accordingly for full displacement, faint siRNA bands were present in all samples with increasing band intensity directly related to increasing lipid:siRNA. This indicated an increasing proportion of total siRNA EE% should be attributed to outer associated siRNA on the R8-PLP surface (Fig. 2.5B.1). When samples were treated with heparin+Triton X-100, for denaturation and displacement, strong siRNA bands further increased in intensity with increasing lipid:siRNA (Fig. 2.5B.2), confirming increasing total siRNA EE% with increasing lipid:siRNA. Additionally, these bands were significantly more intense than equivalent lipid:siRNA samples

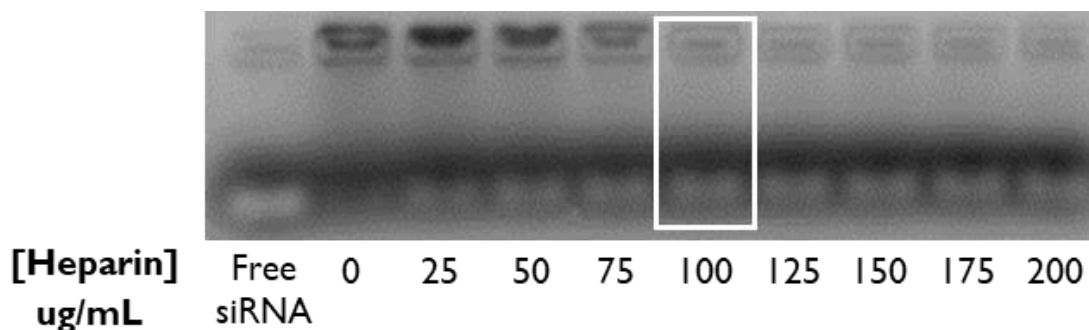


Figure 2.5A: Heparin Displacement Assay that indicates the minimum amount of [heparin] to remove all outer-associated siRNA (white box; 100ug/mL).

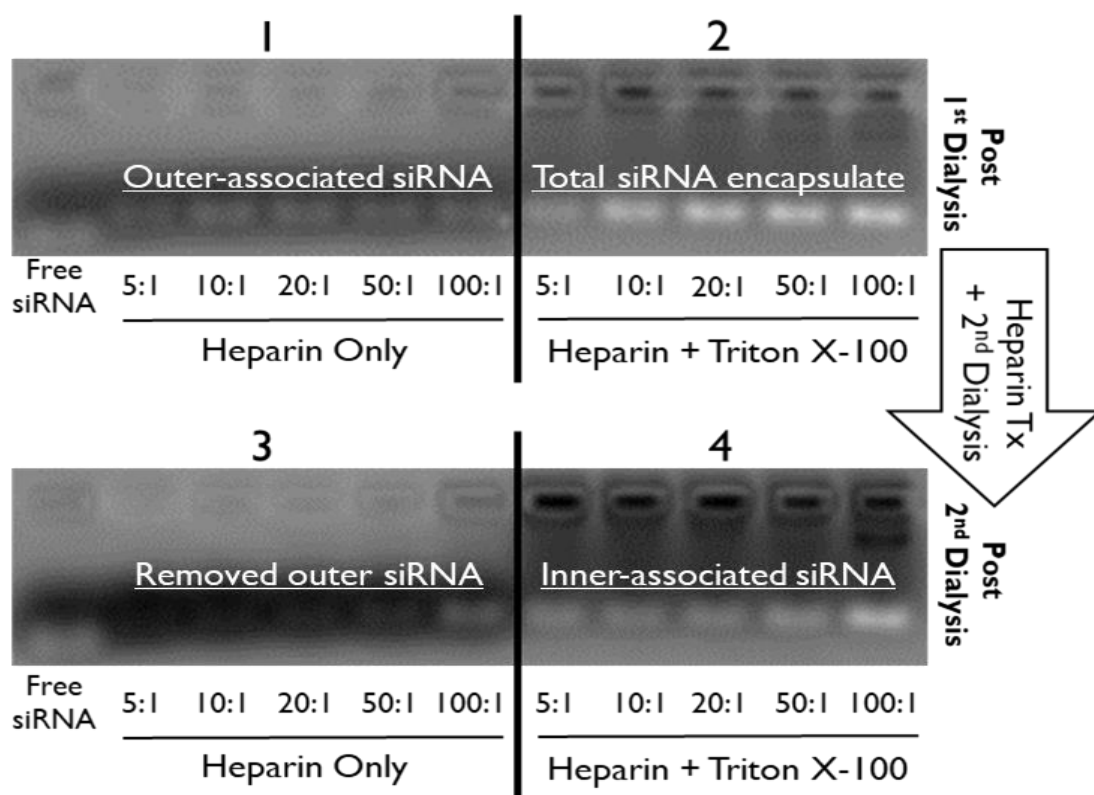


Figure 2.5B: Gel exclusion/Heparin Displacement Assays used to characterize complexation of siRNA with R8-PLP assemblies. (1) R8-PLP assembly with 100:1 lipid:siRNA was treated 100 ug/mL of Heparin to remove outer associated siRNA after first dialysis. (2) Equal fraction of R8-PLP assembly was treated with heparin + Triton X-100 detergent to remove all siRNA encapsulated after first dialysis before electrophoresis. These bands represent total EE% and increase in intensity with increasing lipid:siRNA. R8-PLP assemblies with 100:1 lipid:siRNA were then treated with 100 ug/mL and dialyzed a second time to remove any outer associated siRNA. (3) These siRNA bands represent outer-associated siRNA remaining after second dialysis. (4) Equal fraction of R8-PLP assembly was treated with heparin and Triton X-100. These bands represent EE% of siRNA after removal of outer-associated siRNA from R8-PLP assembly. These bands also increase in intensity with increasing lipid:siRNA.

treated with heparin only, indicating the proportion of outer associated siRNA is minimal compared to total EE%. When lipid:siRNA samples were treated with heparin and re-dialyzed overnight at 4°C to remove outer siRNA, then retreated with heparin+Triton X-100, siRNA representing only internal encapsulated siRNA were similar in intensity to lipid:siRNA samples prior to re-dialysis, indicating the majority of total siRNA encapsulate was internally protected and retained (Fig. 2.5B.4).

2.3.6 R8-PLP Nanoparticles Sufficiently Protected Encapsulated and Complexed siRNA Against RNase A Degradation.

RNase stability assays against free siRNA controls demonstrated that treatment with 0.5ug/ml RNase A enzyme for 30mins at 37°C was sufficient for complete degradation (Fig. 2.6A). When R8-PLPs, assembled as empirically defined at 100:1, were treated with 0.5ug/ml RNase prior to denaturation, there was no demonstrable siRNA degradation, as evidenced by equivalent siRNA bands in denatured R8-PLPs without RNase treatment (Fig. 2.6B). Likewise, free siRNA control samples simultaneously exposed to RNase were completely degraded, indicating complete RNase protection of encapsulated and/or complexed siRNA by the R8-PLP nanoparticle.

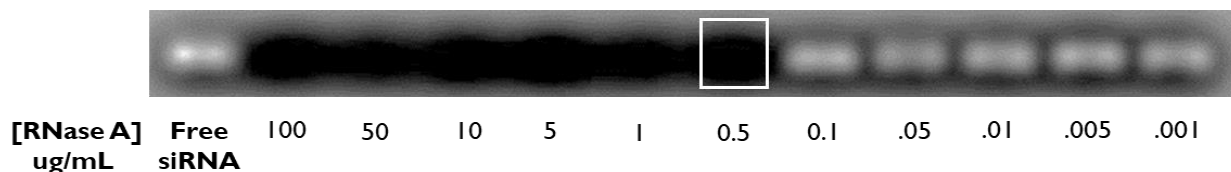


Figure 2.6A: RNase Stability Assay indicating the minimum amount of RNase A required to digest all free siRNA used for assay (white box; 0.5 ug/mL).

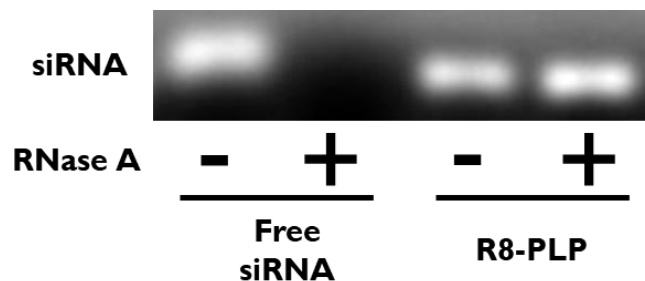


Figure 2.6B: RNase stability assay showing nearly complete protection of siRNA-loaded R8-PLPs. The siRNA bands for R8-PLP assemblies treated and untreated with RNase A are of equal intensity, indicating ~100% protection of siRNA when exposed to nuclease digestion.

2.3.7 Slower Injection Rates During R8-PLP Assembly Resulted in Increased Sample Homogeneity but Showed No Correlation to EE%.

Using the empirically defined parameters for R8-PLP assembly, varying the speed of injection at assembly had no significant effect on EE% (n=4; Fig. 2.7A). Importantly, slower injection rates resulted in a more homogeneous nanoparticle population, with PDI<0.2 at 0.1 and 0.2ml/min (n=3; Fig. 2.7B). Slower injection rates also resulted in an increased average diameter of the nanoparticles, but all remained <65nm (n=3; Fig. 2.7C).

2.3.8 R8-PLP Nanoparticles Demonstrated Enhanced Cell Association *in vitro*.

Qualitative analysis of Rho-PE-labeled liposomes, via fluorescence microscopy, exhibited enhanced cellular association of R8-PLP nanoparticles after 30min and 24hr of exposure, compared to PLP controls (Fig. 2.8).

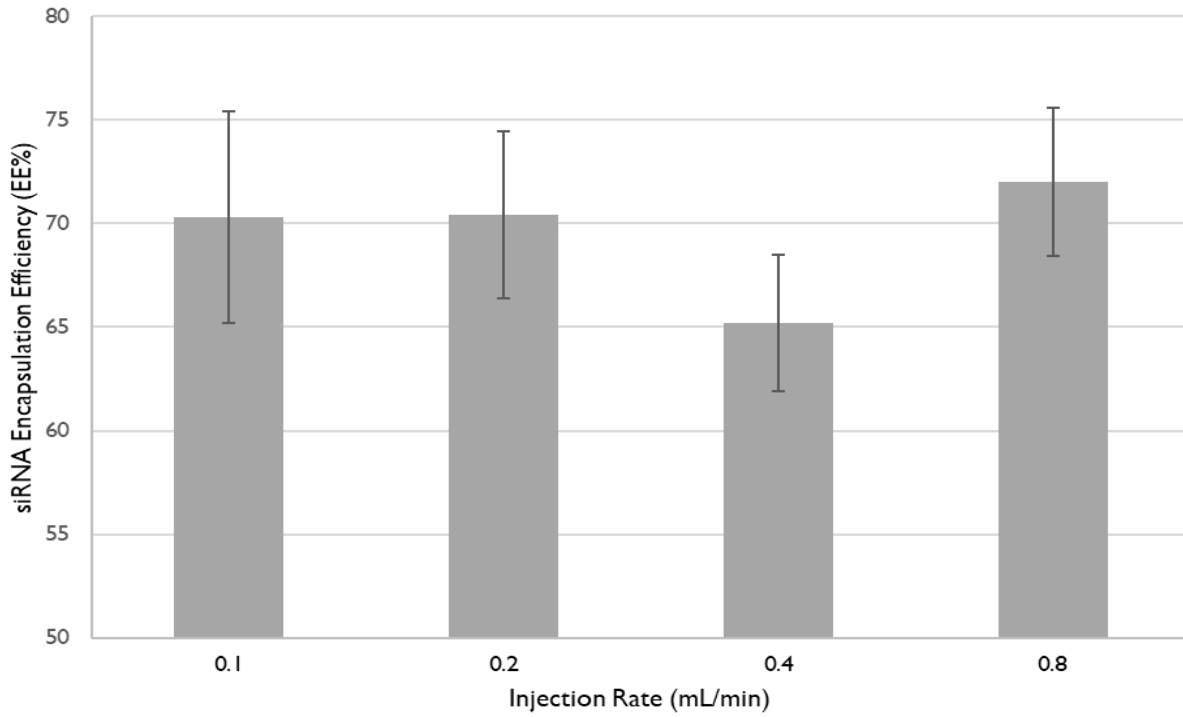


Figure 2.7A: Comparison of siRNA EE% with varied injection rates during EtOH injection assembly of R8-PLPs with 10:1 lipid:siRNA. There were no significant differences in siRNA EE% between injection rate groups (P=NS vs. all groups; n=3)

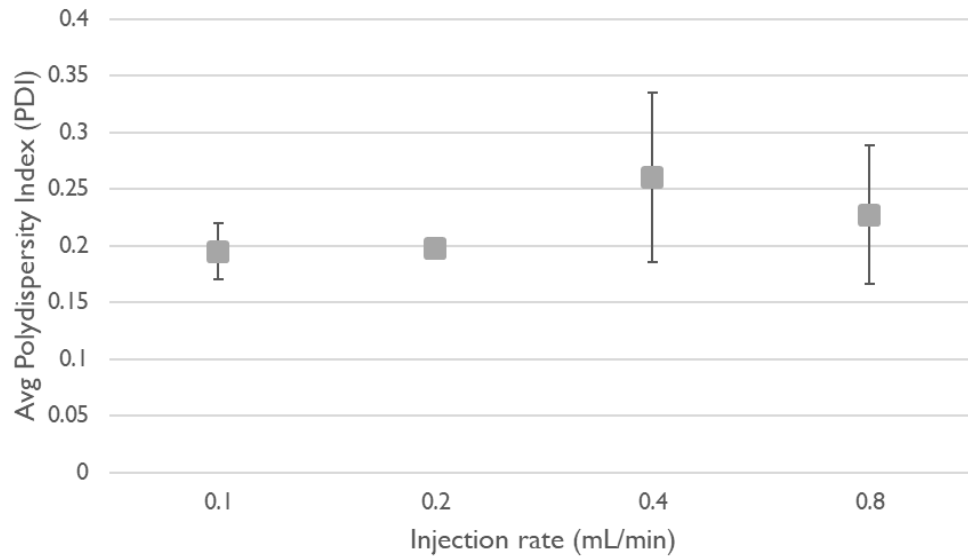


Figure 2.7B: Comparison of PDI upon R8-PLP assembly using varied injection rates (P=NS vs all groups; n=3)

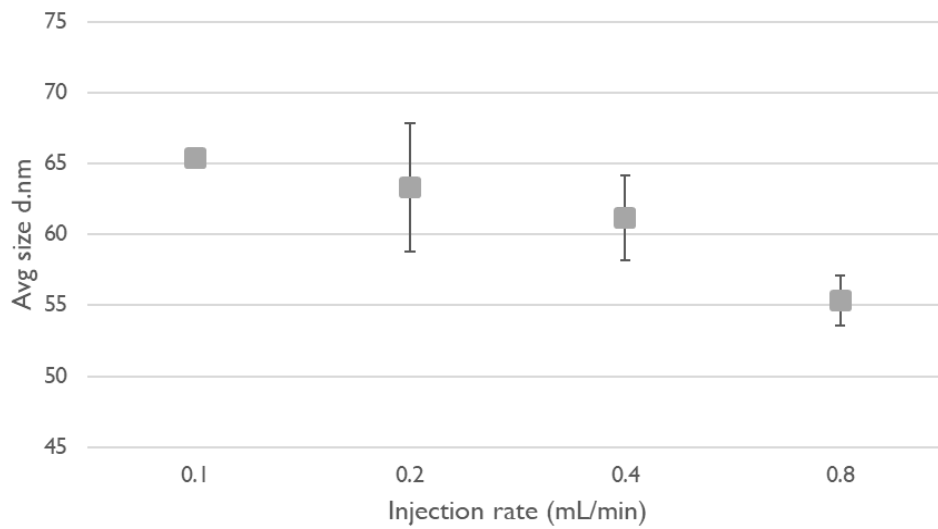


Figure 2.7C: Comparison of average size (d.nm) upon R8-PLP assembly using varied injection rates.

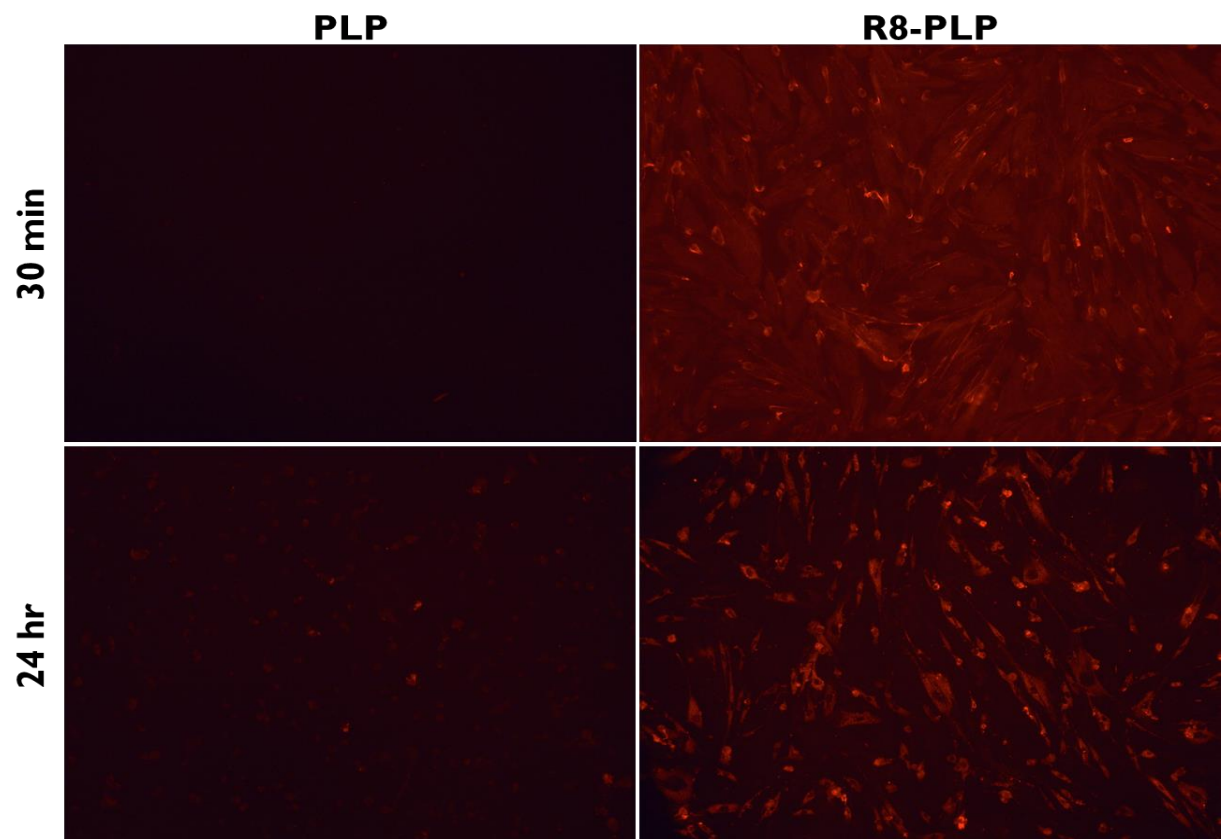


Figure 2.8: Qualitative fluorescent images of HASMCs treated with R8-PLP assemblies with 10mol% STR-R8 and PLP controls at 30 mins and 24 hours. 0.5mol% of Rho-DPPE was added to all liposome groups and cells were treated with 100uM total lipid. Images indicated enhanced cell association of R8-PLPs compared to PLP controls at both 30 mins and 24 hours.

2.4 Discussion

Therapeutic strategies utilizing siRNA have been validated in a broad spectrum of disease pathologies *in vitro*.^{74,75} Unfortunately, the clinical success of siRNA-mediated gene therapeutics is hampered by inadequate delivery technology.⁷⁶ Liposomes have emerged as the most widely tested nanocarriers of siRNA due to biocompatibility, flexibility of assembly, and multifunctional potential.^{57,77} However, effective liposome-mediated transfection typically requires cationic lipids to improve nucleic acid EE% and cell associative properties.⁷⁸ Unfortunately, CLP-induced cytotoxicity and immunogenicity has limited translational efficacy of liposomal gene therapy *in vivo*.⁷⁹ Therefore, the EE% and cell interactive properties of non-cationic PLPs require optimization to achieve the translational success that remains elusive in liposome-mediated gene therapy studies. Here we aimed to establish a noncationic PLP formulation with natural lipid constituents and surface-conjugated CPP as an alternative transfection agent to traditional CLP formulations that often fail in downstream gene therapy applications. The development of a simple, scalable method for assembling noncationic CPP-modified PLPs capable of efficient siRNA loading and enhanced cell association could provide an ideal drug delivery system for gene therapy.

R8 is a well-established CPP that can be incorporated into PLP bilayers using R8-amphiphiles to expose the active peptide on the liposome surface. Examples of R8-amphiphiles include R8 conjugated to DSPE-PEG (R8-PEG), R8 anchored to stearic fatty acid (STR-R8), and others.^{80,81} Common liposome modification techniques that can be used for R8-amphiphile incorporation are (1) inclusion of R8-amphiphile during initial liposome assembly (pre-insertion), (2) insertion of R8 amphiphiles into the bilayers of pre-formed liposomes (post-insertion), and (3) reacting the R8 peptide with functional groups exposed on the surface of pre-formed

liposomes utilizing click chemistry techniques (post-conjugation).^{82,83} However, the optimal process parameters required to assemble CPP-modified noncationic PLPs with efficient siRNA loading and functionally enhanced delivery are previously unknown.

Here, we first examined the modification of non-cationic PLPs with R8 by incorporating R8-PEG into the liposomal formulation via pre-insertion, post-insertion, and post-conjugation techniques. One liposomal attribute that directly affects drug leakage during ligand modification is membrane fluidity.⁸⁴ Therefore, in order to minimize membrane fluidity of pre-formed liposomes during R8 modifications, we tested post-insertion and post-conjugation efficiency at 4°C in addition to previously established reaction conditions of 37°C.^{85,86} With 4°C still being well above phase-transition of liposomes comprised of unsaturated lipids, it was expected that both 4°C and 37°C would provide the thermal energy required for adequate insertion. This allowed for the assessment siRNA leakage and retention upon R8 incorporation based on the effects of temperature on membrane fluidity. As expected, when performing post-insertion at 4°C for increased membrane stability, a slightly higher retention of siRNA was achieved when compared to post-insertion at 37°C (Table 2.3), but final EE% was still only ~5%. Post-conjugation is often avoided when dealing with CPPs, due to their membrane perturbing effects and siRNA leakage upon incorporation. Here we confirmed that using R8 with unnatural lysine(azide) residues to decorate the surface of pre-formed PLPs by post-conjugation resulted in significant siRNA leakage irrespective of temperature. In fact, the final siRNA encapsulation for post-insertion and post-conjugation in all conditions was no higher than ~7%, limiting the overall feasibility of assembling R8-modified PLPs using post-insertion or post-conjugation of R8-PEG. Ultimately, pre-insertion of R8-PEG resulted in enhanced encapsulation above all other R8-PEG groups, but the PDI of these liposomes was significantly higher even after extrusion (Fig. 2.2,

Table 2.4). When conjugated to PEG, peptides have more degrees of freedom compared to peptides conjugated directly to lipid molecules, due to the many degrees of freedom that the polyethylene glycol polymer exhibits under physiological conditions.⁸⁷ It is possible this highly dynamic scenario of the R8 peptide interferes with liposome assembly when using the pre-insertion technique. Therefore, while the encapsulation of siRNA is modestly increased by R8-PEG pre-insertion vs. post-insertion or post-conjugation techniques, the efficient assembly of liposomal siRNA nanocarriers is still compromised due to low overall EE%.

Next we examined the modification of non-cationic PLPs with STR-R8. With R8 anchored to the stearic fatty acid, the entrapment of liposomal siRNA was highly efficient. Contrary to pre-insertion using R8-PEG, the pre-insertion of STR-R8 had little effect on size dispersity (PDI < 0.25) and still resulted in liposomes below 50nm (Table 2.4). Furthermore, pre-insertion of STR-R8 enhanced the overall encapsulation of siRNA to ~56%, the highest EE% achieved when comparing all R8-amphiphile incorporation techniques. To our knowledge, there is no established one-step method to encapsulate siRNA above ~50% efficiency in noncationic PLPs. The method demonstrated here is a one-step assembly whereby all lipid constituents, including ligand-conjugated lipids, are solubilized together in organic solvent prior to injection into aqueous buffer containing siRNA encapsulate. This one-step assembly method is inherently simpler than post-insertion or post-conjugation techniques, which require multiple assembly and purification steps. Harashima et al. previously demonstrated the unique ability of STR-R8 to condense nucleic acid through electrostatic complexation.⁸⁸ We propose that the enhanced EE% seen in R8-PLPs assembled via pre-inserted STR-R8 is a result of the condensation of siRNA during liposome assembly. A portion of the STR-R8 is integrated into the PLP bilayer to help enhance delivery, but much of it may also promote condensation and enhanced encapsulation of siRNA upon

incorporation into PLPs. In this way, the STR-R8 moiety provides a bifunctional element to R8-PLP assembly and application.

To further elucidate the process parameters for R8-PLP formulation and assembly for optimal encapsulation of siRNA, we examined the synergistic contribution of Ca^{2+} -mediated nucleic acid condensation. Similar to previously reported results, EtOH injection of non-modified PLPs in the presence of Ca^{2+} enhanced the EE% of siRNA with as little as 10mM Ca^{2+} ($14.03 \pm 1.18\%$) compared to PLPs with no Ca^{2+} ($6.82 \pm 1.62\%$, Fig. 2.3A).⁷⁰ When assembling R8-PLPs with pre-insertion of STR-R8 in the presence of Ca^{2+} there was a synergistic enhancement of siRNA EE% with $\geq 10\text{mM}$, whereby encapsulation approached $\sim 70\%$ at all concentrations and no deleterious effect was seen in nanoparticle size or homogeneity (Fig. 2.3A-C). Moving forward, this one-step assembly technique of R8-PLPs, using STR-R8 modification via pre-insertion and 10mM Ca^{2+} at injection, was utilized to assemble all liposome groups to define additional assembly parameters for optimized siRNA retention and enhanced cell association. A schematic representing this empirically defined and modified EtOH injection technique is presented in Fig. 2.9.

For further optimization of assembly parameters, next siRNA loading and carrying capacity was examined by varying lipid:siRNA wt-to-wt ratios at injection. We demonstrated increased siRNA loading with increased lipid:siRNA, where 50:1 and 100:1 lipid:siRNA samples achieved $>90\%$ and $>97\%$ EE%, respectively (Fig. 2.4A-B). In order to differentiate outer associated vs. inner entrapped siRNA proportions constituting this final EE% value, a series of gel electrophoresis assays were utilized. When all lipid:siRNA samples (5:1-100:1) were treated with heparin only for outer siRNA disassociation, faint bands indicated an increasing proportion of

outer associated siRNA with increasing lipid:siRNA conditions (Fig. 2.5B.1). However, when equivalent fractions of each lipid:siRNA sample were treated with heparin+Triton to release both associated and entrapped siRNA, bands of greater intensity were revealed, indicating more siRNA is entrapped within the liposomal core than that which is associated with the outer surface (Fig. 2.5B.2). Subsequently, when additional equivalent fractions were heparin treated and re-dialyzed overnight to clear outer associated siRNA from the samples, these re-dialyzed lipid:siRNA samples were treated with heparin+Triton to release total remaining siRNA encapsulate from the inner core. These siRNA bands remained nearly as intense as lipid:siRNA samples prior to re-dialysis, reconfirming that the majority of siRNA encapsulate is protected from heparin displacement and encapsulated within the liposomal core (Fig. 2.5B.4).

Given that a proportion of the nearly 100% encapsulation efficiency demonstrated here in our 100:1 sample could be attributed to merely outer associated nucleic acid, one could postulate that the delivery efficacy of our empirically derived R8-PLP platform described herein might be overestimated for *in vitro* and/or *in vivo* translation due to nucleic acid instability in the presence of serum. Therefore, to determine R8-PLP stability and siRNA protection, R8-PLPs with the highest EE% (assembled as described at 100:1) were subjected to RNase A enzymatic degradation prior to gel electrophoresis. As indicated in Fig. 6B, R8-PLPs exposed to RNase degradation exhibited siRNA bands of equal intensity to untreated R8-PLP controls, while free siRNA was completely degraded. This qualitative assay confirmed complete protection of siRNA when encapsulated within our R8-PLP nanocarrier using the assembly method described herein.

Our ultimate goal is to elucidate the most efficient method for producing CPP-modified PLPs that have the potential for downstream gene therapy applications. To this end our

methodology must have the potential for scalable production and the resultant delivery platform must demonstrate functionality in a dynamic biological environment. While our laboratory manually derived and validated many of these specifications, the development of instrumentation to control these and other parameters is a source of ongoing collaborative efforts among our group and others. Consequently, the data presented here regarding controlled injection rates and the absence of a significant effect on EE% (Fig. 2.7A-C) may point to an assembly method that could be highly scalable for industrial applications. Furthermore, to test the dual-functionality of the STR-R8 in increasing siRNA EE% while simultaneously enhancing the cell associative properties noncationic PLP assemblies, HASMCs were treated with R8-PLPs and PLP controls. Here, Rhodamine-labeled lipid (0.5mol%) was added to PLP and R8-PLP assemblies for liposome tracking. As revealed through fluorescent analysis, R8-PLPs significantly enhanced cell association at both 30 mins and 24 hours post treatment compared to unmodified PLP controls. This preliminary *in vitro* validation supports the need for further studies of functionality and delivery efficacy *in vitro* and *in vivo*. As such our future assays will focus on the cytotoxicity profiles, *in vitro* gene targeting efficacy, *in vivo* biodistribution analysis, and pharmacokinetic profiling of the R8-PLP nanocarrier platform.

In conclusion, our research has demonstrated that the addition of STR-R8 into PLPs utilizing the pre-insertion technique is a simple and efficient method to produce noncationic CPP-modified liposomes capable of enhanced cell association and optimal siRNA retention (Fig. 2.9). This development could provide a foundation for future clinical applications of liposomal gene therapy with greater translational success.

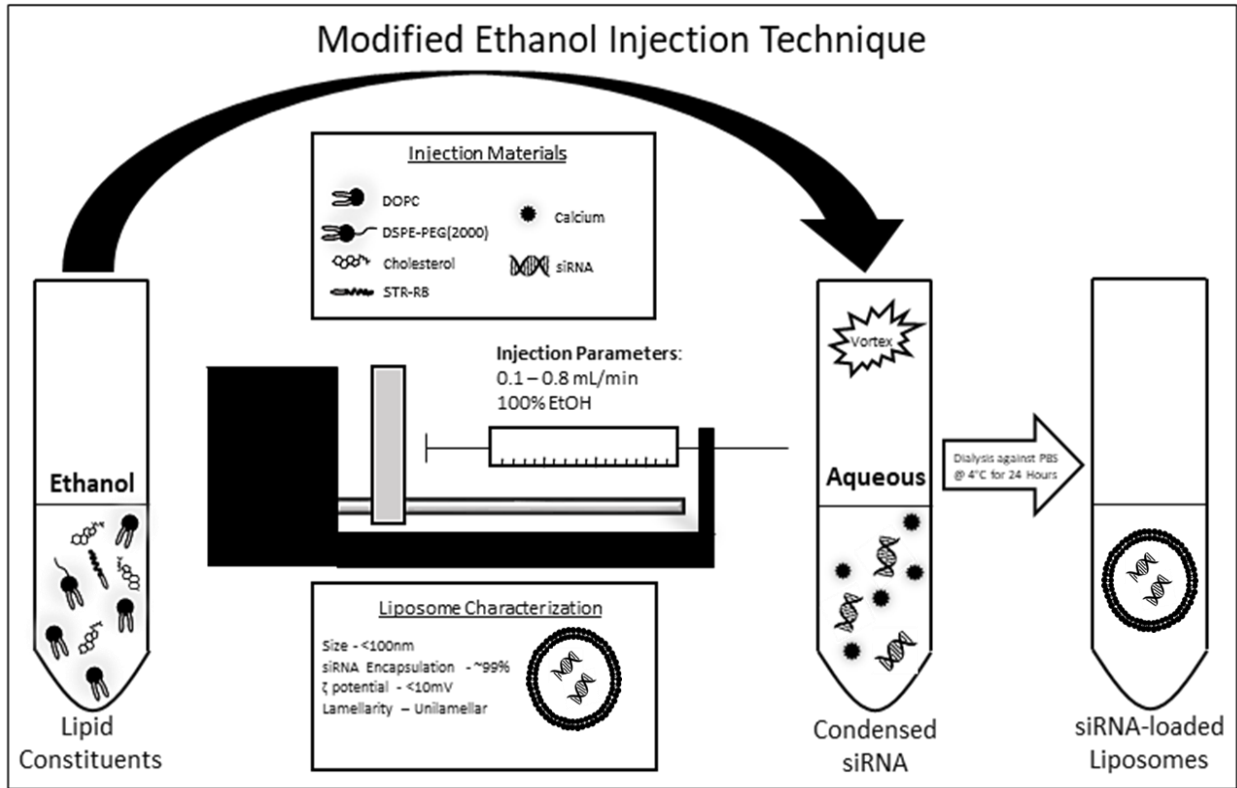


Figure 2.9: Schematic illustration of empirically derived Ca²⁺-mediated EtOH injection technique used to assemble noncationic R8-modified PLPs with nearly complete siRNA EE% and enhanced cell association. These R8-PLP assemblies exhibit critical quality attributes required for optimal in vitro performance in vivo translation with an average size of <100nm in diameter, zeta potential of <10mV, and unilamellar structure.

CHAPTER 3: Improving the Efficacy of Liposomal-mediated Vascular Gene Therapy via Lipid Surface Modifications

The following chapter was published in the *Journal of Surgical Research* and is reprinted here with permission from Elsevier.

3.1 Introduction

Currently there are more than 200 million people worldwide with peripheral vascular disease (PVD).⁸⁹ As average global life expectancy continues to escalate, the prevalence of PVD will also continue to rise. Endovascular interventions are low-risk, minimally invasive procedures that have become increasingly pervasive in the treatment of PVD due to high initial success rates (>90%).⁹⁰ Unfortunately, endovascular procedures are linked to higher re-intervention rates for loss of vessel patency, due to chronic restenosis and injury-induced intimal hyperplasia (IH) development, typically marked by dysfunctional migration and proliferation of vascular smooth muscle cells (VSMC) in the vessel wall along with delayed vascular endothelial cell (VEC) recovery.⁹¹ In fact, IH-induced restenosis occurs in greater than 60% of endovascular cases at 12-months follow-up, often requiring secondary intervention with increased morbidity and mortality rates.^{92,93} An optimal treatment plan to mitigate the development of IH-induced restenosis would improve long-term primary intervention success rates, and help relieve the clinical and financial burden of the PVD health epidemic.

RNA interference (RNAi), or the use of short interfering RNA (siRNA) to transiently attenuate cellular protein expression, shows promise as a gene therapy technology to alter vascular pathology.^{94,95} Our lab has previously defined several molecular mechanisms of IH development that could be potential targets for molecular therapeutics aimed at its attenuation.<sup>96-
¹⁰²</sup> However, the development of molecular nanocarriers is needed in order to overcome the unfavorable physiochemical properties that limit intracellular siRNA uptake. Various transfection agents have been investigated for their application of gene therapy to vascular cell types, including

polymeric nanoparticles, chemical agents, and viral vectors.¹⁰³⁻¹⁰⁵ Recently, our group has successfully deployed multiple classes of biodegradable polymers in the delivery of molecular gene therapy in vascular cell types and tissue *in vitro*.^{106,107} While many of these nanocarriers have shown efficacy with *in vitro* transfection, they often fail to translate to an *in vivo* model due to their cytotoxicity, adverse immune response, and inefficient biodistribution.^{106,108} Therefore, the development of a biocompatible nanocarrier that can provide targeted vascular gene therapy, without immunological or cytotoxic effects, is needed to provide a drug delivery candidate for future *in vivo* testing for the attenuation of IH development in a post-surgical model.

Liposomes are promising drug delivery vehicles due to their biocompatibility, relatively low cytotoxicity, and flexibility of modification. Liposomal phospholipids are arranged in a bilayer that forms a spherical nanoparticle mimicking the cell membrane. Cationic liposomes (CLPs), made with synthetic lipid components, have been successfully used in the delivery of gene therapeutics *in vitro*, due to the high loading capacity of negatively charged phosphate groups present in nucleic acids.^{79,109} Also, the positive surface charge of CLPs promotes cellular interaction due to the electrostatic affinity for the negatively charged cell membrane. Unfortunately, clinical translatability has been limited, as CLPs are often demonstrated to be cytotoxic and immunogenic when administered *in vivo*, partially attributable to their synthetic constituents.¹¹⁰

Neutral liposomes are comprised of naturally occurring phospholipid constituents and have been modified to improve efficacy as targeted nanocarriers while maintaining a lower toxicity profile. Polyethyleneglycol (PEG) can be conjugated to the surface of a liposome to provide “stealth” properties for the nanoparticle. Along with their nanoscale size at <150 nm in

diameter, PEGylation allows the nanocarrier to avoid opsonization clearance from the blood stream, increasing the overall half-life of the carrier.⁵ The most intriguing aspect of neutral PEGylated liposomes (PLPs) is the flexibility of modification and multifunctional potential provided by the PEG shell on the liposome surface. The PEG molecule can provide a scaffold for conjugation of functional ligands, and various ligand classes can be anchored into the lipid bilayer via stearylated fatty acids. These modifications can provide functional modalities such as enhanced intracellular delivery, cell-type specific delivery, triggered release, imaging capabilities, tissue localization, etc.¹¹¹ Specifically, cell-penetrating peptides (CPPs) are short peptide fragments that can enhance cellular uptake of biomolecular cargo.^{67,112} These peptides are typically cationic in nature and can locally and temporarily disrupt the lipid bilayer on the cell surface, leading to direct translocation across the cell membrane. Here, we aim to establish CPP-modified neutral liposomes as efficient molecular nanocarriers in VSMCs, with reduced cytotoxicity and enhanced siRNA delivery as compared to standard CLP formulations previously established in the RNAi literature. Improving the efficacy of liposome-mediated molecular therapeutics in vascular cell types, using lipid surface modifications, could lead to a translatable drug delivery platform for future *in vivo* application in vascular injury models of disease aimed at the prevention of IH.

3.2 Materials and Methods

3.2.1 Neutral and Cationic Liposome Assembly via EtOH Injection

All liposome constituent acronyms are defined in Table 3.1. Lipids and cholesterol were purchased from Avanti Polar Lipids (Alabaster, AL, USA). Octaarginine (R8) peptide, a well-established CPP that has been shown to enhance cytosolic delivery of PLP contents, was purchased from LifeTein LLC (Somerset, NJ, USA).^{112,113} Figure 3.1 illustrates each liposome group

Table 3.1: Liposome constituents.

Liposome Constituents	
Acronym	Lipid Derivative
DOPC	1,2-dioleoyl- <i>sn</i> -glycero-3-phosphocholine
DSPE-PEG	1,2-distearoyl- <i>sn</i> -glycero-3-phosphoethanolamine-N-[methoxy(polyethylene glycol)-2000]
DOTAP	1,2-dioleoyl-3-trimethylammonium-propane
DOPE	1,2-dioleoyl- <i>sn</i> -glycero-3-phosphoethanolamine
Rho-DOPE	N-(lissamine rhodamine B sulfonyl)-1,2-dioleoyl- <i>sn</i> -glycero-3-phosphoethanolamine
Chol	Ovine cholesterol
STR-R8	Stearylated octaarginine

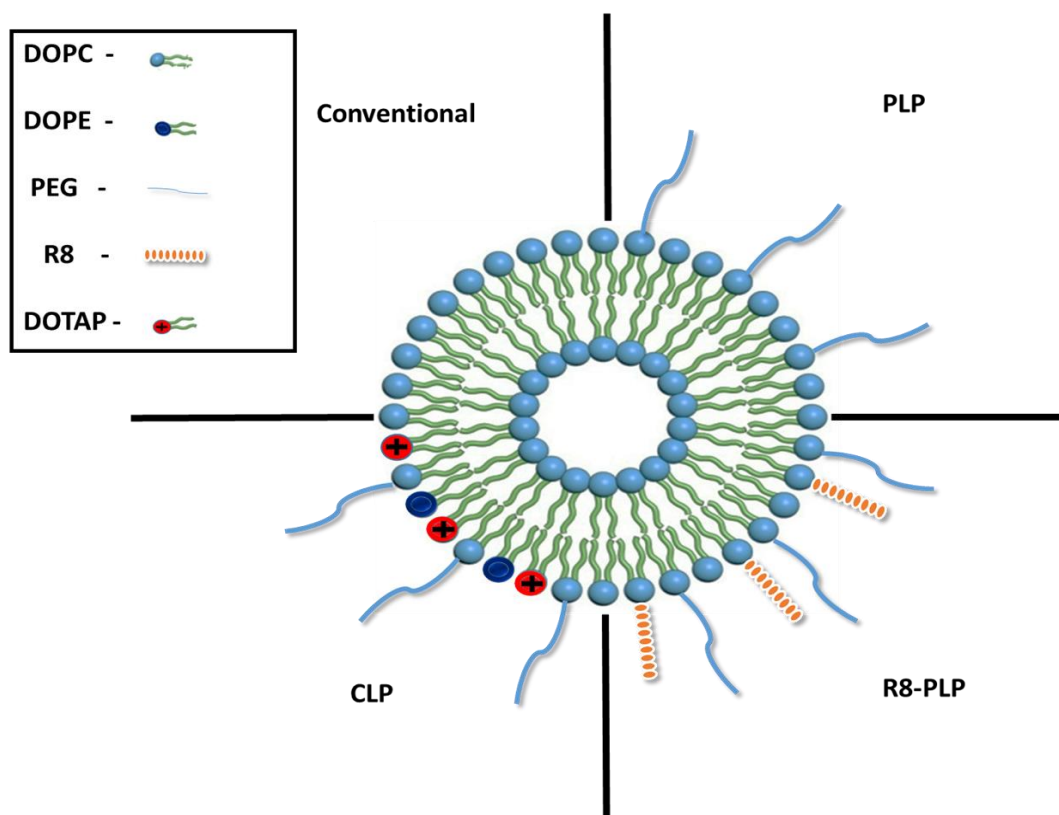


Figure 3.1: Illustration of lipid constituents and their assembly within in liposome classification used for experimental analysis. Constituent abbreviations defined in Table 3.1.

and their constituents in schematic form. Neutral PEGylated non-modified liposomes (PLP) were formed with bulk lipid DOPC:chol at 7:3mol plus 10mol% DSPE-PEG. Neutral PEGylated R8-modified liposomes (R8-PLP) were formed with PLP base plus increasing increments of STR-R8 (1-10mol%). Non-PEGylated neutral controls (LP and R8-LP) were formed with identical bulk lipid base without the addition of DSPE-PEG. PEGylated cationic liposomes (CLP) were formed with DOTAP:DOPE at 1:1mol plus 10mol% DSPE-PEG. All liposome formulations were assembled via the EtOH injection technique previously described⁷⁰. Briefly, lipids were dissolved in CHCl₃, combined as indicated, and dried under N₂ gas and vacuum to remove remaining solvent, and then resuspended in molecular grade 100% EtOH. GAPDH or negative control (NC) siRNA (Thermofisher Scientific, Waltham, MA, USA) at 50ug/300ul 10mM Tris-HCl, pH 8.0 (plus 10nM CaCl₂ for neutral formulations) was injected with 125-1000ug total lipid/200uL 100% EtOH, under constant vortexing at room temp. Liposomes were then purified from un-encapsulated siRNA via overnight dialysis against PBS, pH 7.4 at 4 °C and extruded at 100nm using polycarbonate membranes (Avanti Polar Lipids).

3.2.2 Liposome Characterization Studies

Size and Charge Characterization

The mean size and zeta potential of all liposome preparations were measured in triplicate by dynamic light scattering and electrophoretic mobility on the Zetasizer Nano ZS instrument (Malvern Instruments Ltd., Worcestershire, UK).

Morphological Characterization by Scanning Transmission Electron Microscopy

Liposome morphology and lamellarity were investigated by STEM using a negative-stain method. Liposomes were applied dropwise to a carbon film coated copper grid and allowed to air dry. Liposome films were then stained with 2% phosphotungstic acid and air-dried for 1 min at room temp. Samples were visualized with Zeiss Auriga 40 STEM scope, and images were acquired by SmartSEM image acquisition software (Carl Zeiss, Inc., Oberkochen, Germany).

Encapsulation Efficiency (EE%)

siRNA encapsulation of each preparation was determined using Quant-iT RiboGreen RNA Assay Kit (ThermoFisher Scientific). Briefly, liposomes were solubilized in 1% Triton X-100 at 37°C for 15 min to release encapsulated siRNA, mixed 1:1 with RiboGreen reagent for fluorescent labeling of siRNA, and emission was measured at 525 nm. Fluorescence units of solubilized liposomes were compared to a known standard curve of siRNA in 1% Triton X-100 to determine μg of siRNA encapsulate. EE% of each liposome formulation was calculated as $(\mu\text{g siRNA encapsulate} / 50\mu\text{g total siRNA}) \times 100$.

3.2.3 Vascular Smooth Muscle Cell Culture

Human aortic smooth muscle cells (HASMCs) were obtained from LifeLine Cell Technology (Walkersville, MD) as cryopreserved primary cultures of 49yr old male single-donor cells. Cells were plated at 1.5×10^5 cells/well (6-well plate) for gene expression and cell viability experiments or at 4×10^4 cells/well (24-well plate) for cell association experiments. Cells were incubated at 37°C in an environment of 5% CO₂ and 95% humidity and grown to 60-80% confluency in Vasculife growth medium (Vasculife Basal Medium + Vasculife smooth muscle cell supplement kit + gentamycin/amphotericin; LifeLine Cell Technology). Prior to

experimental use, cells were made quiescent in Dulbecco's Modified Eagle Medium (DMEM; Thermofisher Scientific) + gentamycin/amphotericin overnight.

3.2.4 Cytotoxicity Assays

At ~60% confluency, HASMCs were treated with PLPs, R8-PLPs, and CLPs at 200nM siRNA in DMEM. After 24h treatment, LIVE/DEAD® Viability/Cytotoxicity Kit (Thermofisher Scientific) was used to determine relative cell toxicity, according to the manufacturer's instructions. Briefly, DMEM was removed, cells were washed twice in PBS, and co-stained with calcein-AM + ethidium homodimer (1ul each /1ml PBS) for 15min at 37°C. Stained cells were visualized via fluorescein isothiocyanate (FITC; live) and Texas Red (dead) fluorescent filters. Images were acquired on both filters at 400x using a BX51 Olympus microscope with an Olympus Q-color camera (Olympus Corporation, Shinjuku, Tokyo, Japan) in three independent fields per sample. Cells were counted using ImagePro software (Media Cybernetics, Inc., Rockville, MD). Cellular toxicity was calculated as $[\text{dead cell count}/(\text{dead cell count} + \text{live cell count})]$ in each image, triplicates were averaged per independent sample, and the mean normalized to baseline cell death in non-treated controls of each experimental replicate.

3.2.5 Cell Association Experiments

To measure cell association, liposomes were assembled as described with the addition of Rho-DOPE at 0.1mol%. At ~80% confluency, HASMCs were treated with Rhodamine-labeled PLPs, R8-PLPs, and CLPs at 0.2mM total lipid in DMEM. After 24 hour treatment cells were washed twice in PBS, lysed with 1% Triton X-100, and centrifuged at 12,000 RPM for 5min at 4°C to remove cell debris. Cell lysates (100ul) were plated in duplicate in 96-well plates, and cell association of rhodamine-labeled liposomes was determined by fluorimetry at 575nm. Cell

association was determined by mean arbitrary fluorescence units (AFU) of each sample, minus baseline fluorescence of non-treated controls receiving no Rhodamine source within each experimental replicate. For qualitative analysis microscopy images were acquired with a Texas Red fluorescent filter at 400X under 400msec exposure across all groups.

3.2.6 Liposome Transfection and Gene Expression Analysis

HASMCs were transfected with PLPs, R8-PLPs, and CLPs at 200, 400, and 500nM siRNA in serum-free DMEM. After 24 hour transfection, DMEM was removed, and cells were incubated an additional 24h in Vasculife growth medium before collection for quantitative polymerase chain reaction (qPCR). All qPCR reagents were obtained from ThermoFisher Scientific unless otherwise noted. Total RNA was isolated using Ambion PureLink Total RNA Purification Kit according to manufacturer's instructions, and 200ng was converted to cDNA using the High Capacity RNA-to-cDNA Master Mix. Two microliters of cDNA transcripts were then amplified by qPCR using the TaqMan® Gene Expression Master Mix and predesigned TaqMan Gene Expression Assays specific for human GAPDH on the StepOne PCR system (Applied Biosystems, Foster City, CA, USA). The comparative cycle threshold method was used to determine relative quantity of GAPDH mRNA in liposome treated samples compared with non-treated controls (Control) or in samples receiving encapsulated GAPDH siRNA compared with NC siRNA, as indicated. All mRNA amounts were normalized to 18S ribosomal RNA as an endogenous control.

3.2.7 Statistical Analysis

All data are reported as mean \pm SEM. Statistical analyses were performed using Student's *t*-test or one-way ANOVA and a post-hoc Student-Newman-Keuls test using SigmaStat 3.5

software (Systat Software, Inc., San Jose, CA). Probability (*P*) values ≤ 0.05 were considered to be significant.

3.3 Results

3.3.1 EtOH Injection Assembly of PLPs, R8-PLPs, and CLPs Results in Nanoparticles with Similar Physical Characteristics.

STEM images confirm the spherical morphology and unilamellarity of each liposome class (Fig. 3.2). Dynamic light scattering confirms a narrow size distribution at ~ 50 - 150 nm following EtOH injection and extrusion of all liposome classes (Table 3.2). Zeta-potentials, determined by electrophoretic mobility measurements, demonstrate neutral-low positive charge of PLP and R8-PLP groups and an increased positive charge of CLPs (Table 3.2).

3.3.2 R8 Modification of PLPs Increases Encapsulation Efficiency of siRNA in a Concentration Dependent Manner.

EtOH injection assembly of non-modified PLPs results in siRNA encapsulation at $20.0 \pm 1.9\%$ using $500\mu\text{g}$ total lipid / $50\mu\text{g}$ siRNA ($n=6$; Fig 3.3). Addition of STR-R8 at $2.5\text{mol}\%$, $5\text{mol}\%$, and $10\text{mol}\%$ increases encapsulation to $63.1 \pm 3.8\%$, $68.0 \pm 2.4\%$, and $73.3 \pm 5.0\%$, respectively ($n=5-6$; Fig 3.3). These R8-PLP groups demonstrate an efficiency equivalent to CLPs ($60.3 \pm 12.0\%$; $P=\text{NS}$ vs. CLP; $n=5-6$; Fig 3.3).

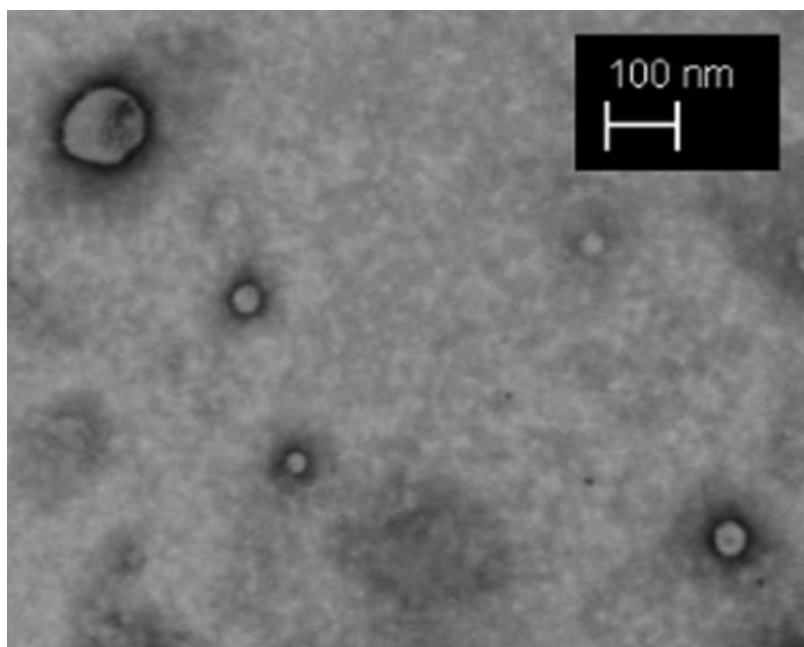


Figure 3.2: Scanning transmission electron microscopy (STEM) images confirming liposome morphology and lamellarity. A 2% phosphotungstic acid negative-stain method is used to visualize the spherical morphology and unilamellarity of liposomes assembled using the described EtOH injection assembly technique. Image is representative of each liposome class. Scale bar = 100nm.

Table 3.2: Liposome characterization.

Liposome Characteristics			
Liposome Class	Size (nm)	PDI	Zeta-potential
PLP	41.6±2.8	0.27±0.08	7.1±0.4
R8-PLP 1mol%	44.7±0.9	0.20±0.03	8.6±1.0
R8-PLP 2.5mol%	39.3±1.1	0.16±0.01	7.7±1.3
R8-PLP 5mol%	35.9±1.0	0.15±0.01	8.8±0.6
R8-PLP 10mol%	40.2±3.1	0.31±0.09	10.5±0.2
CLP	37.0±1.8	0.24±0.03	13.7±1.1

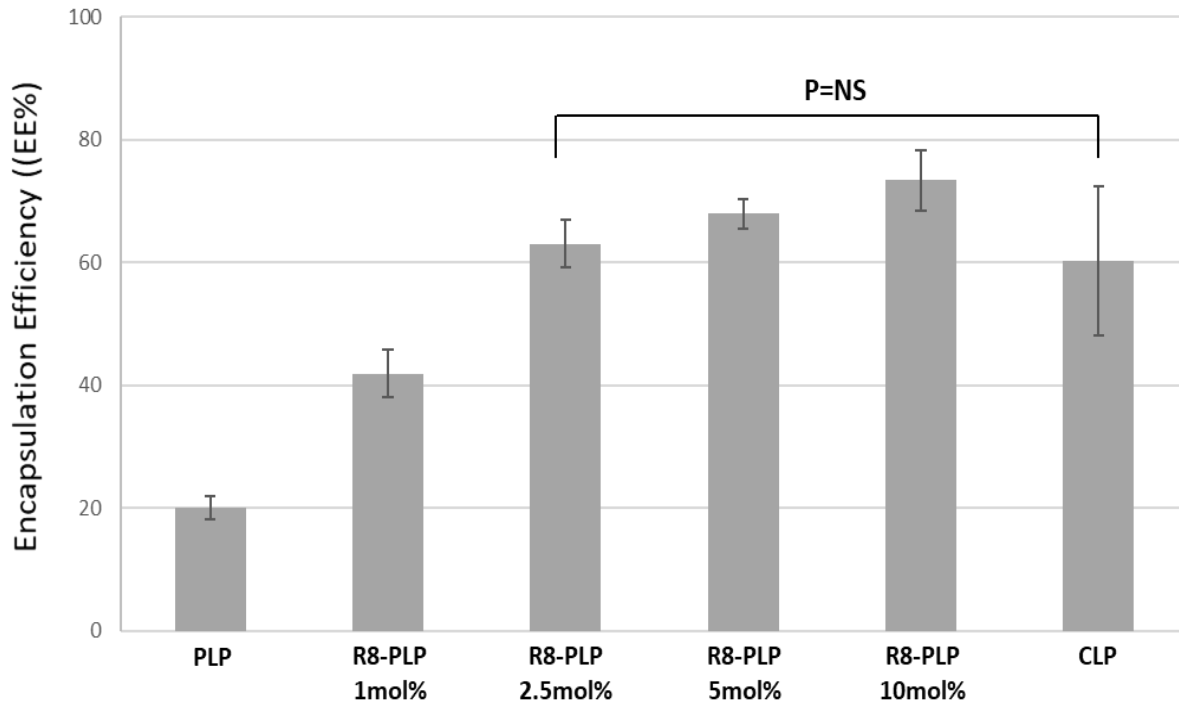


Figure 3.3: Graph showing increased siRNA encapsulation with increasing mol% of STR-R8. siRNA encapsulation of each liposome formulation was determined using Quant-iT RiboGreen RNA Assay Kit, and encapsulation efficiency (EE%) was calculated as $(\mu\text{g siRNA encapsulate} / 50\mu\text{g total siRNA}) \times 100$. R8 modification of PLPs increases EE% of siRNA in a manner equivalent to CLPs. P=NS within groups as indicated, n=5-6.

3.3.3 Non-cationic Liposomes Exhibited Significantly Less Cytotoxic Effects Compared to Cationic Liposomes.

Treatment of HASMCs with CLPs at 200nM siRNA increased cell death by 1.99 ± 0.27 -fold compared to baseline death of non-treated controls ($*P < 0.05$ vs. control; $n=3-6$; Fig 3.4). PLPs had no effect on baseline cell death of non-treated controls (0.98 ± 0.14 vs. 1.00 ; $P=NS$ vs. control; $n=3-6$). R8 modification of PLPs at 5 and 10mol% demonstrated no significant death over baseline (1.14 ± 0.18 and 1.19 ± 0.23 , respectively; $P=NS$ vs. control; $n=3-6$; Fig 3.4). PLP and all R8-PLP groups exhibited significantly lower cytotoxic effect than CLPs ($**P < 0.05$ vs. CLP; $n=3-6$, Fig 3.4).

3.3.4 R8 Lipid Surface Modification Significantly Increases the Cell Association of PLPs.

Treatment of HASMCs with CLPs at 0.2mM total lipid resulted in 22.3 ± 4.9 -fold increase in cell association compared to non-modified PLPs ($*P < 0.05$ vs. PLP; $n=3$; Fig. 3.5). R8 modification at 5 and 10mol% significantly increased cell association compared to non-modified PLPs ($**P < 0.05$ vs. PLP; $n=3$, Fig 3.5), with R8-PLP 10mol% resulting in the largest effect at 10.8 ± 2.4 -fold increase ($***P < 0.05$ vs. all other R8-PLPs; $n=3$; Fig 3.5).

3.3.5 Transfection with R8-PLPs, Modified at 10mol% STR-R8, Resulted in Significant GAPDH silencing, in a Manner Dependent on Lipid-to-siRNA Load Capacity.

R8-PLP-10mol% liposomes were used to deliver 200nM and 400nM siRNA to cultured HASMCs at lipid-to-siRNA weight/weight (w:w) ratios of 2.5:1-20:1. Delivery of GAPDH siRNA at 2.5:1 had no effect on GAPDH expression at either 200nM or 400nM siRNA. However, 400nM siRNA delivered with 5:1, 10:1, and 20:1 w:w liposomes resulted in significant

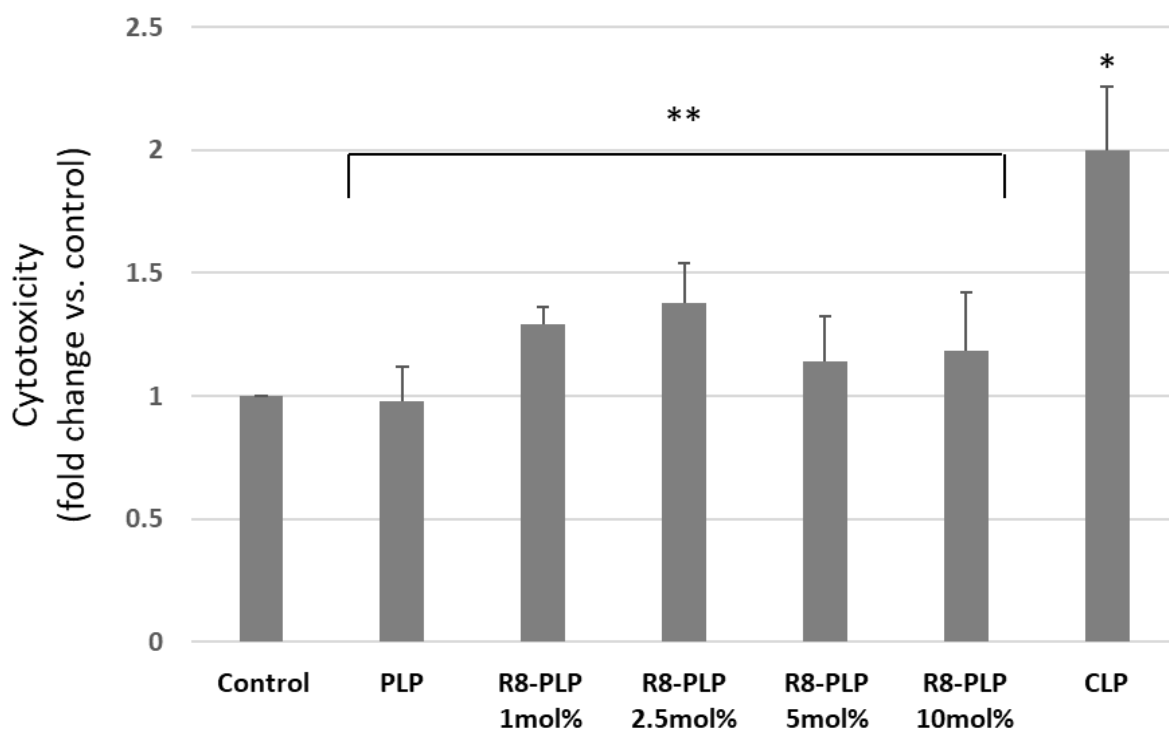


Figure 3.4: Cytotoxicity of R8-PLPs with increasing mol% R8 as compared to PLP and CLP controls. Cellular toxicity of each liposome formulation was determined by Live/Dead co-stain with calcein-AM and ethidium homodimer. Cells were visualized and counted under fluorescent microscopy, and toxicity was calculated as [dead cell count/(dead cell count +live cell count) and normalized to baseline cell death in non-treated controls. PLPs had no cytotoxic effect, and all R8-PLP groups exhibited significantly lower cytotoxic effect than CLPs. P=NS vs. non-treated control; *P≤0.05 vs. non-treated control; **P≤0.05 vs. CLP; n=3-6.

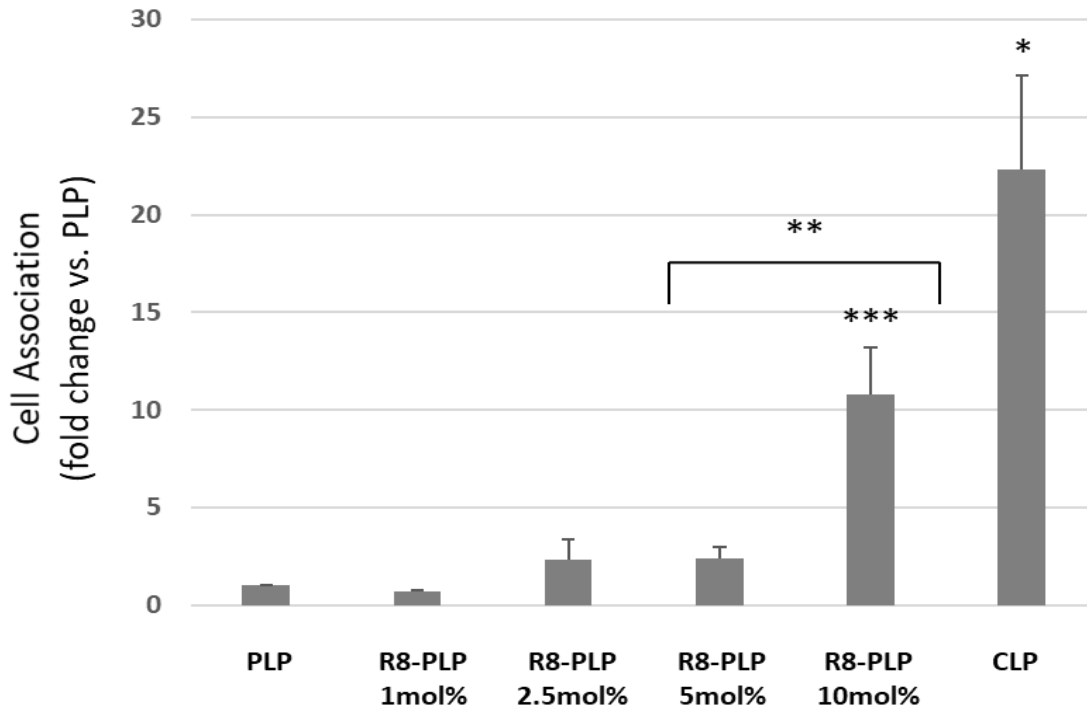


Figure 3.5: Graph of cell association of R8-PLPs as compared to CLPs and normalized to PLPs. Liposomes were assembled as described with the addition of Rho-DOPE at 0.1 mol%, and cell association was determined by mean arbitrary fluorescence units (AFU) of each sample, minus baseline fluorescence of non-treated controls receiving no Rhodamine source. R8 lipid surface modification at 5 and 10 mol% significantly increases cell association compared to non-modified PLPs. * and ** $P \leq 0.05$ vs. PLP; *** $P \leq 0.05$ vs. all other R8-PLPs; $n=3$.

GAPDH silencing when compared to non-treated controls (83 ± 2 , 68 ± 10 , and $41\pm 7\%$ relative expression, respectively; $*P\leq 0.05$ vs. control (non-treated); $**P\leq 0.05$ vs. control and CLP; $n=4-7$; Fig 3.6). Furthermore, 200nM siRNA was sufficient for significant GAPDH silencing when delivered at 10:1 and 20:1 w:w (83 ± 8 and $74\pm 9\%$ relative expression, respectively; $*P\leq 0.05$ vs. control (non-treated); $n=4-7$; Fig 3.6). To account for any off-target effects resulting from exposure to nanoparticle constituents alone, expression was also normalized to HASMCs receiving NC siRNA under identical liposomal delivery conditions. Effective silencing was confirmed with 400nM GAPDH siRNA at 10:1 and 20:1 w:w delivery when compared to NC siRNA controls (59 ± 18 and $42\pm 14\%$ relative expression, respectively; $*P\leq 0.05$ vs. control (NC siRNA); $n=3-4$; Fig 3.7) and with 200nM GAPDH siRNA at 10:1 w:w delivery when compared to NC siRNA controls ($71\pm 8\%$ relative expression; $*P\leq 0.05$ vs. control (NC siRNA); $n=3-4$; Fig 3.7). CLP-mediated delivery also resulted in modest but statistically significant silencing at both 200nM and 400nM (92 ± 4 and $93\pm 5\%$ relative expression vs. non-treated controls or 90 ± 3 and $94\pm 2\%$ relative expression vs. NC siRNA controls; $*P\leq 0.05$ vs. controls; $n=5-7$; Fig 3.6 and 3.7), while non-modified PLPs had no effect on gene silencing under any condition. Importantly, R8-PLP-10mol% formulations demonstrated GAPDH silencing that was significantly better than CLP-mediated silencing under multiple treatment parameters ($**P\leq 0.05$ vs. control and CLP; $n=4-7$; Fig 3.6).

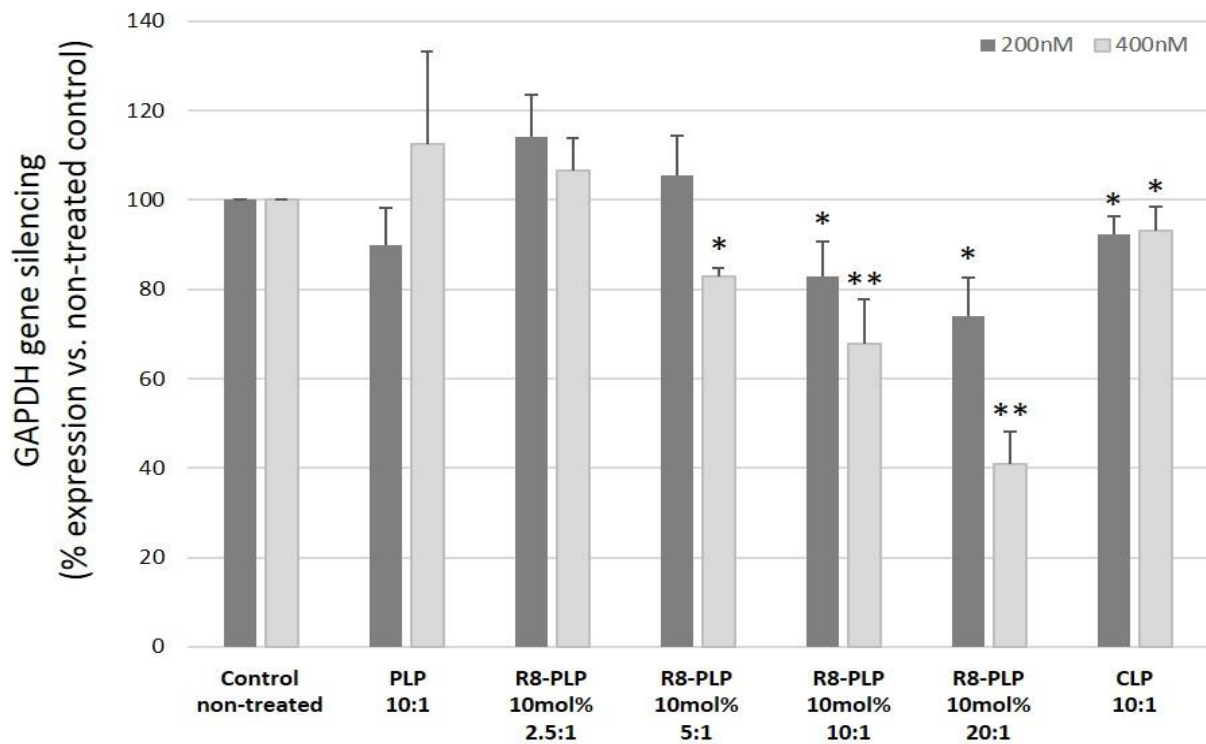


Figure 3.6: Graph of silencing efficiency of R8-PLP siRNA compared CLP-loaded siRNA. R8-PLP-10mol% liposome transfection demonstrated significant silencing, in a manner dependent on lipid-to-siRNA load capacity when tested at w:w ratios of 2.5:1-20:1. * $P \leq 0.05$ vs. non-treated control; ** $P \leq 0.05$ vs. control and CLP; $n=3-7$.

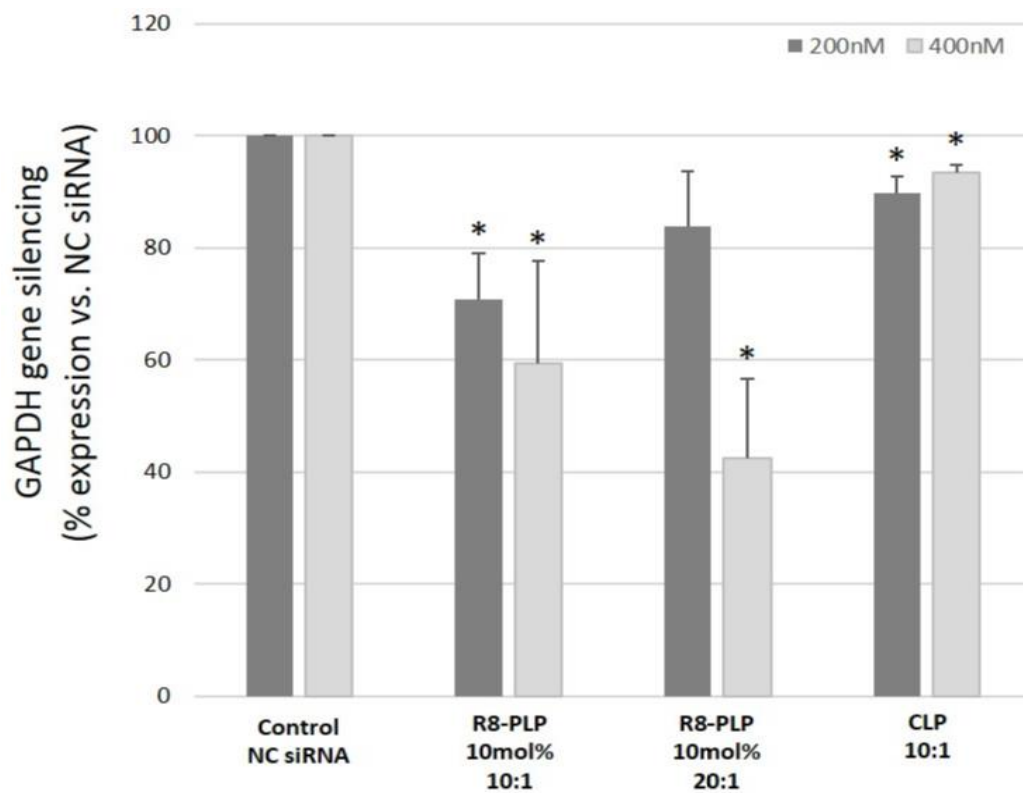


Figure 3.7: Graph of silencing efficiency of R8-PLP-loaded siRNA compared to NC siRNA. Liposomal mediated gene silencing was determined by qPCR, using the comparative cycle threshold method to determine relative quantity of GAPDH mRNA in liposome treated samples compared with non-treated controls (Control) or in samples receiving encapsulated GAPDH siRNA compared with NC siRNA, as indicated. * $P \leq 0.05$ vs. NC siRNA control; $n=3-7$.

3.4 Discussion

Gene therapy has shown promise as a novel therapeutic modality in the treatment of PVD and IH development.^{40,114,115} Specifically, RNAi could be used to alter or inhibit vascular pathologies in a gene-specific manner. An ideal vector for siRNA-mediated gene modulation would require a molecular carrier capable of enhanced transfection, reduced cytotoxicity, and increased stability *in vitro* and *in vivo*. Successful *in vitro* gene silencing has been demonstrated in vascular cell types using viral vectors, cationic polymers, and lipid-based nanoparticles. Cationic liposomes have been demonstrated as effective molecular carriers for vascular cell types *in vitro* due to enhanced association with negatively charged cell membranes, optimal loading efficiency of siRNA during lipoplex formation, and reduced susceptibility to nuclease activity.¹¹⁶ However, translational success of cationic liposome-mediated transfection has been limited due to elevated immunogenicity, cytotoxicity, and hepatic clearance *in vivo*.^{117,118} The design of a CPP-modified neutral liposome, formed with natural lipid constituents, could provide enhanced encapsulation and cell association properties, while avoiding the adverse cytotoxic effects associated with cationic lipid nanocarriers.

Here we aimed to compare neutral liposomes, with and without CPP modification, to a standard CLP formulation frequently described in the RNAi literature, in order to examine their efficacy as nanocarriers in VSMCs. We utilized a modified EtOH injection technique to assemble PLPs, R8-PLPs, and CLP groups with encapsulated siRNA as our molecular cargo for delivery (Fig 3.1, Table 3.2). This method proved to be effective in forming unilamellar liposomes with spherical morphology and a narrow size distribution of <45nm in all groups ($PDI \leq 0.31 \pm 0.09$; Fig 3.2, Table 3.1). Typically, positively charged lipid nanoparticles, with augmented size (>150 nm), have reduced half-life due to opsonin-dependent clearance and elevated hepatic removal

rates.^{119,120} Previous *in vivo* studies using liposome-mediated gene therapy have shown neutrally-charged liposomes <100nm in diameter to have increased half-life *in vivo*.^{121,122} The size and zeta potential data presented here validates our modified EtOH injection assembly method as a valid technique for these *in vitro* and future *in vivo* investigations of liposomal nanoparticles.

R8 is a well-established CPP that has been shown to enhance membrane translocation of a wide variety of biological cargo, including neutral liposomes.^{88,123,124} To construct CPP-modified liposomes in this study, STR-R8 was anchored into the lipid bilayer in order to expose R8 on the liposome surface. Because efficient drug loading of anionic siRNA within neutral PLPs has proven difficult, it is important to note that we were able to demonstrate enhanced siRNA encapsulation with STR-R8 incorporation, to a degree equivalent to that of CLPs (Fig 3.3). This enhanced loading efficiency could be attributed to 1) the Ca²⁺-modulated condensation of siRNA inherent in our modified assembly technique, and 2) the cationic nature exhibited by the R8 peptide, which is attracted to the negatively charged phosphate backbone of the siRNA molecule. In fact, addition of STR-R8 to the liposomal formulation was associated with a modest increase in overall membrane zeta-potential, slightly skewing the charge of our CPP-modified liposome toward a more cationic nature (Table 3.2). However, using this assembly method for R8-PLPs, we were able to achieve CLP-equivalent siRNA loading without reaching elevated CLP-equivalent surface charges. Previous studies using similar EtOH injection techniques have demonstrated enhanced encapsulation of siRNA (~80%) with non-PEGylated liposomes comprised of DOPC and cholesterol as bulk lipid constituents. However, the addition of PEG into the lipid formulation drastically reduced siRNA encapsulation.⁷⁰ Our results confirm the ability to enhance molecular drug loading in PEGylated liposomes via the utilization of STR-R8. This is a significant finding

considering PEGylation would be required to avoid premature clearance in future *in vivo* applications using lipid nanoparticles.

The immunogenicity and cytotoxicity associated with cationic liposomes has prevented *in vivo* translation for CLP formulations frequently described in the RNAi literature. These effects could be attributed to both their cationic nature and the presence of synthetic lipid constituents in their formulations.¹¹⁰ Though the addition of STR-R8 in the assembly of our CPP modified neutral liposome showed modest increases in overall surface charge, all PLP and R8-PLP groups were shown to be significantly less cytotoxic than CLPs (Fig. 3.4). In fact, most neutral liposomes exhibited no cytotoxic effect at all, with cell death rates being equal to that of baseline. Furthermore, consistent with R8's enhanced translocation properties demonstrated in previous gene transfer studies, even low levels of STR-R8 addition (>2.5mol%) enhanced cellular association of neutral liposomes in our study (Fig 3.5).^{69,125,126} Specifically, R8-PLP-10mol% dramatically enhanced cell association of non-modified-PLPs, though not to a level comparable to tested CLP formulation. However, while there was no R8-PLP-10mol% effect on cytotoxicity, CLPs were almost 2-fold more toxic than baseline. Synthetic lipid constituents typically comprising cationic liposomes, such as DOTAP in our CLP formulation, are responsible for imparting their positive charge characteristics. However, once endocytosed, these unnatural lipids cannot be efficiently degraded by the cell, thus promoting unfavorable interaction with other cellular components.¹²⁷ Alternatively, because STR-R8 is comprised of natural amino acids, and all neutral PLP groups were composed of native lipid constituents, these liposomal nanoparticles can be more efficiently degraded by the cell upon delivery, thus foregoing the cytotoxic effects commonly seen in CLP-mediated transfection. The negligible cytotoxicity, concurrent with

enhanced cellular association, exhibited by R8-PLPs here has revealed this class of CPP-modified PLPs as an ideal candidate for *in vitro* and future *in vivo* applications.

Due to the ideal cytotoxicity and cellular association profiles demonstrated here, R8-PLP-10mol% was empirically identified as an optimal R8-PLP for further investigation in its efficacy as a molecular nanocarrier for liposomal-mediated RNAi in VSMCs. Based on our previous studies with polymeric bioconjugates, suggesting differential cargo carrying capacities across nanoparticle materials, we tested variations in lipid-to-siRNA w:w ratios as a means of delineating the optimal carrying capacity of our R8-PLP-10mol% liposomal formulation. For this proof-of-concept analysis, GAPDH was targeted as our gene of interest due to its abundant expression, ease of knockdown evaluation, and our groups previously established protocols to demonstrate chemical and polymeric transfection efficacy of VSMCs *in vitro* using siGAPDH screening.^{106,107} Here w:w was adjusted between 2.5-20:1 using R8-PLP-10mol% and tested alongside PLP and CLP groups to compare gene silencing efficiency using qPCR analysis of GAPDH expression. We were able to demonstrate significant silencing at both 10:1 and 20:1 w:w R8-PLP-10mol% when compared to non-treated controls, while silencing with non-modified PLP and CLPs was not significant. While the requirement for CPP modification of PLPs in order to achieve significant silencing was an expected result, the lack of CLP effectiveness was an interesting finding. This may be explained by reduced cytosolic uptake and increased lysosomal degradation imposed by the addition of PEG molecules to the CLP surface. The PEG shell around the exterior of the liposome nanoparticle is roughly 5nm in thickness and completely surrounds the CLP surface, reducing the interaction between the cationic lipid head group of DOTAP and the endosomal membrane, thereby effectively eliminating endosomal fusion and escape. In the case of STR-R8 it would appear that the extension of R8 peptide into the PEG shell allows for a more favorable interaction for

endosomal escape into the cytosol required for the siRNA-mediated gene silencing.^{124,128-130} To account for any non-specific effects on baseline gene expression that may result from exposure to nanoparticle constituents alone, comparative analysis was also performed against cells transfected with NC siRNA under identical exposure conditions. Significant silencing efficiency was further confirmed, eliminating the possibility for off-target effects of the lipid constituents playing a role in gene regulation including possibilities such as mRNA half-life regulation, cellular metabolism regulation, etc. Interestingly, w:w analysis demonstrated a high lipid requirement for effective siRNA delivery. This suggests the need to form nanoparticles with a low liposomal carrying capacity for efficient drug delivery (i.e. concentrated liposomes carrying reduced siRNA cargo per liposomal carrier). This information can be important for the future development of efficient transfection protocols to test molecular targets of IH-associated genes for *in vitro* phenotypic analyses. But more importantly, defining an appropriate nanoparticle carrying capacity range will be imperative for translation to *in vivo* models where lipid load and biodistribution studies will be paramount in determining efficacy.

Further modifications for optimizing R8-PLP mediated transfection are still warranted, as the level of silencing achieved in this study, using our liposomal carriers of interest, was lower than levels that could be considered efficacious. This may be attributable to steric hindrance provided via the PEG “shield”.¹³¹ The thickness of the linear PEG shell surrounding the liposome surface (at ~5nm) is still about twice the length of the R8 peptide. It is plausible the PEG chain is partially shielding the R8 peptide and thereby preventing its full cell penetrating properties. However, maintaining the PEGylated properties of our drug delivery platform moving forward will be paramount. The translation of liposomes to *in vivo* animal models has been extensively studied, with results showing that grafting PEG to the surface is essential to reduce opsonization,

improve stability, and increase half-life when administered in the vasculature.¹³² Therefore, our future studies could investigate alternative avenues for the addition of R8 utilizing this PEG moiety as a backbone for assembly, such as post-insertion or post-conjugation to the outer edge of PEG using cyclooctyne as the clickable PEG moiety against azido-equipped peptides via copper-free click chemistry techniques.¹³³

In conclusion, we have established PLPs containing 10mol% STR-R8 as an optimal transfection agent with minimal cytotoxicity and enhanced transfection capacity as compared to CLPs in VSMCs. This nanoparticle could prove to be an optimal molecular nanocarrier in the application of vascular gene therapeutics. More *in vitro* studies are needed to further develop this lipid-based nanoparticle for application in translational medicine, but continued development of this liposome delivery system could provide an avenue to a therapeutic treatment in the pathological development of IH in a surgical model.

CHAPTER 4: The Assembly of Ligand-modified PEGylated Liposomes for Cell-type Selectivity in Vascular Cell Types

The following chapter will be submitted for publication in a peer-reviewed manuscript format at a future date.

4.1 Introduction

The utilization of surgery bypass grafting has gradually declined due to the advancements of minimally invasive endovascular procedures such as percutaneous transluminal angioplasty (PTA) and stent implantation. Unfortunately, intimal hyperplasia (IH) is a common adverse response to PTA with or without stenting that can lead to restenosis and further revascularization procedures with higher mortality and morbidity rates. Endothelial denudation is an avoidable injury event during PTA revascularization procedures that exposes the underlying subendothelial matrix and vascular smooth muscle cells (VSMCs) to hemodynamic flow. The endothelium, along with producing vasoactive compounds and providing an impermeable barrier to the underlying medial layer, has been shown to preserve the quiescent state of VSMCs through the local production of nitric oxide (NO).¹³⁴ For this reason, reendothelialization is considered a necessary cellular event for long-term inhibition of neointimal formation after vascular injury. In fact, a recent study demonstrated that VSMCs only appear in intimal layer areas lacking vascular endothelial cell (VEC) recovery seven days after injury.¹³⁵

Despite recent studies suggesting a focus on reendothelialization as therapeutic strategy for IH-induced restenosis, the dysfunctional migration and proliferation of VSMCs has been traditionally labeled as the key target of pharmacological interventions aimed at reducing restenotic development in a surgical setting. Accordingly, most therapeutic interventions for IH-induced restenosis are aimed at attenuating the proliferative response of VSMCs at the site of the treated lesion. For example, the use of antimitotic agents, like paclitaxel and sirolimus, have

been successfully deployed in drug-eluting stents to reduce acute intimal thickening.¹³⁶ However, chronic restenosis still occurs in up to 60% of patients at 12-month follow-up angiography primarily due to the concomitant inhibition of VEC recovery inherent in anti-proliferative strategies. To increase therapeutic efficacy of current medical interventions in the reduction of IH-induced restenosis, a cell-specific therapeutic strategy that inhibits the proliferative response of VSMCs while promoting VEC recovery is required.

Liposomes are highly biocompatible drug delivery systems (DDS) that can be surface decorated with ligands for a variety of downstream applications, including the directed cell-specific interaction within diseased tissues. This so-called “active targeting” through cell-targeting peptide (CTP) modification has emerged as a valuable strategy to enhance liposomal DDS properties and improved therapeutic index. The short peptide fragments REDV and VAPG have recently been shown to selectively bind vascular VECs and VSMCs, respectively.¹³⁷ We have postulated that these vascular cell-specific ligands, when conjugated to a noncationic PEGylated liposome (PLP) surface, could impart a nanotechnology capable of delivering pharmacological cargo in a cell-specific manner. Here we aim to establish the cell selective potential of VEC-specific (EC-PLP) and VSMC-specific (SMC-PLP) PLPs through the surface conjugation of REDV and VAPG, respectively. This approach could provide the ability to simultaneously deliver a multitude of gene therapeutics or established pharmaceuticals aimed at the simultaneous reduction of VSMC migration and proliferation while simultaneously promoting VEC recovery.

4.2 Materials and Methods

4.2.1 PLP Assembly via Ethanol Injection Technique

Liposome Constituents

All liposome formulation constituents are defined in Table 4.1. Lipids and cholesterol were purchased from Avanti Polar Lipids (Alabaster, AL, USA). In accordance with previous literature establishing cell-specific capacity of REDV and VAPG peptide fragments, respectively, a glycine spacer was used for the REDV peptide and a valine-glycine dual amino acid spacer was used for the VAPG peptide. The custom REDV peptide was purchased with an azido-modified lysine from P3 Biosystems (Louisville, KY, USA). The custom VAPG peptide was purchased with an azido-modified lysine from P3 Biosystems (Louisville, KY, USA).

Liposome Assembly

Base PLP nanoparticles were formed with bulk lipid DOPC:chol at 7:3mol plus 10mol% DSPE-PEG, and were assembled using a previously described EtOH injection technique. Briefly, lipids were dissolved in CHCl_3 , combined as indicated, and dried under N_2 gas and vacuum to remove remaining solvent. Dried lipids were then resuspended in molecular grade 100% EtOH. 300uL 10mM Tris-HCl at pH 8.0 with 0-50mM CaCl_2 was injected with 1000-2000 ug total lipid/200uL in 100% EtOH, under constant vortexing at room temperature (RT). EtOH and un-encapsulated siRNA was removed from liposomes via 24hr dialysis against PBS, pH 7.4 at 4 °C. Liposomes were extruded using 100nm polycarbonate NanoSizer™ extruders from T&T Scientific prior to characterization (Knoxville, TN, USA).

Table 4.1: Liposome formulation constituents and associated acronyms.

Liposome Formulation Components	
Lipid Constituent	Acronym
I,2-dioleoyl-sn-glycero-3-phosphocholine	DOPC
cholesterol	chol
I,2-distearoyl-sn-glycero-3-phosphoethanolamine-N-[amino(polyethylene glycol)-2000]	DSPE-PEG
I,2-distearoyl-sn-glycero-3-phosphoethanolamine-N-[dibenzocyclooctyl(polyethylene glycol)-2000]	DSPE-PEGdbco
I,2-dioleoyl-sn-glycero-3-phosphoethanolamine-N-(lissamine rhodamine B sulfonyl)	Rho-PE
VAPG-conjugated to DSPE-PEG	VAPG-PEG
REDV-conjugated to DSPE-PEG	REDV-PEG
SMC-targeted PLP	SMC-PLP
EC-targeted PLP	EC-PLP
Cell-targeting peptide-conjugated PLP	CTP-PLP

4.2.2 CTP-PLP assembly via VAPG and REDV Amphiphile Incorporation

REDV-PEG and VAPG-PEG Synthesis

DSPE-PEGdbco, a form of DSPE-PEG with a cyclooctyne modification commonly used in azide-alkyne cycloaddition reactions (i.e. click chemistry), was used to form REDV-PEG and VAPG-PEG amphiphiles for PLP incorporation. Briefly, equimolar azido-modified REDV and VAPG peptides were combined with DSPE-PEGdbco at RT under constant agitation for 2hr, according to previously established reaction conditions.^{71,72}

PLP Modification with REDV-PEG or VAPG-PEG

For all modification strategies, base PLPs were assembled via EtOH injection as described, and were modified by substituting DSPE-PEG with REDV-PEG or VAPG-PEG amphiphiles at equal mol%, respectively. In this way mol% PEG was kept constant across all conditions to control PEG-induced changes in cell association while comparing cell associative contributions from REDV or VAPG, respectively.

Modification via Pre-insertion

REDV-PEG or VAPG-PEG were combined at 1-5mol% with base PLP lipid constituents at the time of lipid drying under N₂ gas. Likewise, lipid hydration with EtOH was performed in one-step and all lipid constituents were incorporated at the time of initial liposome assembly. Liposomes were purified from un-encapsulated siRNA as described, prior to extrusion and characterization.

Modification via Post-insertion

Base PLPs were assembled as described without the incorporation of R8 amphiphiles. Following PLP purification by dialysis, R8-PEG or STR-R8 were combined with pre-formed base PLPs and incubated at 4°C overnight or 37°C for 4 hours, according to previously established conditions for lipid transfer. A second overnight dialysis was performed following R8-amphiphile insertion to remove any un-retained siRNA encapsulate, prior to extrusion and characterization.

4.2.3 Liposome Characterization Studies

Size, Homogeneity, and Charge Characterization

The mean size, associated polydispersity index (PDI), and zeta potential of all liposome preparations were measured by dynamic light scattering and relative electrophoretic mobility in water using the Zetasizer Nano ZS instrument (Malvern Instruments Ltd., Worcestershire, UK).

Morphological Characterization by Scanning Transmission Electron Microscopy

Liposome morphology and lamellarity were investigated by STEM using a negative-stain method. Liposomes were applied dropwise to a carbon film coated copper grid and allowed to air dry. Liposome films were then stained with 2% phosphotungstic acid and air-dried for 1 min at room

temp. Samples were visualized with Zeiss Auriga 40 STEM scope, and images were acquired by SmartSEM image acquisition software (Carl Zeiss, Inc., Oberkochen, Germany).

4.2.4 Vascular Cell Culture

Human aortic smooth muscle cells (HASMCs) and Human aortic endothelial cells (HAECs) were obtained from LifeLine Cell Technology (Walkersville, MD). Cells were incubated at 37°C in an environment of 5% CO₂ and 95% humidity and grown in Vasculife growth medium (Vasculife Basal Medium + Vasculife smooth muscle cell supplement kit OR Vasculife endothelial growth supplement kit + gentamycin/amphotericin; LifeLine Cell Technology).

4.2.5 Cell Association Experiments

To measure cell association, liposomes were assembled as described with the addition of Rho-PE at 0.5mol%. VSMCs were treated with Rhodamine-labeled neutral PLPs and CTP-PLP groups at 100uM total lipid in DMEM at >80% confluency. After 1hr, 4hrs and 24hr liposome exposure, cells were washed three times in PBS and qualitatively imaged by fluorescent microscopy. Images were acquired with a Texas Red fluorescent filter at 400X under 400msec exposure across all groups. For quantitative analysis, cells were washed three times in PBS, lysed with 1% Triton X-100, and centrifuged at 12,000 RPM for 5min at 4°C to remove cell debris. Cell lysates (100ul) were plated in duplicate in 96-well plates, and cell association of rhodamine-labeled liposomes was determined by fluorimetry at 575nm. Cell association was determined by mean arbitrary fluorescence units (AFU) of each sample, minus baseline fluorescence of non-treated controls receiving no Rhodamine source within each experimental replicate.

4.2.6 Statistical Analysis

All data are reported as mean \pm SEM. Statistical analyses were performed using Student's *t*-test or one-way ANOVA and a post-hoc Student-Newman-Keuls test using SPSS 25 software (Systat Software, Inc., San Jose, CA). Probability (*P*) values ≤ 0.05 were considered to be significant.

4.3 Results

4.3.1 The Incorporation of CTP Does Not Significantly Affect Size or Homogeneity of CTP-PLPs Compared to PLP Controls.

The incorporation of VAPG-PEG via pre-insertion or post-insertion does not significantly affect the nanoparticle size or PDI of assembled SMC-PLPs compared to PLP controls (Fig 4.1 and 4.2). Likewise, the incorporation of REDV-PEG does not significantly affect size or PDI of assemblies VEC-PLPs compared to PLP controls (Fig 4.3 and 4.4).

4.3.2 The Incorporation of VAPG-PEG into PLP Base Formulations Results in Desired Morphological Characteristics.

TEM images of SMC-PLPs modified with 5 mol % VAPG-PEG confirms size of < 100 nm in diameter, spherical morphology, and unilamellarity (Fig 4.5). Quantitative measurements made using SmartSEM image acquisition software showed a diameter of 71.35 nm and 73.86 nm, respectively. From this we can see that all liposomal nanoparticles shown in image fall within size distribution exhibited by DLS data.

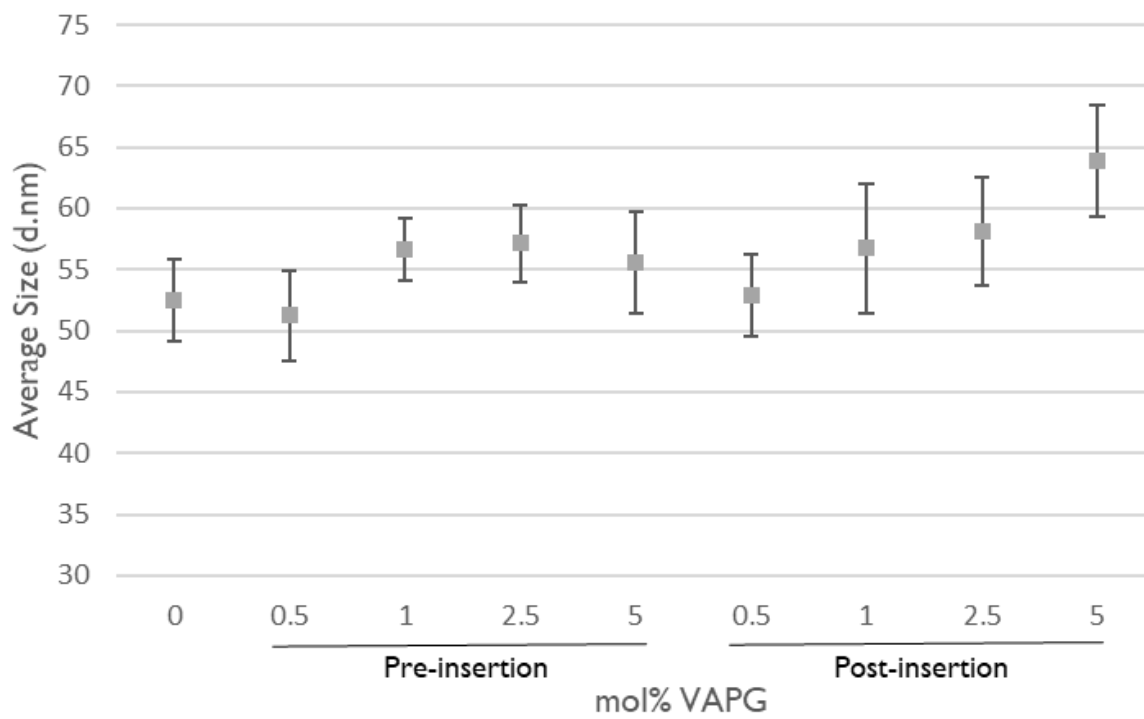


Figure 4.1: Comparison of average size (d.nm) as a result of VAPG incorporation into PLPs using pre-insertion and post-insertion techniques.

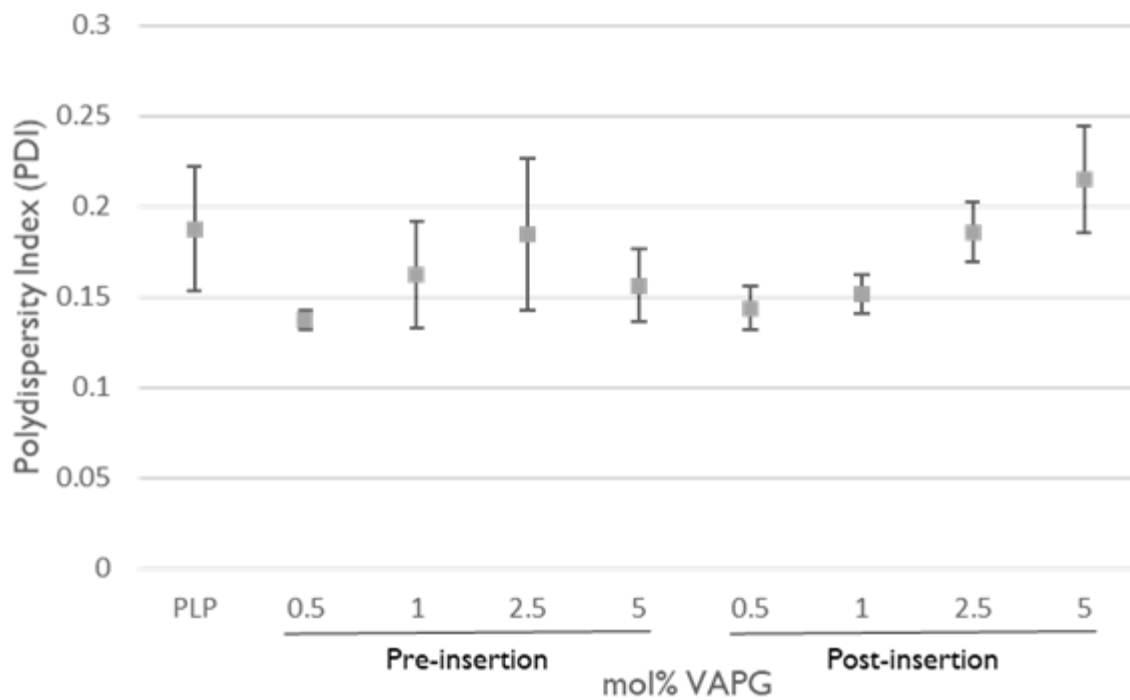


Figure 4.2: Comparison of polydispersity index (PDI) as a result of VAPG incorporation into PLPs using pre-insertion and post-insertion techniques.

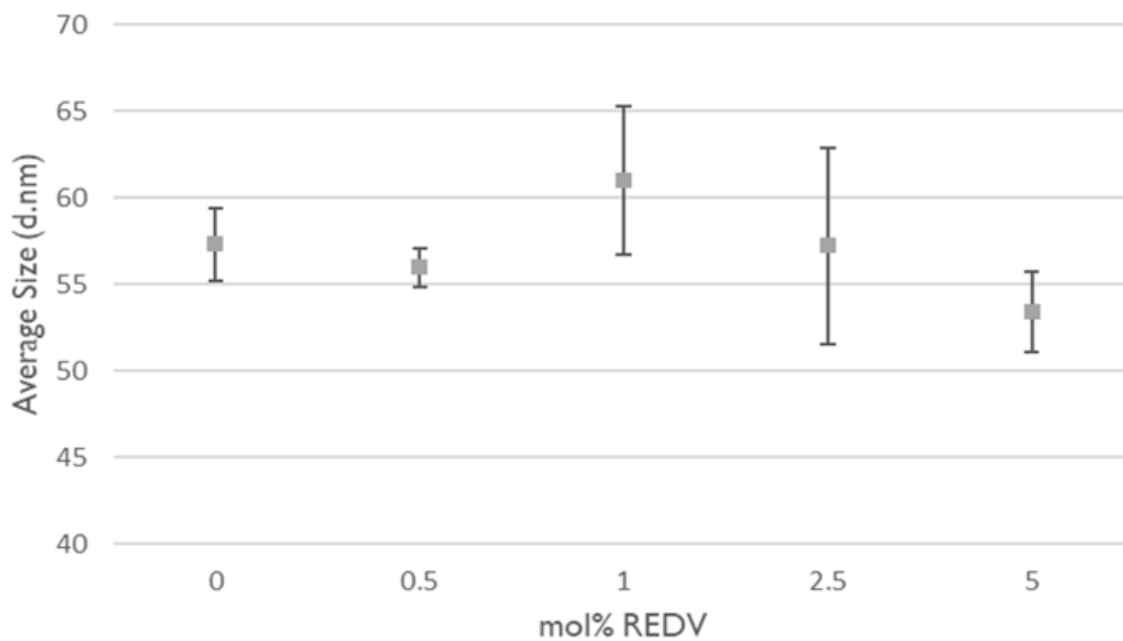


Figure 4.3: Comparison of average size (d.nm) as a result of REDV incorporation into PLPs using pre-insertion technique.

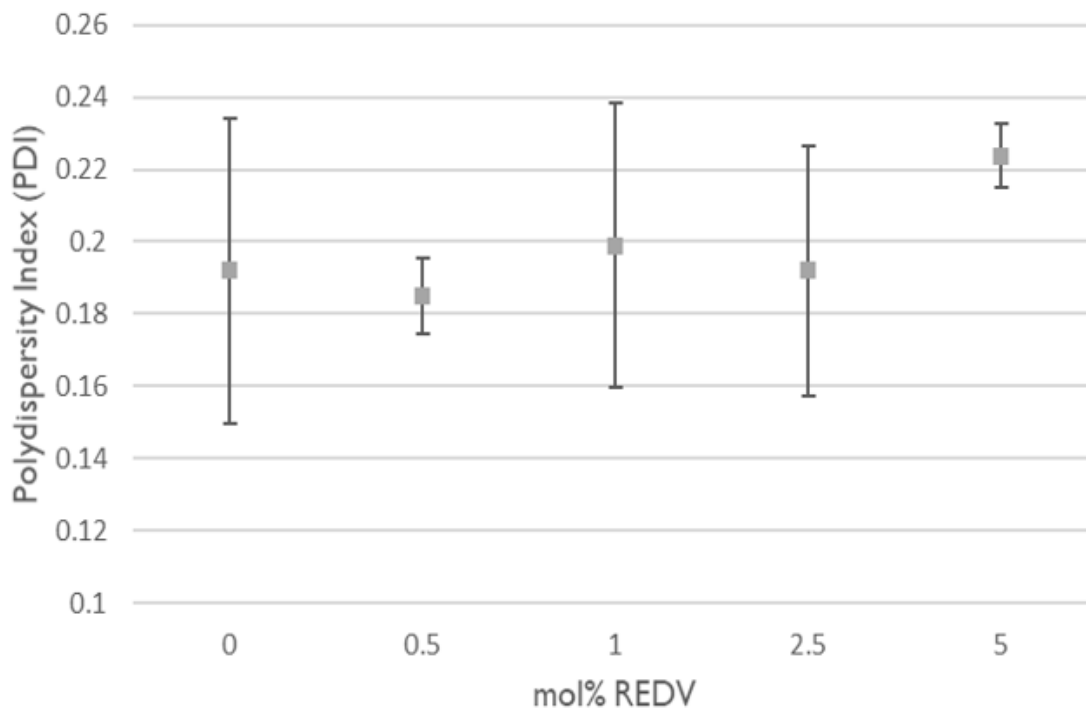


Figure 4.4: Comparison of average size (d.nm) as a result of REDV incorporation into PLPs using pre-insertion technique.

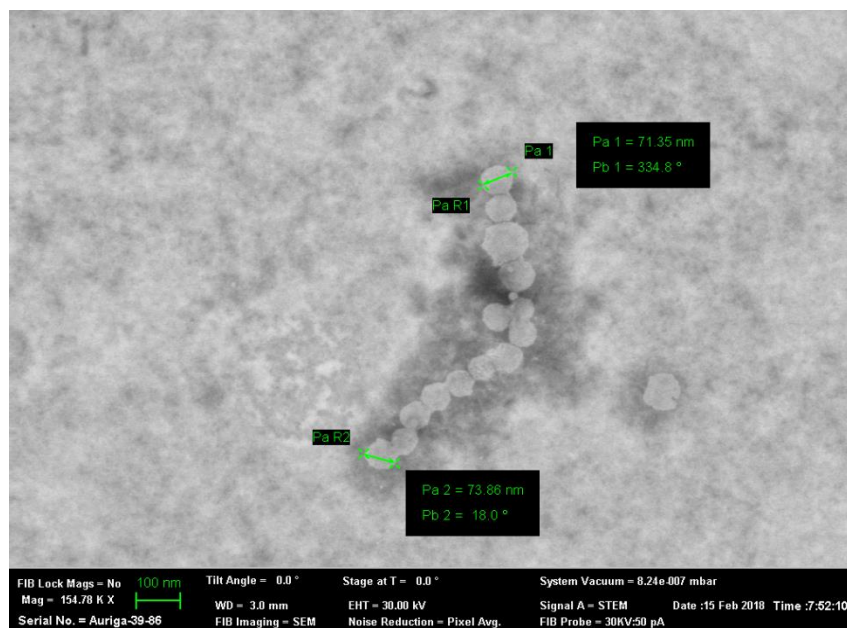


Figure 4.5: STEM images of SMC-PLPs modified with 5 mol % VAPG. This image confirms that the assembly process preserves liposomal morphology and unilamellarity, and confirms quantitative size measurements made with DLS.

4.3.3 The Incorporation of VAPG-PEG into SMC-PLPs Increases Cell Association Above PLP Controls in VSMC but Not VEC.

The incorporation of 0.5, 1.0, 2.5, and 5.0mol% VAPG-PEG via pre-insertion achieved 2.31±0.73, 2.45±0.65, 3.02±0.73, and *3.42±0.77-fold increase in cell association in VSMC and 1.17±0.18, 1.23±0.18, 1.75±0.39, and 2.01±0.59-fold increase in cell association in VEC, respectively, after 4 hour treatment (*P<0.05 vs. PLP in SMC; n=5, Fig. 4.6).

4.3.4 The Incorporation of VAPG-PEG into SMC-PLPs via Post-insertion Does Not Significantly Increase Cell Association in SMCs Compared to PLP Controls.

The incorporation of 0.5, 1.0, 2.5, and 5.0mol% VAPG-PEG via post-insertion achieved 1.93±0.80, 2.11±0.65, 1.86±0.66, and 1.96±0.43-fold increase in cell association in VSMC and 1.57±0.36, 2.26±0.47, 2.03±0.54, and 2.32±0.44-fold increase in cell association in VEC, respectively, after 4 hour treatment (Fig. 4.7).

4.3.5 The Incorporation of REDV-PEG into EC-PLPs Increases Cell Association Above PLP Controls in VEC but Not VSMC at Early Exposure.

The incorporation of 0.5, 1.0, 2.5, and 5.0mol% REDV-PEG via pre-insertion achieved 0.95±0.17, 1.32±0.15, 1.10±0.12, and 1.09±0.28-fold change in cell association in VSMC and 1.11±0.07, *1.59±0.01, 1.38±0.16, and 1.35±0.30-fold change in cell association in VEC, respectively, after 1 hour treatment (*P<0.05 vs. PLP in VEC; n=3, Fig. 4.8).

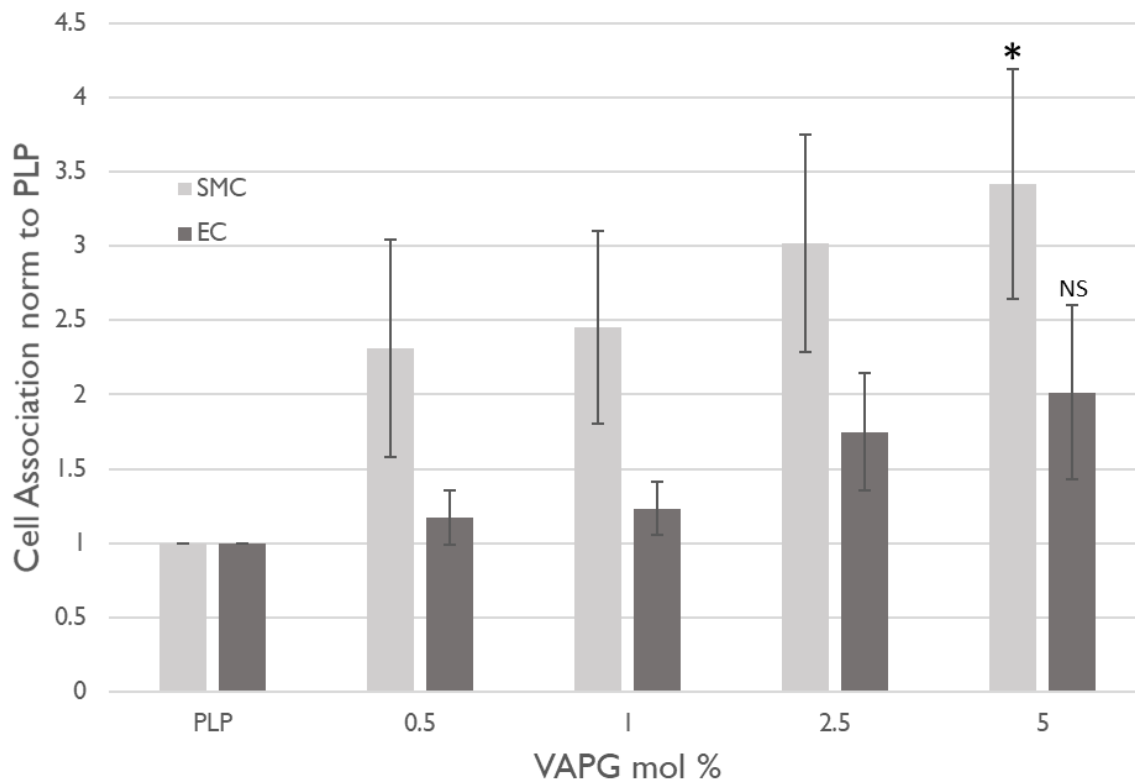


Figure 4.6: The relative cell association of VAPG modified CTP-PLPs compared in HASMCs and HAECs. PLP controls and SMC-PLPs were assembled as described with the addition of Rho-DOPE at 0.5mol%, and cell association was determined by mean arbitrary fluorescence units (AFU) of each sample, minus baseline fluorescence of non-treated controls receiving no Rho-DOPE. *P<0.05 vs. PLP in VSMC; n=5; NS vs. PLP in VEC.

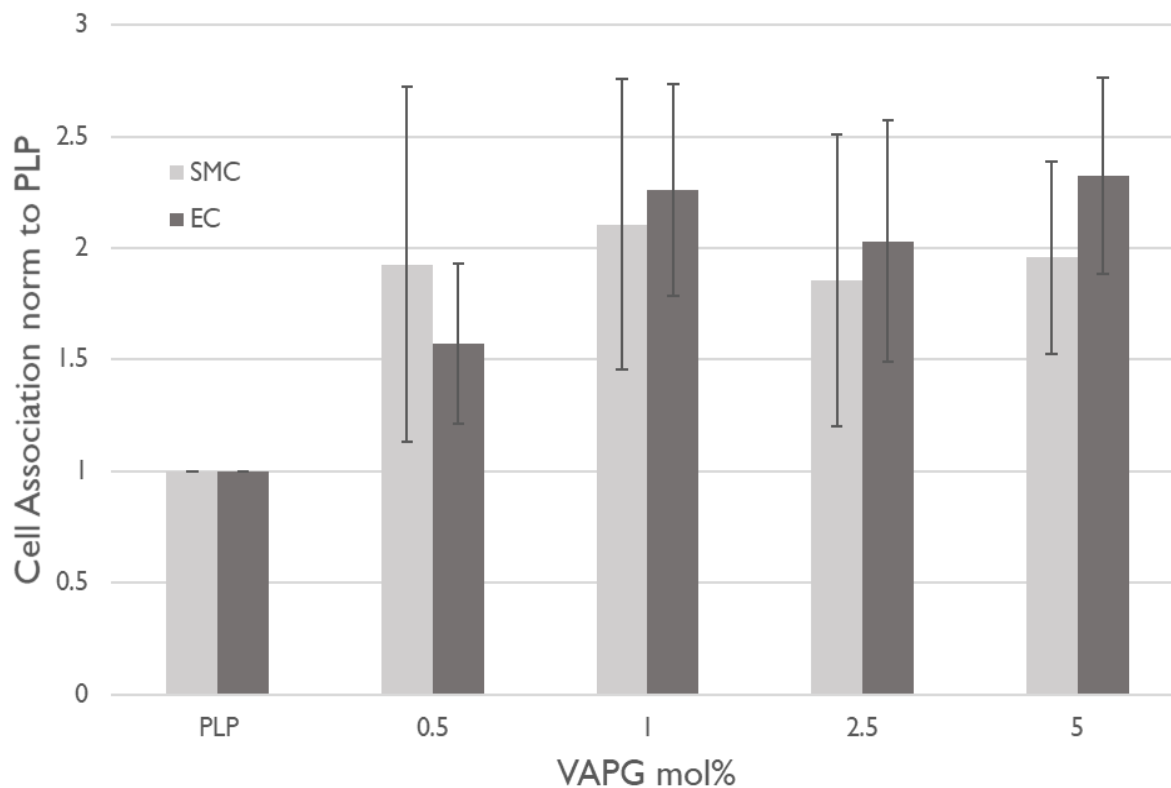


Figure 4.7: The relative cell association of VAPG modified CTP-PLPs using post-insertion technique compared in VSMCs and VECs. PLP controls and SMC-PLPs were assembled as described with the addition of Rho-DOPE at 0.5mol%, and cell association was determined by mean arbitrary fluorescence units (AFU) of each sample, minus baseline fluorescence of non-treated controls receiving no Rho-DOPE.

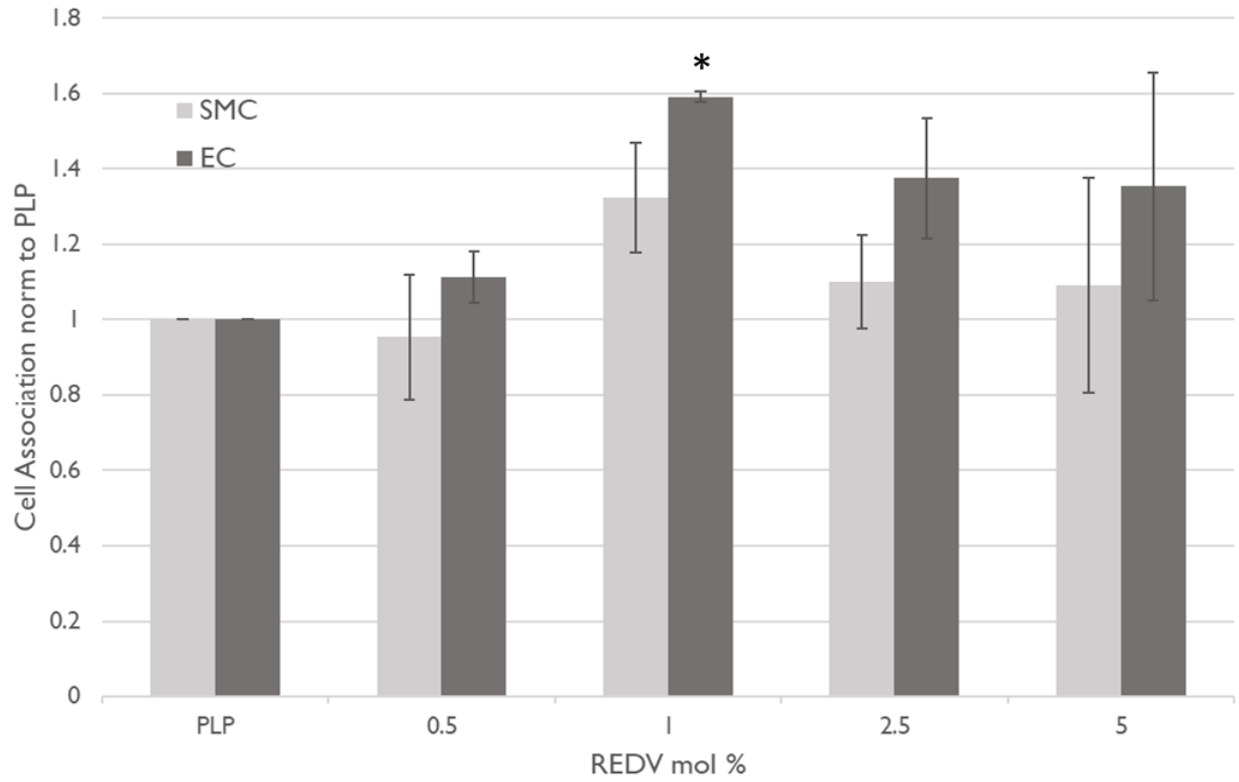


Figure 4.8: The relative cell association of REDV modified CTP-PLPs using pre-insertion compared in VSMCs and VECs after 1 hour treatment. PLP controls and EC-PLPs were assembled as described with the addition of Rho-DOPE at 0.5mol%, and cell association was determined by mean arbitrary fluorescence units (AFU) of each sample, minus baseline fluorescence of non-treated controls receiving no Rho-DOPE. *P<0.05 vs. PLP in VEC; n=3

4.3.6 The Incorporation of REDV-PEG into EC-PLPs Does Not Significantly Increase Cell Association Above PLP Controls at Later Time Points.

The incorporation of 0.5, 1.0, 2.5, and 5.0mol% REDV-PEG via pre-insertion achieved 0.83 ± 0.11 , 1.16 ± 0.10 , 1.19 ± 0.18 , and 1.04 ± 0.10 -fold change in cell association in VSMC and 0.78 ± 0.19 , 1.19 ± 0.18 , 1.08 ± 0.04 , and 0.91 ± 0.02 -fold change in cell association in VEC, respectively, after 4 hour treatment (Fig 4.9).

4.4 Discussion

Therapeutic strategies using ligand-modified CTP-PLPs for cell-specific targeting have been studied in wide variety of disease targets, including atherosclerotic lesions and vascular injury. Targeted nanomedicine is a promising approach in treating vascular injury in a surgical model due to the contradictory outcomes produced by current therapeutic paradigms.¹³⁸ Most therapeutic modalities are geared towards the inhibition of VSMC contribution to neointima formation. Unfortunately, these anti-proliferative therapies also prohibit the effective healing of the *intimal layer* comprised of VECs. We propose that an optimal pharmacological strategy would provide a therapeutic application that discretely inhibits VSMC migration and proliferation, while also promoting VEC recovery.

The extracellular matrix (ECM) helps delineate where specific cell types reside within tissues based on cell selectivity with common ECM components. For this reason drug discovery and proteomics studies have revealed “cell-selective” peptides based on their interaction with the ECM. VAPG (val-ala-pro-glycine) and REDV (arg-glu-asp-val) have been chosen as the SMC-specific and EC-specific ligand candidates in this study due to their small size and simplicity. VAPG,

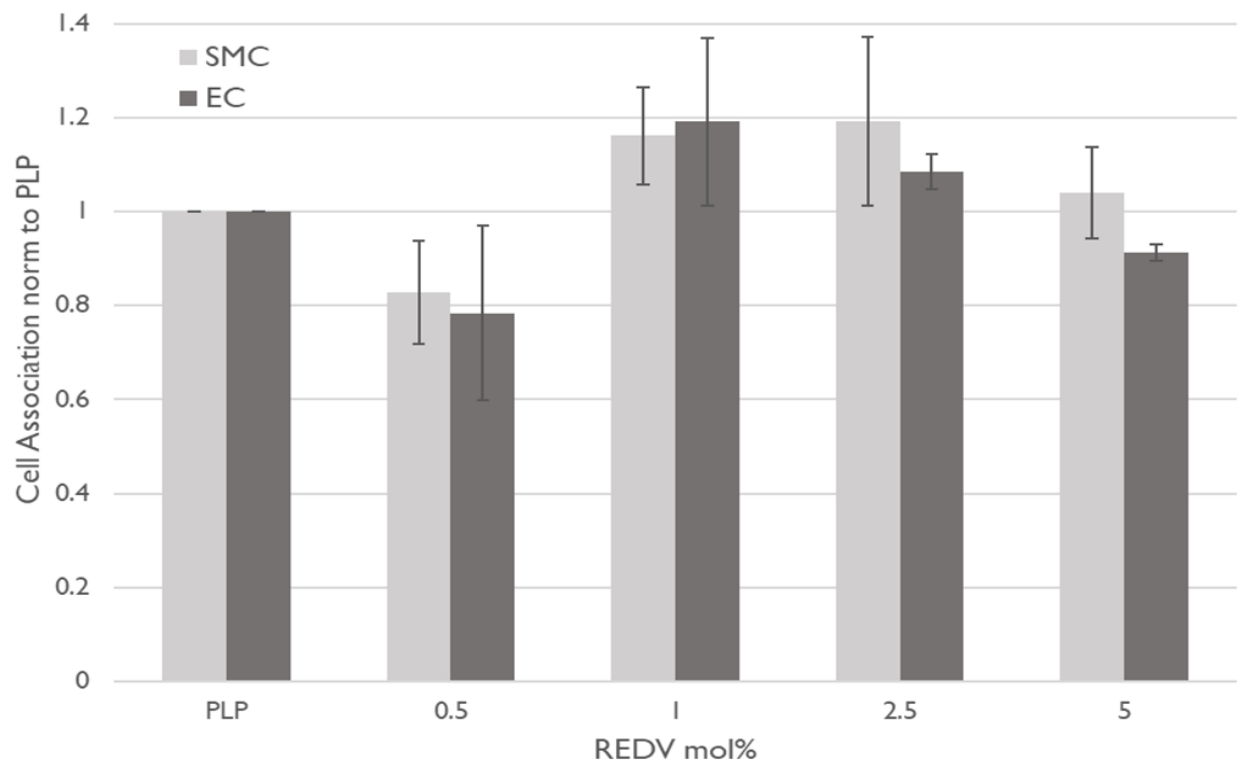


Figure 4.9: The relative cell association of REDV modified CTP-PLPs sing pre-insertion compared in VSMCs and VECs after 4 hour treatment. PLP controls and EC-PLPs were assembled as described with the addition of Rho-DOPE at 0.5mol%, and cell association was determined by mean arbitrary fluorescence units (AFU) of each sample, minus baseline fluorescence of non-treated controls receiving no Rho-DOPE. *P<0.05 vs. PLP in VEC; n=3

an elastin-derived ECM binding sequence, and REDV, a fibronectin-derived ECM binding sequence, were shown to have VSMC and VEC specific attachment under shear flow conditions.¹³⁹ The previously established cell-specific fragments, VAPG and REDV, were attached to PLP surfaces via azide-alkyne click chemistry techniques, exposing them on the edge of the PEG scaffold.

First, we examined the effect of VAPG-PEG and REDV-PEG incorporation on PLP characterization. We looked at size, PDI, liposome morphology, and lamellarity. The incorporation of VAPG-PEG and REDV-PEG into PLPs showed no significant difference in size or PDI when compared to unmodified PLP. STEM images confirm that VAPG modified liposomes display a spherical morphology, consistent with liposomal assembly. The measured sizes using STEM imaging are less than 100 nm in diameter and fall within the range of measured average size using DLS. Also, these liposomes are unilamellar in nature, a characteristic required for functional gene delivery.

Next, we investigated the VSMC-specific cell association of SMC-PLPs modified with VAPG-PEG. VSMCs and VECs were given 4 hour treatments with SMC-PLPs containing 0.5, 1.0, 2.5, and 5mol %, respectively, due to previously optimized cell association of PLPs in VSMCs (data not shown). The addition of 5 mol % VAPG-PEG to PLP enhanced cell association ~3.5-fold in VSMCs when normalized to PLP controls with no VAPG. On the other hand, no significant enhancement of cell association was shown in VECs using this SMC-PLP formulation. Additionally, there was no significant difference between VSMC-related and VEC-related cell association within VAPG groups. This would indicate that, even though VSMC-specific association was shown by SMC-PLPs when compared to PLP control, the cell-specific affinity is

diminished due to the fact that there is some increase in cell associative potential in VECs. The addition of VAPG-PEG via post-insertion did not convey any enhanced cell association in VSMCs when normalized to PLP. This would indicate that post-insertion of VAPG-PEG is inefficient. Chemical and physical studies utilizing high performance liquid chromatography (HPLC) in line with evaporative light scattering detection (ELSD) to measure relative abundance of ligand-conjugated lipids would be required in the future. Regardless, these assays confirm that VAPG-decorated PLPs confer some VSMC-specific potential.

Similarly, we conjugated REDV to the surface of PLPs to produce EC-PLPs. Interestingly, when treated for 4 hours with EC-PLP, there was no significant enhancement of cell association in VSMCs or VECs. However, when we shortened this treatment time to 1 hour, the addition of 1 mol % REDV-PEG was shown to significantly enhance cell association in VECs ~1.59-fold. There was no observed increase in VSMCs for EC-PLPs when normalized to PLP.

The lack of cell-specific differences observed within each group for both SMC-PLP and EC-PLP treatment *in vitro* would suggest that these “targeted” liposomes are inadequate for *in vivo* translation. This could be due to the presence of the PEG shell in PLP formulations, which can inhibit short peptides from interacting with cell surface even if exposed on surface. Also, these experiments were performed in static cell culture conditions, unlike previous studies where cell-specificity of VAPG and REDV were established under flow conditions. Future studies utilizing a flow chamber for cell culture may be required to elucidate cell-specific attachment.

Our ultimate goal was to establish cell-specific potential of SMC-PLPs and EC-PLPs modified with VAPG and REDV, respectively. Although both peptides conferred cell-specific affinity when compared to PLP controls, further investigation is necessary before *in vivo*

administration is warranted. It may be necessary to use folded peptides or monoclonal antibodies with recognized affinity to create the cell-specific affinity necessary for translational studies. In conclusion, we have established a proof-of-concept technique whereby our previously established ethanol injection assembly method and resulting noncationic PLP vector can be modified via click chemistry techniques to confer cell-targeting capabilities.

CHAPTER 5: Conclusions and Future Directions

5.1 Study Conclusions and Future Directions

Technological advancements in medicine have revolutionized how surgeons treat occlusive disorders of the vasculature. Endovascular surgery is a minimally invasive technique that provides surgeons with a low-risk treatment option for PVD patients to restore adequate blood flow at the site of atherosclerotic lesions. Unfortunately, these procedures inherently induce endothelial damage, which triggers adverse remodeling of the vessel, otherwise known as IH. IH can lead to restenosis and subsequent revascularization procedures with higher costs and morbidity. Gene therapy has the potential to mitigate restenosis by targeting specific gene targets previously implicated in IH development. Although there is a large volume of optimistic basic science research in the field of gene therapy, the primary hurdle to translational and clinical success is the delivery system. A nanocarrier system with favorable pharmacokinetic properties and minimal toxicity and immunogenicity is required to realize bench-to-bedside success of gene therapeutics.

As an *in vitro* proof-of-concept study, this dissertation project aimed to accomplish the following main objectives:

- 1) Develop a noncationic PLP with reduced cytotoxicity, improved loading efficiency, and enhanced transfection capacity compared to traditional LDS for siRNA delivery.
- 2) Develop a cell-type specific PLP equipped with SMC-specific and EC-specific functional motifs to differentially target vascular cell types for siRNA delivery.

The research herein provides a novel LDS platform for siRNA delivery with a high degree of translational potential. Through continuous optimization and process improvement, this

liposomal siRNA nanotechnology could provide a foundation leading to improved clinical success of gene therapy in vascular disease and other disease pathologies.

In chapter 2, we demonstrated a novel assembly technique that produces PEGylated liposomes with CQAs required for the effective delivery of gene therapeutics in a downstream translational model. Specifically, the research herein shows that the addition of STR-R8 into PLPs utilizing the pre-insertion technique is a simple and efficient method to produce noncationic CPP-modified liposomes with enhanced cell association and optimal siRNA loading efficiency. The siRNA encapsulate is stable within the CPP-PLP nanocarrier, which provides nearly complete protection from nuclease digestion in the external environment. This technique provided a foundational procedure to assemble noncationic liposomal siRNA delivery systems for *in vitro* investigation in vascular cell types.

In chapter 3, we established neutral, CPP-modified liposomes as efficient nanocarriers in VSMCs. We confirmed that incorporating 10mol% STR-R8 in PLP formulations provides an optimal transfection agent with minimal cytotoxicity and enhanced transfection capacity as compared to cationic liposomes. The cytotoxicity associated with common cationic vectors like CLPs and PEI has plagued the gene therapy field for decades, and is the primary reason LDS fail en route to clinical approval. The ability of these nanocarriers to employ functional siRNA-mediated gene knockdown with minimal cytotoxicity is crucial to the downstream success of noncationic platforms in liposomal siRNA delivery.

Chapter 4 is a proof-of-concept study that demonstrates the ligand-mediated, discriminate targeting of noncationic PLPs to VSMCs and VECs, respectively. Modification of PLP base formulations with VAPG-PEG and REDV-PEG enhanced cell association above PLP controls in

respective vascular cell targets. Although we achieved discrete enhancement above unmodified PLP controls with both SMC-specific and EC-specific liposomes, the addition of VAPG and REDV did not significantly improve cell-selective association within ligand-modified groups. The level of cell-selectivity would need to be clear and palpable for effective cell-targeted delivery *in vivo*, therefore further optimization is required.

We will continue to expand development of cell-selective liposomal platform in future studies using customary modification strategies established in LDS literature. Monoclonal antibodies provide much higher affinity for their respective cell targets than small peptide fragments like VAPG and REDV. The incorporation of antibodies to PLP surfaces to convey cell-type specific delivery has been successfully demonstrated *in vitro* and *in vivo*. Although the surface chemistry and orientation of large molecules introduces greater complexity to the PLP assembly process, we aim to incorporate monoclonal antibodies and antibody fragments onto the PLP surface to provide cell-type specific capabilities to our previously established noncationic siRNA-loaded PLPs. Also, the use of pre-insertion technique, while simplistic and scalable, can produce inefficient assemblies where the ligand is internalized and rendered useless. We intend to investigate the use water-in-oil emulsification techniques for tightly controlled surface-decoration of functional ligands in noncationic PLPs.

We are committed to continuous *in vitro*, *ex vivo*, and *in vivo* validation of our noncationic liposomal siRNA platform in hopes of establishing a gene therapeutic aimed at attenuating IH development in a surgical model. Likewise, the simple, scalable assembly technique, established in Chapters 2 and 3, provides a springboard for the development of other LDS modalities for improved drug delivery and effective RNAi therapy in vascular disease and beyond. As assembly

parameters and surface chemistry techniques continue to be optimized by our group novel LDS modalities for clinical application will continue to be developed with ancillary projects. This includes the development of spatially-controlled liposomes, cell-mimetic liposomes, and theranostic liposomes.

For example, our group recently aimed to tailor PLP lipid formulations to mimic membranes of vascular cell types. For instance, the addition of phosphatidyl serine (PS) and diacyl glycerol (DAG) adds lipid complexity to our unilamellar liposome system commonly seen in cells, which could augment liposomal drug delivery. These specific lipids are highly involved in lipid signaling and vesicular trafficking within the cell, which could plausibly promote cellular uptake of noncationic PLPs. Utilizing the assembly method herein, a recently published study from our group demonstrates that the use of DAG and PS could enhance therapeutic potential of our R8-PLP via enhanced cell associative properties.¹⁴⁰

Also, our group is interested in the spatial control of siRNA-loaded PLPs within the vasculature. Recently, we demonstrated successful localization and collagen-specific affinity of ligand-conjugated liposomes. A novel peptide with specific affinity for human collagen Type IV was chosen as a ligand candidate for future studies. In a study recently submitted for peer-review publication, our group established that, by decorating PLP surface with collagen-binding peptides, ligand-conjugated liposomes demonstrated increased binding affinity to collagen matrices under flow conditions. The idea is that, by targeting exposed subendothelial collagen in vascular injuries, liposomes can be directed to vascular lesions for downstream therapeutic and diagnostic applications.

The purpose of this dissertation was to establish a noncationic PLP capable of augmented transfection potential, enhanced siRNA encapsulation, reduced cytotoxicity, and cell selectivity in vascular cell types, while meeting all CQAs required for effective systemic administration of liposomal nanomedicine. Our research has elucidated a simple and efficient method for producing noncationic R8-modified liposomes with enhanced cell association and siRNA loading efficiency. We have confirmed that these novel liposomal nanocarriers containing STR-R8 amphiphiles are effective transfection agents in VSMC with minimal cytotoxicity compared to traditional CLPs. In addition, PLPs produced using this novel assembly method can be further modified to convey cell-specific properties in VSMC and VEC alike. The novel LDS developed in this study will provide the foundation for future pre-clinical *in vivo* validation studies using our previously established animal model of vascular injury and IH development in rat carotid arteries. However, further *in vitro* development is required to move towards an animal model and increase translational potential in a clinical setting. We have proposed that the development of a targeted liposomal vector capable of discrete delivery of therapeutic genes to VSMCs and VECs, respectively, could provide an optimal pharmacological approach to prevent IH-induced restenosis in response to vascular injury. The novel siRNA-loaded PLP developed herein will provide the foundation for future clinical applications of gene therapy aimed at preventing IH-induced restenosis.

BIBLIOGRAPHY

1. Johnson CO, Nguyen M, Zipkin B, Alam T, Roth GA. Abstract P135: Prevalence of Peripheral Vascular Disease: Results of the Global Burden of Disease 2016 Study. *Circulation* 2018;137:AP135-AP.
2. Taha AG, Byrne RM, Avgerinos ED, Marone LK, Makaroun MS, Chaer RA. Comparative effectiveness of endovascular versus surgical revascularization for acute lower extremity ischemia. *Journal of vascular surgery* 2015;61:147-54.
3. Ylä-Herttua S, Baker AH. Cardiovascular gene therapy: past, present, and future. *Molecular Therapy* 2017;25:1095-106.
4. Ballantyne M, McDonald R, Baker A. IncRNA/MicroRNA interactions in the vasculature. *Clinical Pharmacology & Therapeutics* 2016;99:494-501.
5. Patti BS, Chupin VV, Torchilin VP. New developments in liposomal drug delivery. *Chemical reviews* 2015;115:10938-66.
6. Aryasomayajula B, Salzano G, Torchilin VP. Multifunctional Liposomes. *Cancer Nanotechnology: Springer*; 2017:41-61.
7. Reis A, Paulino D, Abrantes C, Machado I, Barroso J. Usage of mobile devices to help people suffering from peripheral arterial disease upkeep a healthy life. *J Phy Med Rehab* 2017;1:103.
8. Criqui MH. Peripheral arterial disease-epidemiological aspects. *Vascular medicine* 2001;6:3-7.
9. Aronow WS, Ahn C. Prevalence of coexistence of coronary artery disease, peripheral arterial disease, and atherothrombotic brain infarction in men and women ≥ 62 years of age. *The American journal of cardiology* 1994;74:64-5.
10. Armstrong EJ, Chen DC, Westin GG, et al. Adherence to guideline-recommended therapy is associated with decreased major adverse cardiovascular events and major adverse limb events among patients with peripheral arterial disease. *Journal of the American Heart Association* 2014;3:e000697.
11. Suri JS, Kathuria C, Molinari F. *Atherosclerosis disease management: Springer Science & Business Media*; 2010.
12. Bennett MR, O'Sullivan M. Mechanisms of angioplasty and stent restenosis: implications for design of rational therapy. *Pharmacology & therapeutics* 2001;91:149-66.
13. Marks DS, Vita JA, Folts JD, Keaney JF, Welch GN, Loscalzo J. Inhibition of neointimal proliferation in rabbits after vascular injury by a single treatment with a protein adduct of nitric oxide. *The Journal of clinical investigation* 1995;96:2630-8.
14. Collins JA, Munoz JV, Patel TR, Loukas M, Tubbs RS. The anatomy of the aging aorta. *Clinical Anatomy* 2014;27:463-6.
15. Sung H-J, Eskin SG, Sakurai Y, Yee A, Kataoka N, McIntire LV. Oxidative stress produced with cell migration increases synthetic phenotype of vascular smooth muscle cells. *Annals of biomedical engineering* 2005;33:1546-54.
16. Corselli M, Chen C-W, Sun B, Yap S, Rubin JP, Péault B. The tunica adventitia of human arteries and veins as a source of mesenchymal stem cells. *Stem cells and development* 2011;21:1299-308.
17. Libby P, Ridker PM, Maseri A. Inflammation and atherosclerosis. *Circulation* 2002;105:1135-43.
18. Gimbrone Jr MA, García-Cardena G. Endothelial cell dysfunction and the pathobiology of atherosclerosis. *Circulation research* 2016;118:620-36.

19. Woodward M, Parrinello C, Matushita K, Wagenknecht LE, Coresh J, Selvin E. Risk prediction of major complications in persons with diabetes: The Atherosclerosis Risk in Communities Study. *Diabetes, Obesity and Metabolism* 2016;18.
20. Mäkikallio T, Holm NR, Lindsay M, et al. Percutaneous coronary angioplasty versus coronary artery bypass grafting in treatment of unprotected left main stenosis (NOBLE): a prospective, randomised, open-label, non-inferiority trial. *The Lancet* 2016;388:2743-52.
21. Mazari F, Khan J, Samuel N, et al. Long-term outcomes of a randomized clinical trial of supervised exercise, percutaneous transluminal angioplasty or combined treatment for patients with intermittent claudication due to femoropopliteal disease. *British Journal of Surgery* 2017;104:76-83.
22. Bosiers M, Deloose K. Results for Infrapopliteal Endovascular Interventions: Angioplasty, Stenting, and Atherectomy. *Critical Limb Ischemia: CRC Press; 2016:190-204.*
23. Siontis GC, Stefanini GG, Mavridis D, et al. Percutaneous coronary interventional strategies for treatment of in-stent restenosis: a network meta-analysis. *The Lancet* 2015;386:655-64.
24. Verma SK, Garikipati VNS, Krishnamurthy P, et al. IL-10 accelerates re-endothelialization and inhibits post-injury intimal hyperplasia following carotid artery denudation. *PloS one* 2016;11:e0147615.
25. Newby AC, Zaltsman AB. Molecular mechanisms in intimal hyperplasia. *The Journal of pathology* 2000;190:300-9.
26. Nagai A, Yamashita K, Imamura M, Azuma H. Hydroxyapatite electret accelerates reendothelialization and attenuates intimal hyperplasia occurring after endothelial removal of the rabbit carotid artery. *Life sciences* 2008;82:1162-8.
27. Leidenfrost JE, Khan MF, Boc KP, et al. A model of primary atherosclerosis and post-angioplasty restenosis in mice. *The American journal of pathology* 2003;163:773-8.
28. Cortese B, Micheli A, Picchi A, et al. Paclitaxel-coated balloon versus drug-eluting stent during PCI of small coronary vessels, a prospective randomised clinical trial. The PICCOLETO study. *Heart* 2010;96:1291-6.
29. Kałuza GL, Joseph J, Lee JR, Raizner ME, Raizner AE. Catastrophic outcomes of noncardiac surgery soon after coronary stenting. *Journal of the American College of Cardiology* 2000;35:1288-94.
30. Dangas GD, Claessen BE, Caixeta A, Sanidas EA, Mintz GS, Mehran R. In-stent restenosis in the drug-eluting stent era. *Journal of the American College of Cardiology* 2010;56:1897-907.
31. Wessely R. New drug-eluting stent concepts. *Nature Reviews Cardiology* 2010;7:194.
32. Raymond J, Metcalfe A, Salazkin I, Gevry G, Guilbert F. Endoluminal cryotherapy to prevent recanalization after endovascular occlusion with platinum coils. *Journal of vascular and interventional radiology* 2006;17:1499-504.
33. Torguson R, Sabate M, Deible R, et al. Intravascular brachytherapy versus drug-eluting stents for the treatment of patients with drug-eluting stent restenosis. *The American journal of cardiology* 2006;98:1340-4.
34. DeCunha J, Janicki C, Enger S. A retrospective analysis of catheter-based sources in intravascular brachytherapy. *Brachytherapy* 2017;16:586-96.
35. Ginn SL, Alexander IE, Edelstein ML, Abedi MR, Wixon J. Gene therapy clinical trials worldwide to 2012—an update. *The journal of gene medicine* 2013;15:65-77.

36. Gill DR, Pringle IA, Hyde SC. Progress and prospects: the design and production of plasmid vectors. *Gene therapy* 2009;16:165.
37. Mishra PJ. The miRNA–drug resistance connection: a new era of personalized medicine using noncoding RNA begins. *Pharmacogenomics* 2012;13:1321-4.
38. Fire A, Xu S, Montgomery MK, Kostas SA, Driver SE, Mello CC. Potent and specific genetic interference by double-stranded RNA in *Caenorhabditis elegans*. *nature* 1998;391:806.
39. Carthew RW, Sontheimer EJ. Origins and mechanisms of miRNAs and siRNAs. *Cell* 2009;136:642-55.
40. Pradhan-Nabzdyk L, Huang C, LoGerfo FW, Nabzdyk CS. Current siRNA targets in the prevention and treatment of intimal hyperplasia. *Discovery medicine* 2014;18:125.
41. Mountain DJ, Arnold JD, Kirkpatrick SS, et al. Targeting MT1-MMP via Polymeric Transfection is More Efficient to Inhibit the Cellular Processes of Intimal Hyperplasia. *Arteriosclerosis, Thrombosis, and Vascular Biology* 2013;33:A215-A.
42. Robbins PD, Ghivizzani SC. Viral vectors for gene therapy. *Pharmacology & therapeutics* 1998;80:35-47.
43. Kay MA, Glorioso JC, Naldini L. Viral vectors for gene therapy: the art of turning infectious agents into vehicles of therapeutics. *Nature medicine* 2001;7:33.
44. Wells D. Gene therapy progress and prospects: electroporation and other physical methods. *Gene therapy* 2004;11:1363.
45. Green JJ, Shi J, Chiu E, Leshchiner ES, Langer R, Anderson DG. Biodegradable polymeric vectors for gene delivery to human endothelial cells. *Bioconjugate chemistry* 2006;17:1162-9.
46. Johnson S, Bangham A, Hill M, Korn E. Single bilayer liposomes. *Biochimica et Biophysica Acta (BBA)-Biomembranes* 1971;233:820-6.
47. Bunker A, Magarkar A, Viitala T. Rational design of liposomal drug delivery systems, a review: combined experimental and computational studies of lipid membranes, liposomes and their PEGylation. *Biochimica et Biophysica Acta (BBA)-Biomembranes* 2016;1858:2334-52.
48. Sercombe L, Veerati T, Moheimani F, Wu SY, Sood AK, Hua S. Advances and challenges of liposome assisted drug delivery. *Frontiers in pharmacology* 2015;6:286.
49. Torchilin VP. Multifunctional, stimuli-sensitive nanoparticulate systems for drug delivery. *Nature reviews Drug discovery* 2014;13:813.
50. Hatakeyama H, Akita H, Harashima H. A multifunctional envelope type nano device (MEND) for gene delivery to tumours based on the EPR effect: a strategy for overcoming the PEG dilemma. *Advanced drug delivery reviews* 2011;63:152-60.
51. Noble GT, Stefanick JF, Ashley JD, Kiziltepe T, Bilgicer B. Ligand-targeted liposome design: challenges and fundamental considerations. *Trends in biotechnology* 2014;32:32-45.
52. Miller AD. Cationic liposomes for gene therapy. *Angewandte Chemie International Edition* 1998;37:1768-85.
53. Kedmi R, Ben-Arie N, Peer D. The systemic toxicity of positively charged lipid nanoparticles and the role of Toll-like receptor 4 in immune activation. *Biomaterials* 2010;31:6867-75.
54. Capodanno D, Gori T, Nef H, et al. Percutaneous coronary intervention with everolimus-eluting bioresorbable vascular scaffolds in routine clinical practice: early and midterm outcomes from the European multicentre GHOST-EU registry. *EuroIntervention* 2015;10:1144-53.
55. Saul JM, Annapragada AV, Bellamkonda RV. A dual-ligand approach for enhancing targeting selectivity of therapeutic nanocarriers. *Journal of controlled release* 2006;114:277-87.

56. Guan S, Rosenecker J. Nanotechnologies in delivery of mRNA therapeutics using nonviral vector-based delivery systems. *Gene therapy* 2017;24:133.
57. Zylberberg C, Gaskill K, Pasley S, Matosevic S. Engineering liposomal nanoparticles for targeted gene therapy. *Gene therapy* 2017;24:441.
58. Li S-D, Huang L. Stealth nanoparticles: high density but sheddable PEG is a key for tumor targeting. *Journal of controlled release: official journal of the Controlled Release Society* 2010;145:178.
59. Gabizon A, Shmeeda H, Barenholz Y. Pharmacokinetics of pegylated liposomal doxorubicin. *Clinical pharmacokinetics* 2003;42:419-36.
60. Garg T, K Goyal A. Liposomes: targeted and controlled delivery system. *Drug delivery letters* 2014;4:62-71.
61. Jiang L, Li L, He X, et al. Overcoming drug-resistant lung cancer by paclitaxel loaded dual-functional liposomes with mitochondria targeting and pH-response. *Biomaterials* 2015;52:126-39.
62. Wasungu L, Hoekstra D. Cationic lipids, lipoplexes and intracellular delivery of genes. *Journal of Controlled Release* 2006;116:255-64.
63. Aramaki Y, Takano S, Tsuchiya S. Cationic liposomes induce macrophage apoptosis through mitochondrial pathway. *Archives of biochemistry and biophysics* 2001;392:245-50.
64. Loney C, Vandenbranden M, Ruyschaert J-M. Cationic lipids activate intracellular signaling pathways. *Advanced drug delivery reviews* 2012;64:1749-58.
65. Antipina AY, Gurtovenko AA. Molecular mechanism of calcium-induced adsorption of DNA on zwitterionic phospholipid membranes. *The Journal of Physical Chemistry B* 2015;119:6638-45.
66. Hatakeyama H, Akita H, Harashima H. The polyethyleneglycol dilemma: advantage and disadvantage of PEGylation of liposomes for systemic genes and nucleic acids delivery to tumors. *Biological and Pharmaceutical Bulletin* 2013;36:892-9.
67. Koren E, Torchilin VP. Cell-penetrating peptides: breaking through to the other side. *Trends in molecular medicine* 2012;18:385-93.
68. Yang S-T, Zaitseva E, Chernomordik LV, Melikov K. Cell-penetrating peptide induces leaky fusion of liposomes containing late endosome-specific anionic lipid. *Biophysical journal* 2010;99:2525-33.
69. Schmidt N, Mishra A, Lai GH, Wong GC. Arginine-rich cell-penetrating peptides. *FEBS letters* 2010;584:1806-13.
70. Somiya M, Yamaguchi K, Liu Q, et al. One-step scalable preparation method for non-cationic liposomes with high siRNA content. *International journal of pharmaceutics* 2015;490:316-23.
71. Manova R, van Beek TA, Zuilhof H. Surface Functionalization by Strain-Promoted Alkyne–Azide Click Reactions. *Angewandte Chemie International Edition* 2011;50:5428-30.
72. Chenoweth K, Chenoweth D, Goddard lii WA. Cyclooctyne-based reagents for uncatalyzed click chemistry: A computational survey. *Organic & biomolecular chemistry* 2009;7:5255-8.
73. Fisher RK, Mattern-Schain SI, Best MD, et al. Improving the efficacy of liposome-mediated vascular gene therapy via lipid surface modifications. *Journal of Surgical Research* 2017;219:136-44.
74. Ozcan G, Ozpolat B, Coleman RL, Sood AK, Lopez-Berestein G. Preclinical and clinical development of siRNA-based therapeutics. *Advanced drug delivery reviews* 2015;87:108-19.

75. Zuckerman JE, Davis ME. Clinical experiences with systemically administered siRNA-based therapeutics in cancer. *Nature reviews Drug discovery* 2015;14:843.
76. Blanco E, Shen H, Ferrari M. Principles of nanoparticle design for overcoming biological barriers to drug delivery. *Nature biotechnology* 2015;33:941.
77. Yin H, Kanasty RL, Eltoukhy AA, Vegas AJ, Dorkin JR, Anderson DG. Non-viral vectors for gene-based therapy. *Nature Reviews Genetics* 2014;15:541.
78. Scherman D, Rousseau A, Bigey P, Escriou V. Genetic pharmacology: progresses in siRNA delivery and therapeutic applications. *Gene therapy* 2017;24:151.
79. Audouy SA, De Leij LF, Hoekstra D, Molema G. In vivo characteristics of cationic liposomes as delivery vectors for gene therapy. *Pharmaceutical research* 2002;19:1599-605.
80. Kim H-K, Davaa E, Myung C-S, Park J-S. Enhanced siRNA delivery using cationic liposomes with new polyarginine-conjugated PEG-lipid. *International journal of pharmaceutics* 2010;392:141-7.
81. Kogure K, Moriguchi R, Sasaki K, Ueno M, Futaki S, Harashima H. Development of a non-viral multifunctional envelope-type nano device by a novel lipid film hydration method. *Journal of controlled release* 2004;98:317-23.
82. Lee S-H, Sato Y, Hyodo M, Harashima H. Topology of surface ligands on liposomes: characterization based on the terms, incorporation ratio, surface anchor density, and reaction yield. *Biological and Pharmaceutical Bulletin* 2016;39:1983-94.
83. Uster PS, Allen TM, Daniel BE, Mendez CJ, Newman MS, Zhu GZ. Insertion of poly (ethylene glycol) derivatized phospholipid into pre-formed liposomes results in prolonged in vivo circulation time. *FEBS letters* 1996;386:243-6.
84. Sułkowski W, Pentak D, Nowak K, Sułkowska A. The influence of temperature, cholesterol content and pH on liposome stability. *Journal of Molecular Structure* 2005;744:737-47.
85. Iden DL, Allen TM. In vitro and in vivo comparison of immunoliposomes made by conventional coupling techniques with those made by a new post-insertion approach. *Biochimica et Biophysica Acta (BBA)-Biomembranes* 2001;1513:207-16.
86. Moreira JN, Ishida T, Gaspar R, Allen TM. Use of the post-insertion technique to insert peptide ligands into pre-formed stealth liposomes with retention of binding activity and cytotoxicity. *Pharmaceutical research* 2002;19:265-9.
87. Mangoni M, Roccatano D, Di Nola A. Docking of flexible ligands to flexible receptors in solution by molecular dynamics simulation. *Proteins: Structure, Function, and Bioinformatics* 1999;35:153-62.
88. Nakamura Y, Kogure K, Futaki S, Harashima H. Octaarginine-modified multifunctional envelope-type nano device for siRNA. *Journal of controlled release* 2007;119:360-7.
89. Fowkes FGR, Rudan D, Rudan I, et al. Comparison of global estimates of prevalence and risk factors for peripheral artery disease in 2000 and 2010: a systematic review and analysis. *The Lancet* 2013;382:1329-40.
90. Fioole B, van de Rest HJ, Meijer JR, et al. Percutaneous transluminal angioplasty and stenting as first-choice treatment in patients with chronic mesenteric ischemia. *Journal of vascular surgery* 2010;51:386-91.
91. Moore WS. *Vascular and endovascular surgery: a comprehensive review*: Elsevier Health Sciences; 2012.

92. Klein WM, van der Graaf Y, Seegers J, Moll FL, Mali WP. Long-term Cardiovascular Morbidity, Mortality, and Reintervention after Endovascular Treatment in Patients with Iliac Artery Disease: The Dutch Iliac Stent Trial Study I. *Radiology* 2004;232:491-8.
93. Atkins MD, Kwolek CJ, LaMuraglia GM, Brewster DC, Chung TK, Cambria RP. Surgical revascularization versus endovascular therapy for chronic mesenteric ischemia: a comparative experience. *Journal of vascular surgery* 2007;45:162-71.
94. Che H-L, Bae I-H, Lim KS, et al. Suppression of post-angioplasty restenosis with an Akt1 siRNA-embedded coronary stent in a rabbit model. *Biomaterials* 2012;33:8548-56.
95. Maheshwari R, Tekade M, A Sharma P, Kumar Tekade R. Nanocarriers assisted siRNA gene therapy for the management of cardiovascular disorders. *Current pharmaceutical design* 2015;21:4427-40.
96. Freeman BM, Univers J, Fisher RK, et al. Testosterone replacement attenuates intimal hyperplasia development in an androgen deficient model of vascular injury. *Journal of Surgical Research* 2017;207:53-62.
97. Grandas OH, Mountain DJ, Kirkpatrick SS, et al. Effect of hormones on matrix metalloproteinases gene regulation in human aortic smooth muscle cells. *Journal of Surgical Research* 2008;148:94-9.
98. Tummers AM, Mountain DJ, Mix JW, et al. Serum levels of matrix metalloproteinase-2 as a marker of intimal hyperplasia. *Journal of Surgical Research* 2010;160:9-13.
99. Mountain DJ, Kirkpatrick SS, Freeman MB, Stevens SL, Goldman MH, Grandas OH. Role of MT1-MMP in estrogen-mediated cellular processes of intimal hyperplasia. *Journal of Surgical Research* 2012;173:224-31.
100. Mountain DJ, Freeman MB, Kirkpatrick SS, et al. Effect of hormone replacement therapy in matrix metalloproteinase expression and intimal hyperplasia development after vascular injury. *Annals of vascular surgery* 2013;27:337-45.
101. Mountain DJ, Freeman BM, Kirkpatrick SS, et al. Androgens regulate MMPs and the cellular processes of intimal hyperplasia. *Journal of surgical research* 2013;184:619-27.
102. Freeman BM, Mountain DJ, Brock TC, et al. Low testosterone elevates interleukin family cytokines in a rodent model: a possible mechanism for the potentiation of vascular disease in androgen-deficient males. *Journal of surgical research* 2014;190:319-27.
103. Ohno T, Gordon D, San H, et al. Gene therapy for vascular smooth muscle cell proliferation after arterial injury. *Science* 1994;265:781-5.
104. Niidome T, Huang L. Gene therapy progress and prospects: nonviral vectors. *Gene therapy* 2002;9:1647.
105. Waehler R, Russell SJ, Curiel DT. Engineering targeted viral vectors for gene therapy. *Nature Reviews Genetics* 2007;8:573-87.
106. Bools LM, Fisher RK, Grandas OH, et al. Comparative analysis of polymers for short interfering RNA delivery in vascular smooth muscle cells. *Journal of Surgical Research* 2015;199:266-73.
107. Arnold JD, Mountain DJ, Freeman MB, et al. Smooth muscle cell polymeric transfection is an efficient alternative to traditional methods of experimental gene therapy. *Journal of surgical research* 2012;177:178-84.
108. Ylä-Herttua S, Martin JF. Cardiovascular gene therapy. *The Lancet* 2000;355:213-22.
109. Zhang S, Zhao B, Jiang H, Wang B, Ma B. Cationic lipids and polymers mediated vectors for delivery of siRNA. *Journal of Controlled Release* 2007;123:1-10.

110. Lv H, Zhang S, Wang B, Cui S, Yan J. Toxicity of cationic lipids and cationic polymers in gene delivery. *Journal of Controlled Release* 2006;114:100-9.
111. Torchilin VP. Multifunctional nanocarriers. *Advanced drug delivery reviews* 2012;64:302-15.
112. Gao H, Zhang Q, Yu Z, He Q. Cell-penetrating peptide-based intelligent liposomal systems for enhanced drug delivery. *Current pharmaceutical biotechnology* 2014;15:210-9.
113. Copolovici DM, Langel K, Eriste E, Langel U. Cell-penetrating peptides: design, synthesis, and applications. *ACS nano* 2014;8:1972-94.
114. Thomas JW, Kuo MD, Chawla M, et al. Vascular gene therapy. *Radiographics* 1998;18:1373-94.
115. Hayashi K, Nakamura S, Morishita R, et al. In vivo transfer of human hepatocyte growth factor gene accelerates re-endothelialization and inhibits neointimal formation after balloon injury in rat model. *Gene therapy* 2000;7:1664-71.
116. Pankajakshan D, Agrawal DK. *Clinical and Translational Challenges in Gene Therapy of Cardiovascular Diseases: INTECH Open Access Publisher; 2013.*
117. Xu L, Anchordoquy T. Drug delivery trends in clinical trials and translational medicine: Challenges and opportunities in the delivery of nucleic acid-based therapeutics. *Journal of pharmaceutical sciences* 2011;100:38-52.
118. Pecot CV, Calin GA, Coleman RL, Lopez-Berestein G, Sood AK. RNA interference in the clinic: challenges and future directions. *Nature Reviews Cancer* 2011;11:59-67.
119. Karmali PP, Chaudhuri A. Cationic liposomes as non-viral carriers of gene medicines: resolved issues, open questions, and future promises. *Medicinal research reviews* 2007;27:696-722.
120. Safinya CR, Ewert KK, Majzoub RN, Leal C. Cationic liposome–nucleic acid complexes for gene delivery and gene silencing. *New Journal of Chemistry* 2014;38:5164-72.
121. Panyam J, Labhasetwar V. Biodegradable nanoparticles for drug and gene delivery to cells and tissue. *Advanced drug delivery reviews* 2003;55:329-47.
122. Prabha S, Zhou W-Z, Panyam J, Labhasetwar V. Size-dependency of nanoparticle-mediated gene transfection: studies with fractionated nanoparticles. *International journal of pharmaceutics* 2002;244:105-15.
123. Sakurai Y, Hatakeyama H, Akita H, et al. Efficient short interference RNA delivery to tumor cells using a combination of octaarginine, GALA and tumor-specific, cleavable polyethylene glycol system. *Biological and Pharmaceutical Bulletin* 2009;32:928-32.
124. El-Sayed A, Khalil IA, Kogure K, Futaki S, Harashima H. Octaarginine-and octalysine-modified nanoparticles have different modes of endosomal escape. *Journal of Biological Chemistry* 2008;283:23450-61.
125. Kogure K, Akita H, Yamada Y, Harashima H. Multifunctional envelope-type nano device (MEND) as a non-viral gene delivery system. *Advanced drug delivery reviews* 2008;60:559-71.
126. Khalil IA, Kogure K, Futaki S, Harashima H. High density of octaarginine stimulates macropinocytosis leading to efficient intracellular trafficking for gene expression. *Journal of Biological Chemistry* 2006;281:3544-51.
127. Soenen SJ, Brisson AR, De Cuyper M. Addressing the problem of cationic lipid-mediated toxicity: the magnetoliposome model. *Biomaterials* 2009;30:3691-701.

128. Mishra S, Webster P, Davis ME. PEGylation significantly affects cellular uptake and intracellular trafficking of non-viral gene delivery particles. *European journal of cell biology* 2004;83:97-111.
129. Holland JW, Hui C, Cullis PR, Madden TD. Poly (ethylene glycol)-lipid conjugates regulate the calcium-induced fusion of liposomes composed of phosphatidylethanolamine and phosphatidylserine. *Biochemistry* 1996;35:2618-24.
130. El-Sayed A, Futaki S, Harashima H. Delivery of macromolecules using arginine-rich cell-penetrating peptides: ways to overcome endosomal entrapment. *The AAPS journal* 2009;11:13-22.
131. Chan C-L, Majzoub RN, Shirazi RS, et al. Endosomal escape and transfection efficiency of PEGylated cationic liposome-DNA complexes prepared with an acid-labile PEG-lipid. *Biomaterials* 2012;33:4928-35.
132. Lächelt U, Wagner E. Invading target cells: multifunctional polymer conjugates as therapeutic nucleic acid carriers. *Frontiers of Chemical Science and Engineering* 2011;5:275-86.
133. Best MD. Click chemistry and bioorthogonal reactions: unprecedented selectivity in the labeling of biological molecules. *Biochemistry* 2009;48:6571-84.
134. Haruguchi H, Teraoka S. Intimal hyperplasia and hemodynamic factors in arterial bypass and arteriovenous grafts: a review. *Journal of Artificial Organs* 2003;6:227-35.
135. Lan H, Wang Y, Yin T, et al. Progress and prospects of endothelial progenitor cell therapy in coronary stent implantation. *Journal of Biomedical Materials Research Part B: Applied Biomaterials* 2016;104:1237-47.
136. Stone GW, Moses JW, Ellis SG, et al. Safety and efficacy of sirolimus-and paclitaxel-eluting coronary stents. *New England Journal of Medicine* 2007;356:998-1008.
137. Green JV, Murthy SK. Microfluidic enrichment of a target cell type from a heterogeneous suspension by adhesion-based negative selection. *Lab on a Chip* 2009;9:2245-8.
138. Lammers T, Hennink W, Storm G. Tumour-targeted nanomedicines: principles and practice. *British journal of cancer* 2008;99:392.
139. Murthy S, Plouffe B, Radisic M. Surface Engineering in Microfluidic Devices for the Isolation of Smooth Muscle Cells and Endothelial Cells. *MRS Online Proceedings Library Archive* 2007;1004.
140. Mattern-Schain SI, Fisher RK, West PC, et al. Cell mimetic liposomal nanocarriers for tailored delivery of vascular therapeutics. *Chemistry and physics of lipids* 2019;218:149-57.

VITA

Richard Fisher was born in Memphis, TN, and raised by Rick and Tammy Fisher. He has one younger sibling named Ashley Fisher. He attended Cordova High School in Cordova, TN and graduated in 2004 with honors. He then moved to Knoxville, TN to attend the University of Tennessee-Knoxville (UTK) where he studied Biochemistry and Molecular Biology. After receiving his Bachelor's of Science in Biological Sciences, he then studied under Dr. Dixie Thompson in the Kinesiology Department at UTK. Richard would soon earn a Master's of Science in Kinesiology with a concentration in Exercise Science. He would then go on to be hired at the Vascular Research Lab (VRL) as a research technician studying molecular mechanisms of intimal hyperplasia development in peripheral vascular disease. His work at the VRL would not go unnoticed as he soon would ascertain funding for his doctoral studies from the Department of Surgery and the Graduate School of Medicine. Under the tutelage of Dr. Deidra Mountain in the Comparative and Experimental Medicine Program (CEM), Richard was able to establish the novel assembly of a lipid nanoparticle for gene therapy applications. He received his Ph.D in CEM in the spring of 2019. He is currently working for a local biotech company in East Tennessee where he lives with his wife, Lauren Fisher, and daughter, Harper Fisher.